Draft Final Report
April 2005

EVALUATING THICK LIFT LIMEROCK-BASE COURSE SR-826 MIAMI FLORIDA

FDOT No: C-7984
UF No: 00030917

Research Team:

Dr.Sastry Putcha, Project Manager, State Construction Office
Robert Werner, P.E., Project Administrator, Ardaman and Associates, Inc
Dr. Michael C. McVay, Principal Investigator, University of Florida
Dr.David Horhota, State Geotechnical Materials Engineer
Tim Ruelke, P.E., District-2 Construction Engineer
Jack Banning, President, Florida Limerock&Aggregate Institute
Ron Wettlaufer, Compaction Sales Consultant, Nortrax Equipment Company

Report By:

Dr. Michael C. McVay, Principal Investigator, University of Florida
Jeongsoo Ko, Researcher, University of Florida

TABLE OF CONTENTS

page

LIST OF TABLES

LIST OF FIGURES

SUMMARY

Based on the research results, to perform base thick lift compaction on select projects, FDOT specification 200 has been developed as follows:

200-5.2 Number of Courses:

If, through field tests, the Contractor can demonstrate that the compaction equipment can achieve the density required by 200-7.2.1 for the full depth of a thicker lift, and if approved by the Engineer, the base may be constructed in successive courses of not more than 12-inch [300 mm] compacted thickness, provided that the average LBR of the subgrade material is not less than 120 with no individual LBR values less than 100 and the thickness of the subgrade layer is not less than12 inches.

Prior to construction of the test sections, the contractor will submit a plan to construct the single 12-inch thick lift section, including the equipment and procedures to be used. Approval of the plan by the State Construction Office will be required prior to construction of the test sections. Once the plan has been approved, the Engineer will base final approval on results of density tests and stiffness measurements on two test sections each of the length of one LOT. Notify the Engineer prior to beginning construction of the two test sections.

Construct the first test section of 12-inch thick base in two lifts each 6-inch thick using the Contractor's specified compaction effort. Identify the test section with the compaction effort and thickness in the Logbook. After compaction of the first lift, perform five QC density tests at random locations within the test section. All QC tests

and a Department Verification test performed on the first lift must meet the density required by 200-7.2.1. After compaction of the second lift, perform QC density tests at five random locations within the test section. At each location, test the top 6-inch [150 mm] in addition to the entire course thickness. All QC tests and a Department Verification test performed on the second lift must meet the density required by 200-7.2.1. The Engineer will perform a series of at least ten Falling Weight Deflectometer (FWD) tests at random locations within the test section. FWD testing will be conducted in accordance with ASTM D4694.

Construct the second test section consisting of a single 12-inch thick lift using the Contractor's proposed compaction effort for thick lift construction (e.g., vibratory pad-foot roller finished with a vibratory smooth drum roller). The maximum dynamic force of the compaction equipment shall be not less than 60,000 lbf. Identify the test section with the compaction effort and thickness in the Logbook. After compaction of the thick lift, perform QC density tests at five random locations within the test section. At each location, test the top 6 inches [150 mm] in addition to the entire 12-inch [300 mm] course thickness. All QC tests and a Department Verification test must meet the density required by 200-7.2.1.

The Engineer will perform a series of at least ten FWD tests per test section. Engineer's acceptance of the thick lift test section will require that the average FWD impulse stiffness of the thick lift test section be equal to or greater than the average FWD impulse stiffness of the two conventional 6-inch lifts and the required density for thick lift construction must meet the density required by 200-7.2.1. If the average FWD impulse stiffness of the thick lift test section is not greater than the average FWD impulse

stiffness of the conventional two 6-inch lifts, the Contractor may increase the compaction effort until the required average FWD value is achieved. f additional compaction effort is applied to the test section, additional QC density tests and a Department Verification test shall be performed, and the average of these density tests will be considered representative of the test section for determining the required density for thick lift base construction.

After construction of the test sections, approval of the thick lift base construction will require 3 days to obtain the FWD test report.

If unable to achieve the required density and FWD impulse stiffness, remove and replace or repair the test section to comply with the specifications at no additional expense to the Department.

Once approved, a change in the source of base material will require the construction of ~~a~~ new test sections. Do not change the compaction effort once the test sections are approved. The Engineer will verify the density of the bottom 6-inch [150 mm] during thick lift operations with one VT per every 16 LOTs. The Contractor may elect to place material in 6-inch [150 mm] compacted thickness at any time. The Engineer may terminate the use of thick lift construction and instruct the Contractor to revert to the 6-inch [150 mm] maximum lift thickness if the Contractor fails to achieve satisfactory results or meet applicable specifications including the minimum impulse stiffness value determined from FWD tests.

200-6.2 Moisture Content:

Moisture content of the base material shall be 1 to 3% dry of the optimum moisture content as determined by AASHTO FM 1-T 180, Method D. During the phase of test

sections, microwave oven (ASTM D4643) shall be used to measure the initial moisture content. Moisture contents will be obtained from five random locations within both test sections. At each of these locations, two moisture contents will be obtained at depths of 0 to 6-inch and from 6 to 12-inch. After the moisture content results have been obtained, if all of the results are 1 to 3% dry of the optimum moisture content, compaction of the test sections will begin within 24 hours of sampling.

200-7.2.1 Density: Within the entire limits of the width and depth of 12-inch and 6-inch thick base, obtain a minimum density in any LOT of 98% of maximum density as determined by AASHTO FM 1-T 180, Method D. The difference between densities measured in 12-inch and 6-inch tests shall not vary by more than 2 pcf.

The Engineer shall perform FWD testing, as needed, with frequency not exceeding three tests per eight LOTS.

CHAPTER 1
INTRODUCTION

1.1. General

Mechanical compaction of earthen materials has been used for thousands of years. In the US, static/dynamic smooth, pad, or sheep-foot rollers is common in construction of roadway embankments, bases, dams, and so on. The level of effort required in field compaction is typically controlled through comparison between dry densities achieved in the field and dry density resulting from standard laboratory compaction test (e.g., Modified Proctor tests). In the latter, multiple layers of soil are compacted in a standard mold using regulated and standardized compaction effort at different moisture contents to determine the maximum dry density for a specific compactive effort and the corresponding "optimum" moisture content for compaction. The higher the dry density of given material, the higher the expected strength and stiffness of that material.

In the field, contractors have several means and methods that can be employed to meet or exceed a specified minimum dry density for a given material, which include:

1. Compaction equipment selection (e.g., vibratory, static, smooth, pad, etc.)
2. Number of passes
3. Lift thickness
4. Moisture content
5. Stiffness of subgrade soil and base course materials

In Florida, most if not all limerock-base courses (FDOT Specification 200) have a maximum particle size of 3 inches and minimum percentage of fines (i.e., passing 200 sieve) of 35%. Current FDOT practice (Specification 200) allows maximum lift thickness of 6-inch. Specification allows up to maximum of 8-inch thick base lift, if through field test, the contractor can demonstrate that the compaction equipment can achieve density for the full depth of 8-inch and if approved by the engineer. Specification does not any controls on moisture. Generally, moisture contents vary widely based on location (5% - south Florida to 14% - central Florida and north) of mine material, humidity, seasonal rainfall and so on. Most, if not all limerock base courses are compacted with either single or dual steel rollers with vibratory dynamic forces less than 50,000 lbf.

Strong interest has developed in the feasibility of compacting thicker lifts, e.g., a single 12-inch lift for roadway base courses for several reasons. 1) Typical limerock base design thickness exceeds the currently specified lift thickness, thus requiring two lifts of construction. 2) Industry in producing more compaction equipment capable of delivering higher static and dynamic forces. Thicker lift base compaction, if feasible, could benefit both the contractor and the State of Florida in terms of reduced construction cost and time. Note for two conventional 6-inch lifts, the contractor must transport, spread, grade and compact the material twice, and quality control (density, moisture, etc.) must be undertaken twice vs. once with a 12-inch lift.

1.2. Objective

The focus of this research was the placement and compaction of a single 12-inch limerock lift instead of two 6-inch lifts over competent subgrade using compaction equipment readily available to contractors, as well as materials with no special gradation.

Successful placement was to be judged based on similarities of stiffness and strength between the thick lift (12-inch) and two 6-inch lifts constructed using the same material, conditions and subgrade conditions.

To evaluate the appropriate compaction equipment, number of passes, moisture content, and so on, test sections were constructed rigorously monitored, using stress cells, LVDT strain sensor, and accelerometers, tested for compliance with density specifications, and tested for in-place strength and stiffness performance. The LVDTs were used to validate densities measured with nuclear density probe (NDP), and the stress cells and accelerometers were used to measure stiffness and energies within the compacted fill.

Since thick lift limerock compaction has had minimal application within Florida, it was decided to select a site, materials and equipment which had a high potential for success. The following were selected: 1) vibratory pad foot roller or heavy smooth wheel vibratory roller; 2) well graded limerock with limited fines at moisture content dry of optimum (higher stiffness & strength) and 3) stiff/strong subgrade (LBR > 100).

1.3. Scope

The site selected for thick lift compaction study by the FDOT was SR 826 in Miami Florida, District 4. Located near Miami International Airport, SR 826 has Oolitic limestone near the surface (i.e., a strong subgrade, LBR>100) with ongoing placement of two conventional 6-inch limerock lifts which were well graded, low fine contents and moisture content varying from 5 to 9% from the source, i.e. dry of optimum.

After discussion with FDOT, Ardaman & Associates and UF personnel, it was decided to compact three one hundred foot test sections. The first section was

constructed using conventional means, i.e. two 6-inch lifts, compacted with a typical smooth wheel vibratory compactor. The second test section was constructed in a single 12-inch lift using a vibratory pad-foot roller (55,000 lbf). The third test section was also constructed in a single 12-inch lift, but was compacted using a heavier smooth wheel vibratory compactor equipped with "intelligent" compaction control devices. The latter roller has the capability of measuring the soil stiffness, and varying the applied vertical dynamic force depending on the preset target stiffness (modulus).

All three sections were to be instrumented to measure vertical stresses, accelerations, and strains at different depths for each pass of the roller. Nuclear density probe (NDP) and moisture content measurements using lab oven dried were taken prior to, during and upon completion of test section construction. To measure strength and stiffness, dynamic cone penetration, falling weight deflectometer, and soil stiffness gauge test were to be performed at ten locations along each section. In addition, multiple bag samples were collected both pre and post compaction from each section, and sieved to identify particle breakage due to compaction.

The following tasks were completed by FDOT, Ardaman & Associates and University of Florida to complete the scope of services.

1.3.1. Task 1

FDOT District CEI performed laboratory Modified Proctor compaction tests on representative samples of the limerock material to identify optimum moisture contents and maximum dry densities. The FDOT State Materials Office personnel performed the Falling Weight Deflection (FWD) Testing, Automatic Dynamic Cone Penetrometer Testing (ADCPT), Soil Stiffness Gage (SSG) Testing, bag sampling, and laboratory sieve analyses of pre- and post-compacted limerock samples from the three test sections.

1.3.2. Task 2

Ardaman and Associates placed the instrumentation at multiple depths at in each test section, recorded the data for each pass of the compactor, and performed nuclear density probe (NDP) for measurements of density and moisture for each test section.

1.3.3. Task 3

University of Florida reduced and analyzed all of measured data (stresses, strains, accelerations, FWD, ADCP, SSG, etc.) for each section, and evaluated the results (stiffness, moduli, energies, etc.) from section to section (i.e. 6-inch lift vs. 12-inch).

This report summarized the analysis and comparisons, and provides recommendations for implementation and further study. Based on the report, thick lift specifications are developed to be used on select projects.

CHAPTER 2
COMPACTION BACKGROUND

This chapter reviews field vibratory compaction equipment, both conventional and intelligent (feedback loop), as well as the influence of moisture content, and compaction energy, on stiffness and strength of compacted backfill.

2.1. Field Vibratory Compaction

Typical vibratory compaction equipment includes hand held plates (i.e. tampers), as well as single and multiple wheels drum rollers. For this project vibrating smooth and pad- foot rollers were investigated.

The basic concept of vibratory roller is the use of unbalanced weights to develop sinusoidal forces. In addition all vibratory rollers, i.e., towed, self-propelled, and/or tandem have the static weight (motor, frame, etc.) separated from the vibratory mass through shock absorbers. As identified by Koulbert (2004), the total force imparted to the ground is given in Eq. 2.1. The first term is inertia (dynamic) force due to the static weight of the drum. The second term is the varying dynamic force due to the rotating masses within the drum, and the third term is the static weight of both the drum and the rotating masses. Note the second term is a function of the frequency, f, of the rotating masses.

$$F_B = -m_d \ddot{x}_d + m_u r_u \Omega^2 \cos(\Omega t) + (m_f + m_d) g \quad (2.1)$$

Where,
m_d = mass of the drum (kg)
x_d = vertical displacement of drum (m)

$\ddot{x}_d$ = acceleration of drum (m/s2)
m_f = mass of the frame (kg)
m_u = unbalanced mass (kg)
r_u = radial distance at which mu is attached (m)
$m_u r_u$ = static moment of the rotating shaft (kg.m)
$\Omega = 2\pi f$
t = time elapsed (sec)
g = acceleration due to gravity (m/sec2)
f = frequency of the rotating shaft (Hz)

Generally, the second term is much less than the other terms (1st and 3rd) contribution. For instance, Forssblad (1965) studied the effect of the vibratory masses on a vibratory roller's compaction. He found by adding 24% of the total roller weight to the frame, a considerable increase in a soil's compacted density occurred; however, a similar change in the drum's weight did not result in an analogous increases in soil density.

Parsons et al (1962) focused on the amplitude of the vibratory motion, i.e. $\ddot{x}_d$ in Eq. 2.1. Besides increasing the dynamic force, Eq. 2.1, Parsons et al found little effect in typical 6 to 9 inch thick lifts which couldn't be accomplished with more passes of the roller.

Yoo (1978) improved field instrumentation through the use of inductance coil strain gages for field compaction studies. Their experiments also varied compactor weight and layer thickness for gravel-sand mixtures compacted dry (4%) of optimum moisture content. Both 12-inch and 36-inch thick fills were compacted under various energies and moisture content. They concluded that the maximum compact layer thickness should be limited to 12-inch (vs. 36-inch) from stiffness and densities measurements with depth. Similarly, WES (USACE-WES, 1976) carried out

compaction on lean clay (PI=13) with various water contents using a sheep-foot roller. Based on that study, they recommended a limitation of lift thickness of 7-inch.

2.2. Strength, Moisture Content and Compactive Effort

Even though field compaction is generally controlled by dry density and moisture contents, the stiffness and strength of the placed backfill are the properties of interest. For instance, deflection, rutting, and bearing failure of a base course control its design (from AASHTO 2002). Since stiffness and strength measurements are difficult to perform on a routine basis in field, they have been equated to a materials density and moisture content.

Seed and Chan (1959) were one of the first to study the relationship between material strength, compaction effort and moisture for fine-grained soils. Their experiments were performed with Harvard Compaction setup (62.4 cm^3 specimen, 0.5-inch compacting rod with variable spring stiffness). Shown in Figure 2.1 is the change in dry density (bottom), small strain stiffness (middle) and large strain stiffness (top figure) vs. moisture content for different compaction energies. Evident from the figure, stiffness, and density increase with compaction energy for a moisture content dry of optimum. Note the significant reduction in stiffness for a given compactive effort as the moisture content passes wet of optimum.

Turnbull and Foster (1956) studied the influence of moisture and compactive effort on granular soils in Fig. 2.2. Instead of performing triaxial compression, they conducted California Bearing Ratio (CBR). Similar results as shown in Fig. 2.1 are seen in Fig. 2.2.

Ping et al (1996) has suggested a correlation of 1.25 between the Florida Limerock Bearing Ratio Test (LBR) and CBR results.

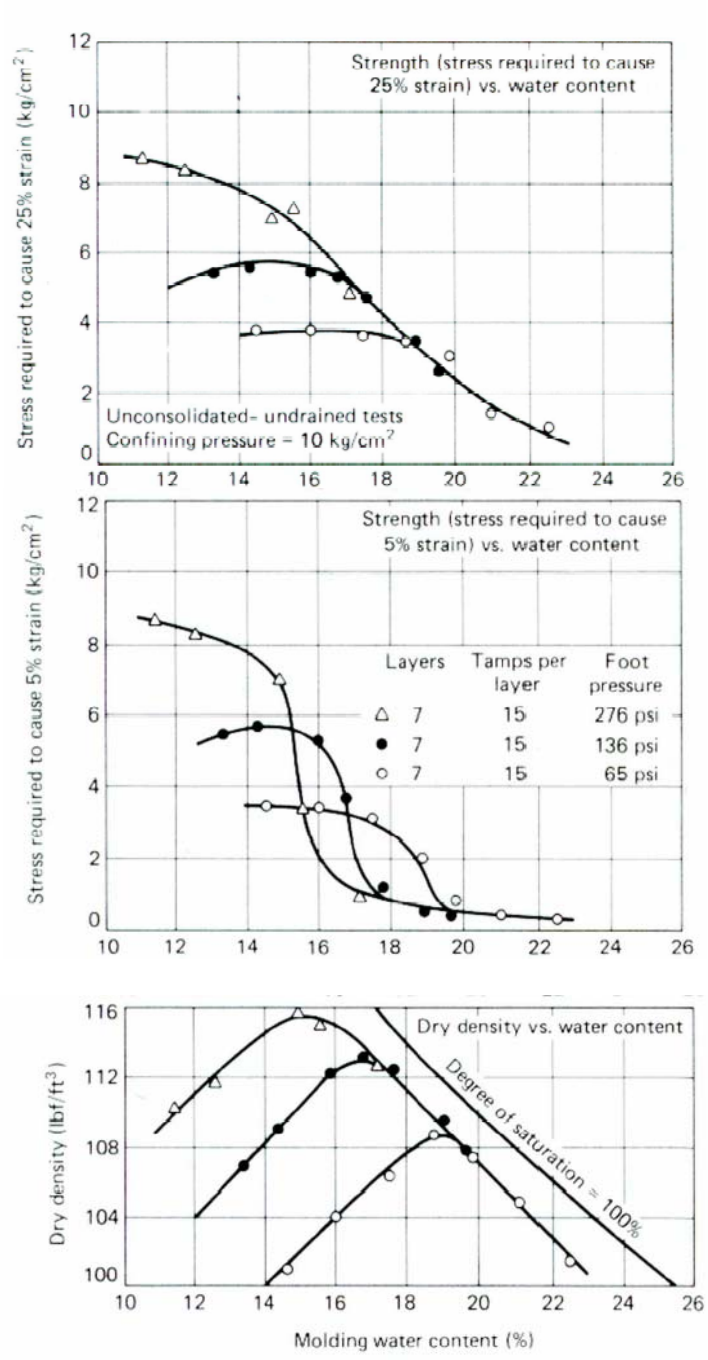

Figure 2.1 Relationships between Density, Compaction Energy and Strength vs. Moisture Content (Seed & Chan, 1959)

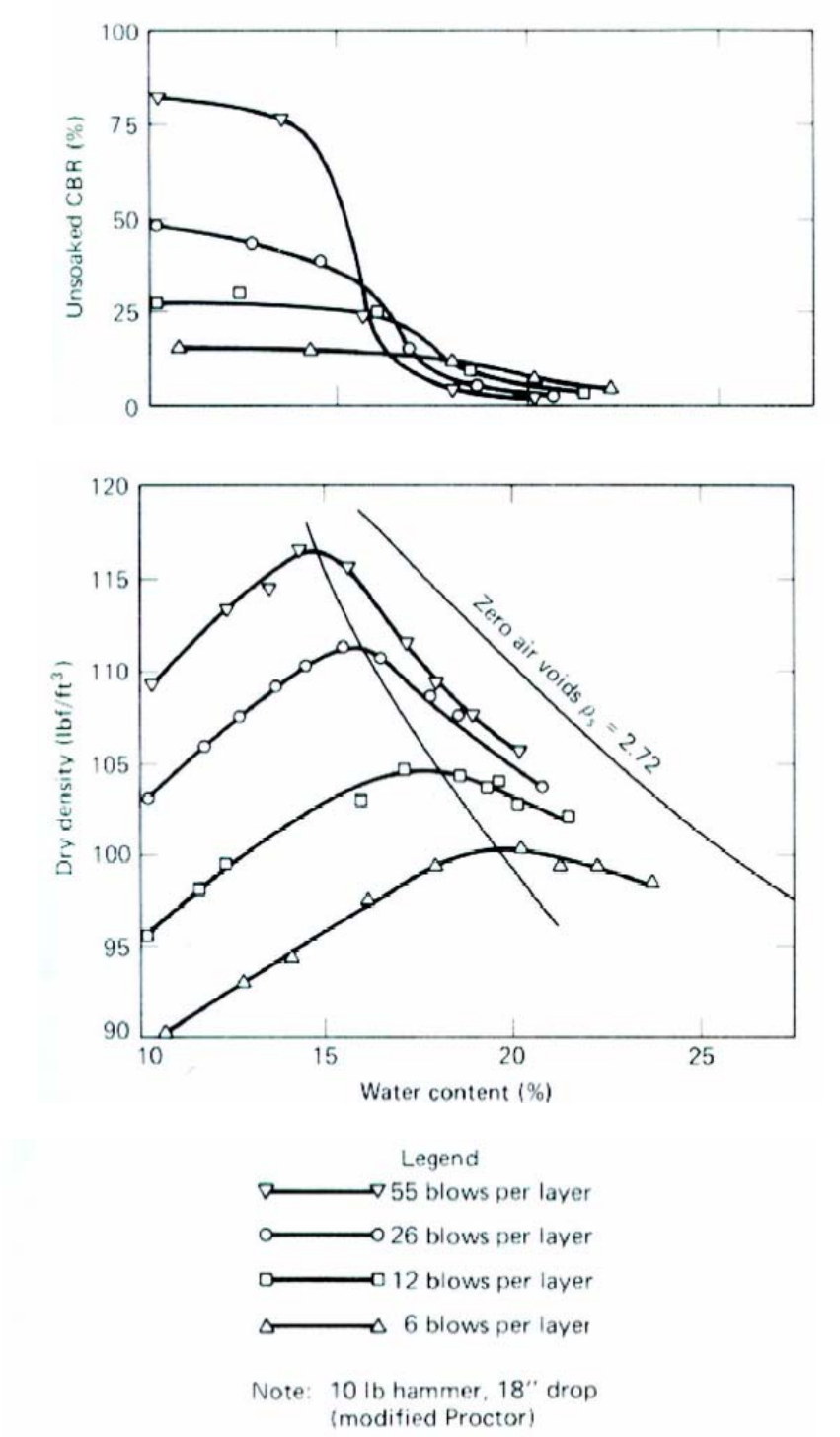

Figure 2.2 Relationships between Strength Parameter (CBR) vs. Moisture Content and Density vs. Various Compaction Energies (Turnbull & Foster, 1956)

The FDOT State Materials Office (SMO) compacted the Florida Limerock to meet LBR requirements. As part of this research, SMO compacted additional specimens to a constant dry density, 123 pcf, at different moisture contents with subsequent LBR testing. Shown in Fig. 2.3 is the variation of LBR value with moisture content for both soaked and un-soaked samples. Evident is the higher stiffness/strength of the un-soaked samples dry of optimum (10.5% - standard proctor). The latter agrees with Seed & Chan, and Turnbull & Foster that compaction dry of optimum for a specific dry density would ensure a higher strength and stiffness.

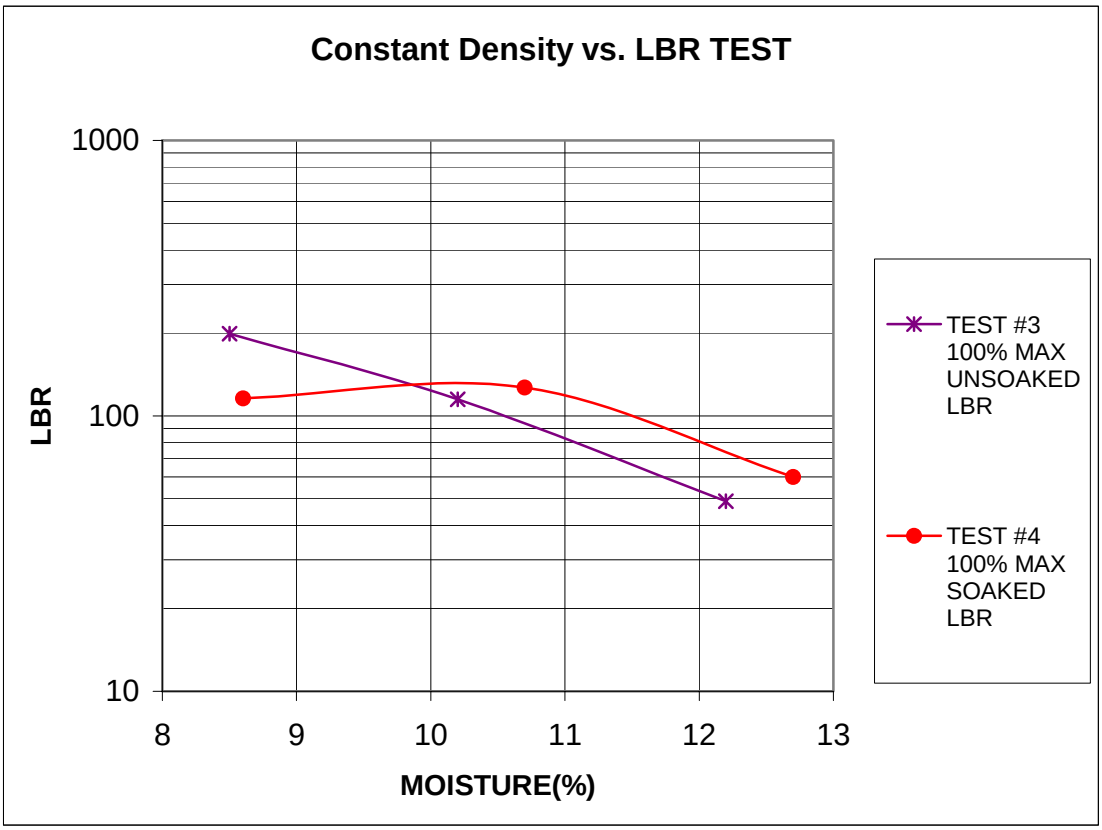

Figure 2.3 LBR vs. Moisture Content – Compacted to Dry Density of 123pcf

2.3. Intelligent Compaction

To perform thick lift placement, one of the compactor manufacturers, Bomag, recommended the use of their Intelligent Compaction Control (ICC) devices. Conventional vibratory steel wheel rollers, Fig 2.4 employ rotating eccentric masses to develop vertical dynamic forces, Eq. 2.1. Moreover, circular motions of the masses are aligned such that the dynamic forces are always vertical. In addition, conventional vibratory rollers operate at either high frequency and low amplitude or low frequency and high amplitude to prevent damage to the equipment.

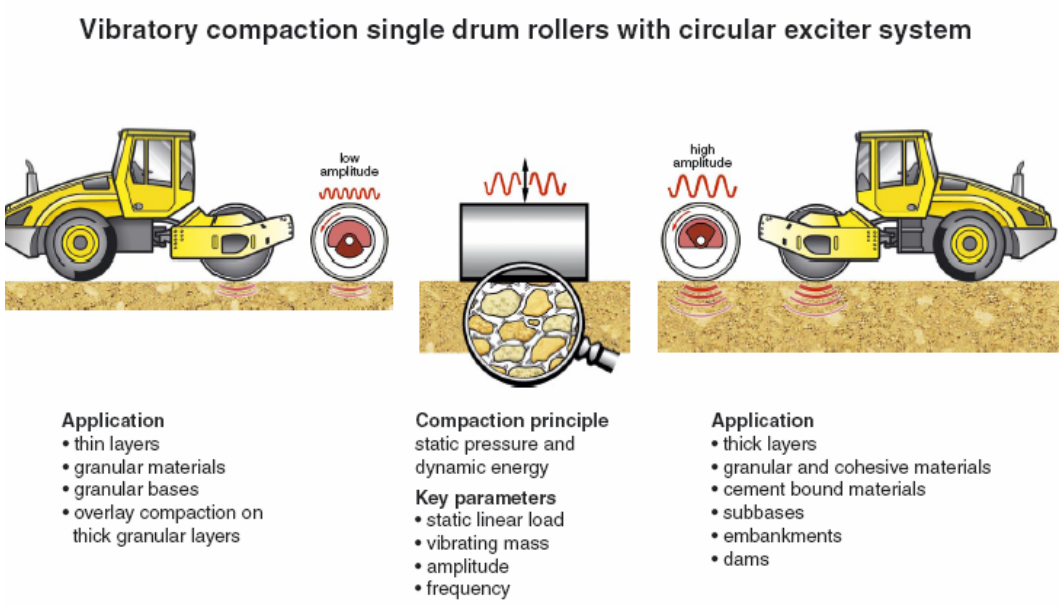

Figure 2.4 Conventional Vibratory Roller (Source:http://www.bomag.com/media/WM9703_0403_rdr.pdf, Last accessed Mar.18.2005).

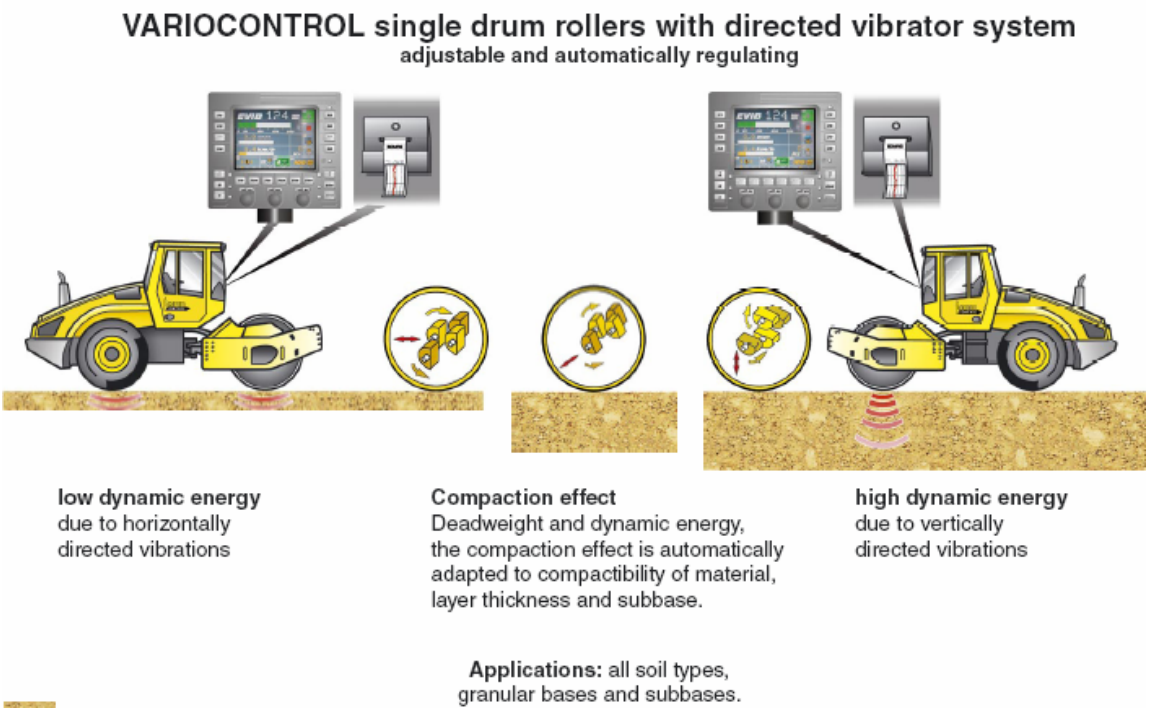

Figure 2.5 Vario-control Vibratory Rollers
(Source:http://www.bomag.com/media/WM9703_0403_rdr.pdf, Last accessed Mar.18.2005).

Recently, a number of manufacturers have implemented more control or feedback between the instrumentation (accelerometer) on the compactor's drum, and the force delivered to the ground. One such unit is Bomag's vario-control Roller, shown in Fig. 2.5. Assuming a one-degree of freedom model for the compacted backfill, Fig. 2.6, the static stiffness, k_B, of the base is computed from:

$$F_B = k_B\, x_d + d_B\, \dot{x}_d \qquad (2.2)$$

Where,
k_B = stiffness of soil (F/L)
x_d = vertical displacement of soil
d_B = damping coefficient (value of 0.2 assumed)
$\dot{x}_d$ = velocity of soil mass (measured at drum)

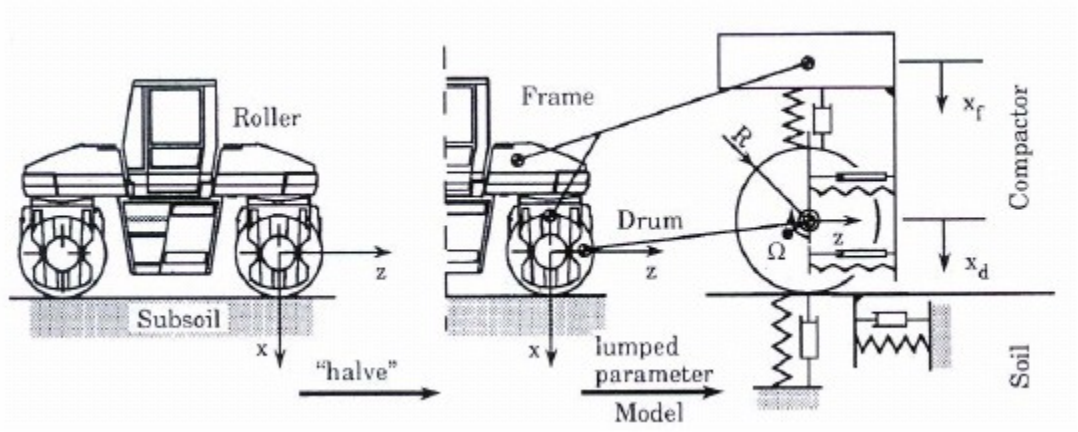

Figure 2.6 One Dimensional Model of Compactor and Subsoil

Next using Lundberg's (1939) work, the Young's Modulus, E_{vib} of the compacted soil is found from the soil stiffness, k_b, Eq. 2.3:

$$k_B = \frac{E_{vib} L \pi}{2\left(1-\upsilon^2\right)\left[2.14+\frac{1}{2}\ln\left(\frac{\pi L^3 E_{vib}}{\left(1-\upsilon^2\right)16\left(m_f+m_d\right)Rg}\right)\right]} \tag{2.3}$$

Where,
L = length of roller
R = radius of roller
ν= poisson's ratio of the soil

The vario-control unit in the manual mode will automatically display the E_{vib} measurements of the compacted base material, which may be used as quality assessment. In the automatic mode, the user identifies a target E_{vib} value as potential specification; the unit then alters the orientation of rotating masses, automatically directing more or less dynamic force into the ground. One of Bomag's vario-control units, B-225D-3 was tested at the SR-826 site.

CHAPTER 3
TEST SITE AND INSTRUMENTATION

3.1. Materials, Site Layout, and Equipment

A typical grain size distribution curve for the compacted Florida limerock at SR-826 is shown in Figure 3.1. AASHTO classification of the material is A-1-a, or GW within the Unified Soil Classification System. Grain Size distributions for all of test sections are given in Appendix A as reported by the State Materials Office. Laboratory Modified Proctor analysis revealed a maximum dry density of 131 pcf and an optimum moisture content of 9%. FDOT Standards Specification 200 required a final placed dry density of 128.4 pcf (i.e. 98% of maximum dry density) for successful base construction.

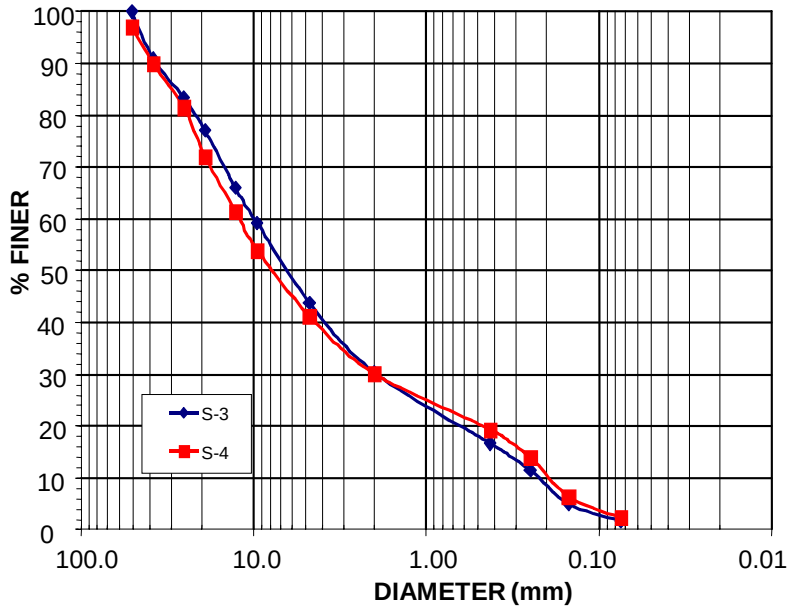

Figure 3.1 Limerock Grain Size Distribution

Presented in Figure 3.2 is the plan view for all three-test sections at SR-826. All sections were placed over preexisting limerock with LBR values above 100.

Section 1, located from stations 227 to 228, at the northeastern quadrant of the site had two conventional 6-inch lifts placed over existing subgrade. The section was compacted with a Bomag 211-D3, a smooth wheel vibratory compactor with a maximum vertical dynamic force of 53,000 lbf, Fig. 3.3

Sections 2 and 3 on the eastern portion of the site, involved placing loose limerock with dump trunks, and spreading with a dozer to a depth of approximately 13-inch (i.e. compacted 12-inch) prior to compaction. Section 2 was compacted with a Bomag 213-PD pad foot roller with maximum dynamic force of 62,000 lbf and a pad height of approximately 4-inch. This device was selected to ensure higher stresses, energies, etc. deeper within the limerock, i.e. densification of the bottom 1/3 of the lift.

Section 3 was compacted with a new Bomag vario-control unit, 225 BV-3. The unit is the largest smooth wheel vibratory roller that Bomag manufactures, capable of developing 85,000 lbf of dynamic force. As identified in Chapter 2, the unit either measures the Modulus, E_{vib}, of the layer (manual mode) or will adjust the dynamic force imparted to the base to obtain a preset E_{vib} values with travel. The unit was run in both modes for this effort.

Shown in Figure 3.1 are the 10 locations of the of the Falling Weight Deflectometer (FWD), Soil Stiffness Gage (SSG), and Automatic Dynamic Cone Penetrometer Tests (ADCPT) which were preformed at the finish of compaction for each test section by the FDOT State Materials Office Personnel. Also shown in Figure 3.1 is the location of buried instrumentation, discussed in the next section.

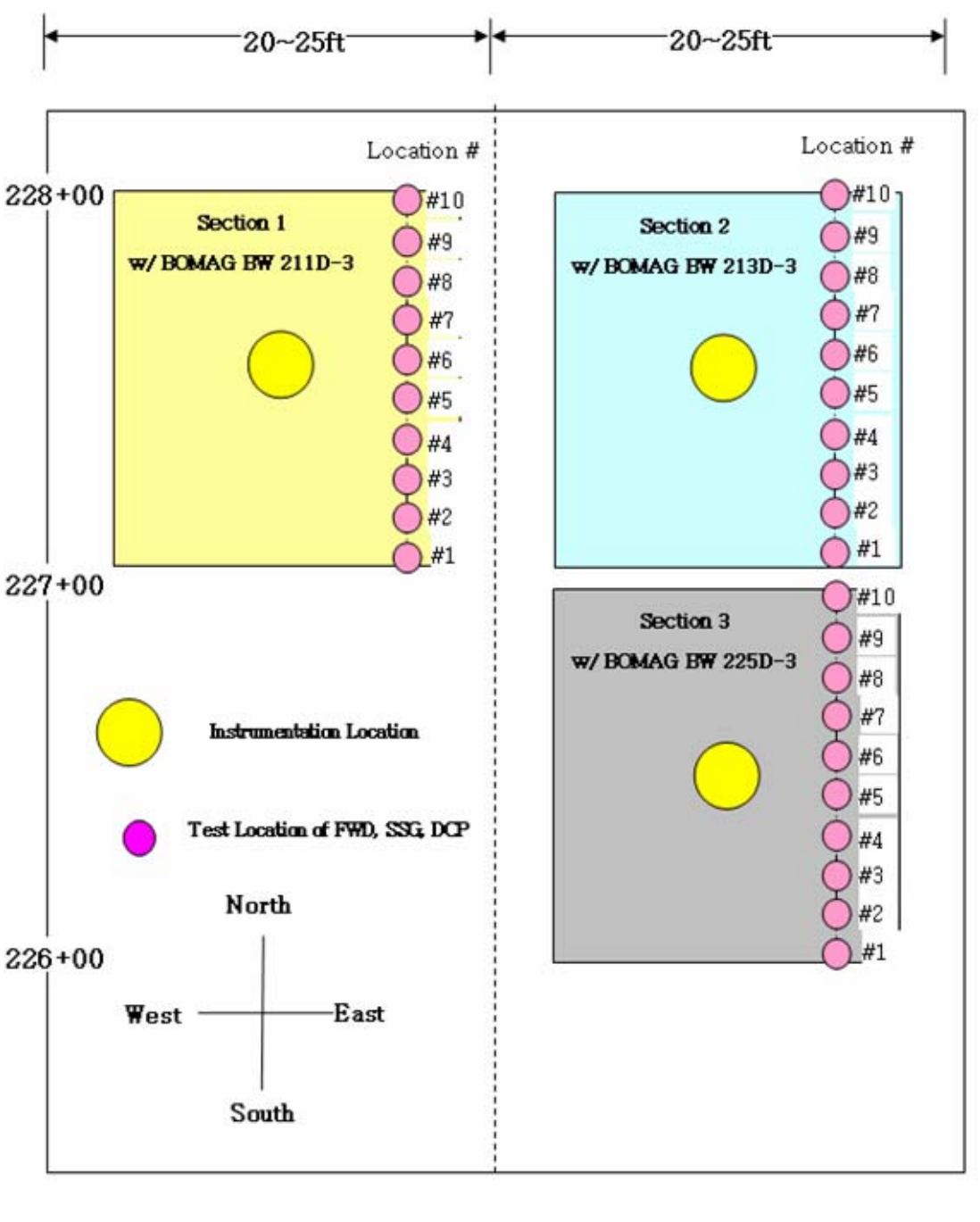

Figure 3.2 Plan Views of Test Strips at SR-826

Figure 3.3 Test Section Compactors

3.2. Embedded Instrumentation

To evaluate the compaction process with depth, instrumentation was placed at 1/3 points within the base layer. Since one of the compaction units was a pad foot roller with the potential of damaging the instrumentation, it was decided to locate all the equipment at the bottom of each 1/3 locations.

Of interest are the stresses, energies, stiffness, and strains with depth as compared to the observed laboratory response (i.e. Proctor, LBR, etc.). For instance, it is expected that dry densities found in the laboratory would be achievable in the field if similar energies (compaction) were applied. In addition, comparisons of density at the bottom of the thick lift computed from nuclear density probe (NDP) vs. measured strains are of

interest (i.e., verification). To accomplish the latter the following instrumentation was installed:

3.2.1. Accelerometers

Of interest are displacements as a function of dynamic vibrations due to the roller. Initial attempts used velocity sensors like those employed in seismic geophones. Unfortunately, the latter generally do not provide the necessary response times. Subsequently, it was decided to employ accelerometers and integrate the response to obtain displacements. To provide accurate, repeatable information, DC accelerometers of the capacitive resistance type were employed, i.e. capable of 0Hz or 1g response. The devices were attached or placed in the vicinity of the stress cells.

3.2.2. Strain Sensor LVDTs

Initially, it was planned to read the LVDTs only after a pass of compactor. However, from the analog nature of the device and with a sufficiently sampling frequency with the data acquisition system, the relative displacements or strains may be obtained during the compaction process. To maintain the location of the devices, as well as their orientation, the LVDTs had 3-inch plastic plates attached to the top of the LVDT housing as well end of sensing rod.

3.2.3. Stress Cells

To measure the vertical stress as a function of compactor motion, 0.375 by 12-inch diameter stress cells were employed. The sensing face was filled with incompressible fluid and the pore transducer was attached 18-inch from the sensor with steel lines. Ardaman and Associates calibrated the devices using a fabricated laboratory pressure chamber. Presented in Figures 3.4 –3.6 are the cross-sectional views of all the

embedded instrumentation at the three test sections at SR-826. Note all the instrumentation was placed at similar depths for comparison purposes by Ardaman and Associates.

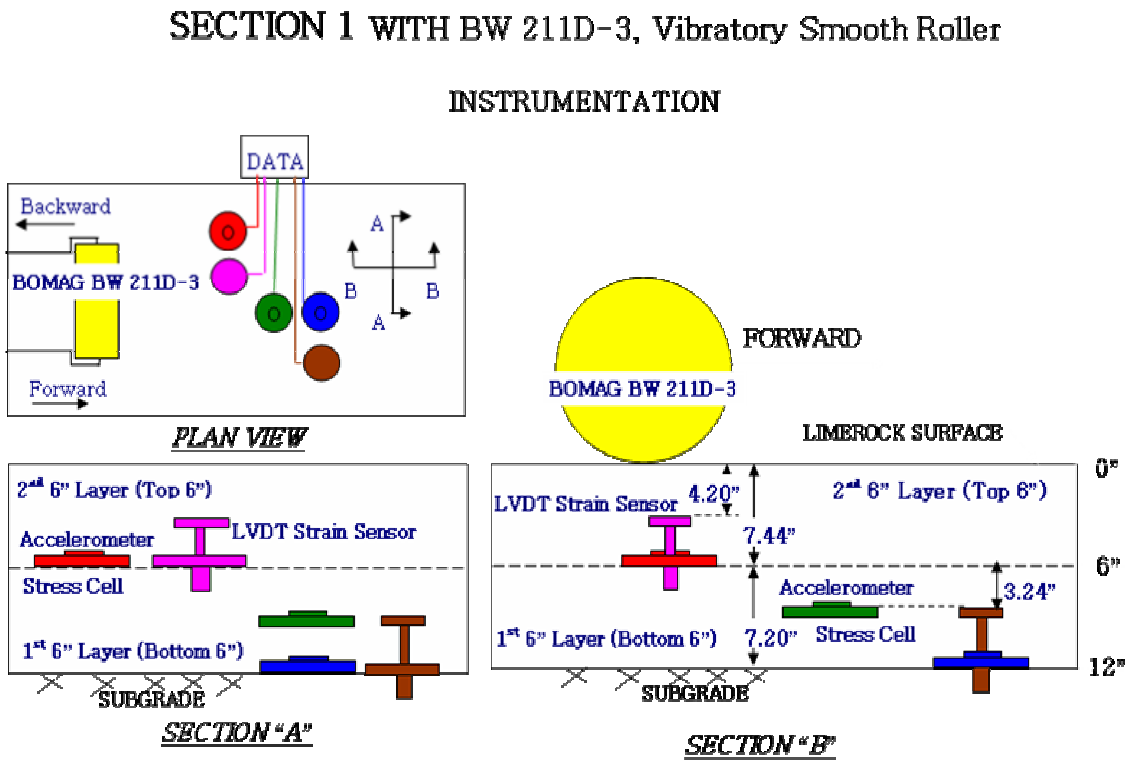

Figure 3.4 Section 1 Instrumentation – Two 6-inch Lifts

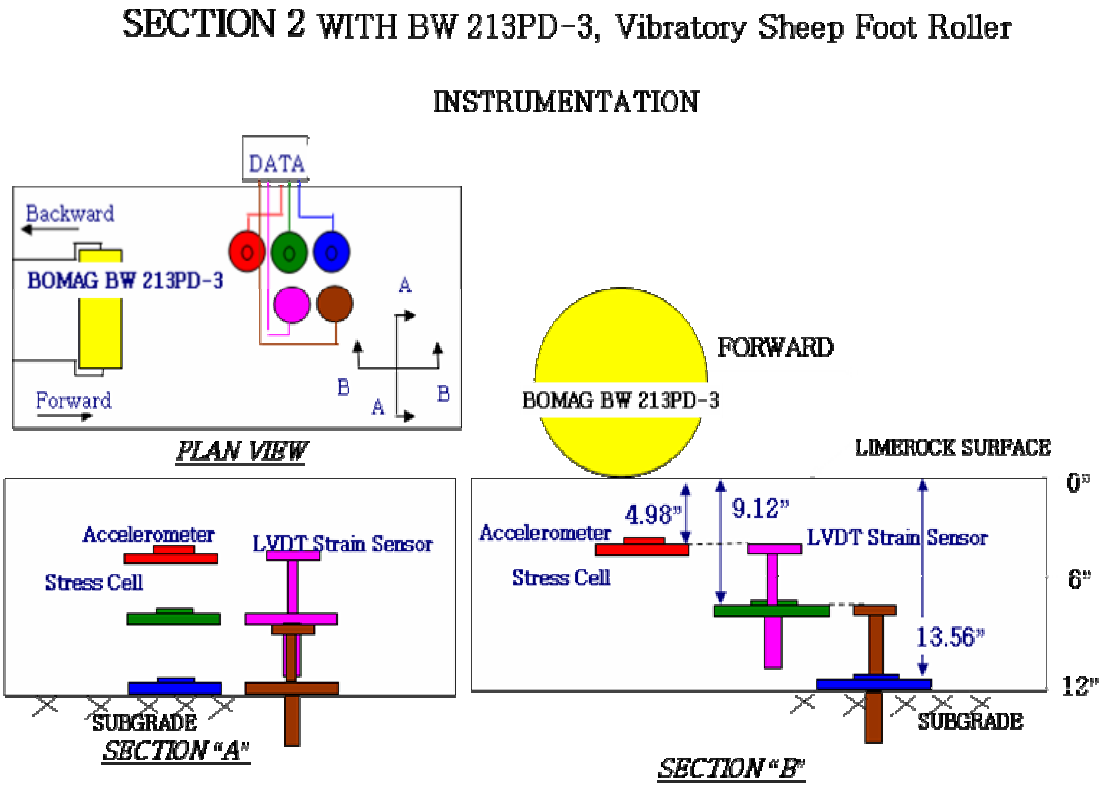

Figure 3.5 Section 2 Instrumentation – Single 12-inch Thick Lift, Pad-Foot Roller

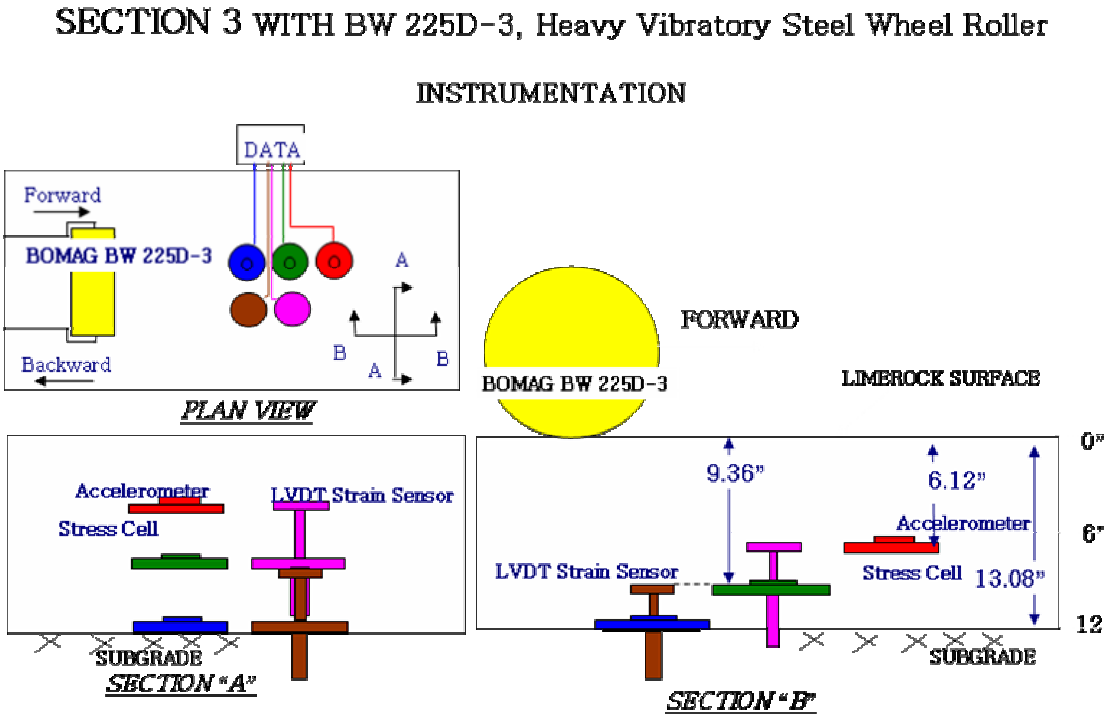

Figure 3.6 Section 3 Instrumentation – Single 12-inch Thick Lift, Vario-Control Roller

CHAPTER 4
RESULTS AND DISCUSSION

4.1. Stress Measurements

Typical recorded vertical stresses as a function of time due to a passing vibratory roller is shown in Fig. 4.1. Each peak represents a rotation of the vibratory mass, which is happening at approximately 30 Hz (i.e. 6 peaks or rotations/0.2sec). Evident is the buildup of stresses as the roller approaches the instrumentation, with the maximum occurring with roller over the gage. Of interest are the stress changes vs. particle motions, e.g. stiffness and energies, as well the peak stresses at various depths within the base layer. Presented in this section are the peak (maximum) stresses as function of depth vs. the number of passes.

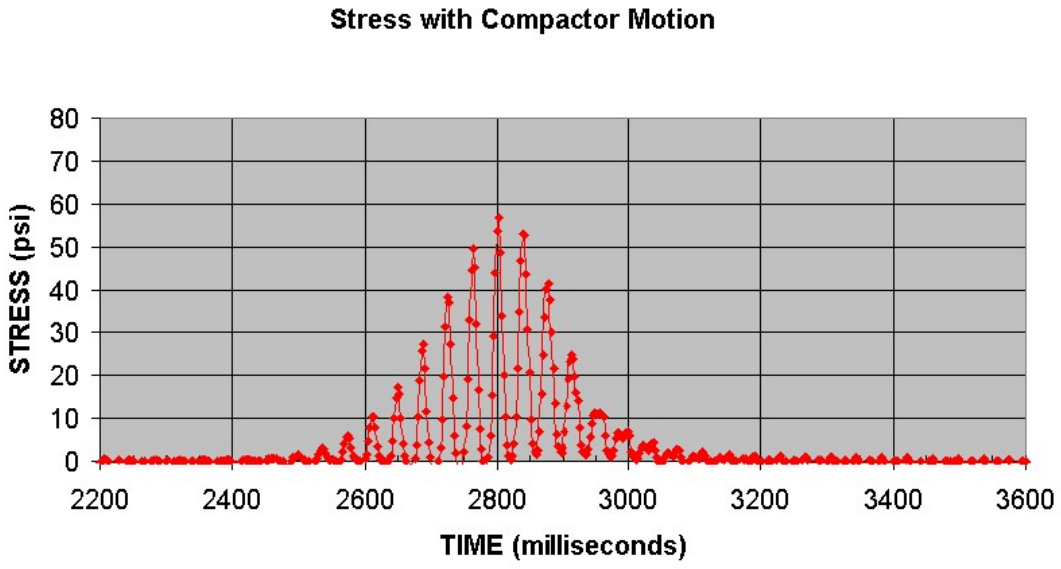

Figure 4.1 Measured Stress as Function of Time Due to a Passing Vibratory Roller

Shown in Figure 4.2 are the peak stresses for section 1 vs. pass of the Bomag 211D. The left side of the figure depicts the stresses at the middle and bottom (Fig. 3.4) of the first 6-inch lift for three passes. The right side of the figure show the stresses at the middle and bottom of the first lift, as well as stresses at the bottom of the second 6-inch lift for an additional 4 passes of the 211D compactor. Evident from the figure is the large difference in stresses between the middle and bottom (i.e. 3-inch vs. 6-inch) of the 1st layer. However, with the placement of the second lift, there is little difference in stresses from 6 to 12-inch as seen from the right side of Fig. 4.2. The larger difference in stresses at top vs. bottom was attributed to Boussinesq's equation and the influence of the square of the depth below compactor on stress.

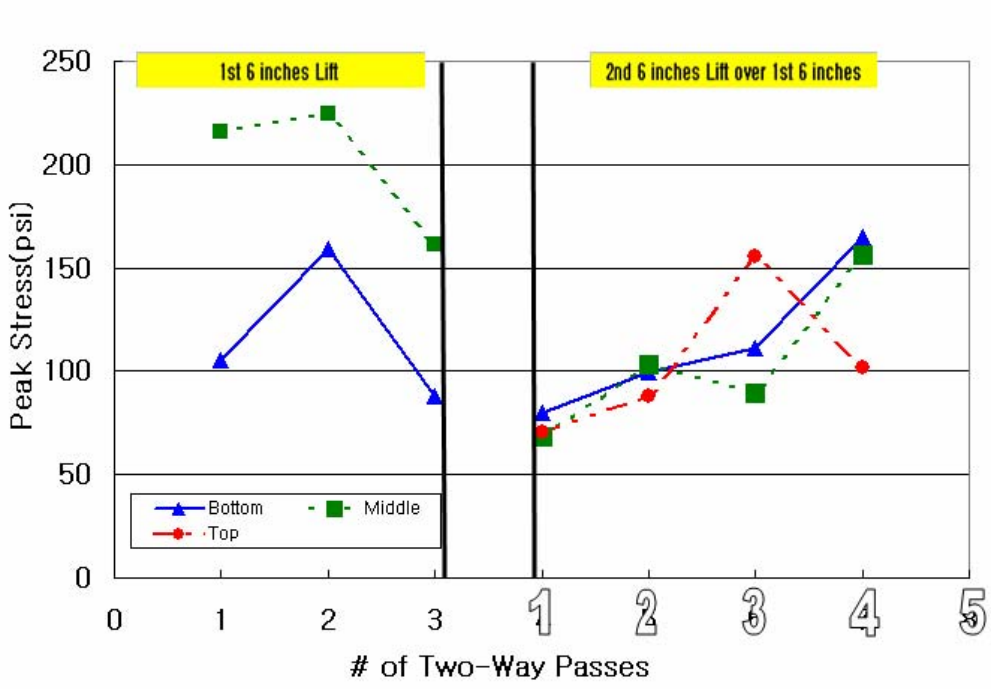

Figure 4.2 Stress vs. Number of Passes in Two 6-inch Lifts on Section 1

Shown in Figure 4.3 are the maximum stresses at depths of 4.98-inch, 9.12-inch, and 13.5-inch in the base for each pass of the BW 213D-3 pad-foot roller (passes 1-3, and

5-6), and BW211D-3 smooth wheel roller (pass 4, and 7-8) in section 2. Note, that a pass, i.e. from 6 to 7, has two points, i.e. 6.5 and 7, which represent the compactor traveling from the south to the north side of the site (i.e. 6.5), and subsequently back from the north to south side, i.e. 7, of section 2. Note passes, 4, 7, and 8 with the smooth wheel vibratory roller were performed to ensure a smooth surface required in nuclear density probe (NDP) backscatter moisture monitoring.

Apparent from Fig. 4.3, the stresses measured at all three instrumented depths were quite similar for the pad foot versus the smooth wheel roller. The latter is attributed to the larger contact area provided by the pads as well as their deeper penetration (i.e. 4-inch high pads) vs. the smooth wheel roller. Also, note the similarity in stress (150psi) reported in section 2 vs. section 1 for 1st set of gages for the smooth wheel roller.

Presented in Figure 4.4 are the maximum vertical stresses with depth (6.1-inch, 9.4-inch, and 13-inch) as a function of pass for the heaviest of the smooth wheel rollers, i.e. BOMAG BW 225D-3 (85,000 lbf). Apparent from a comparison of Figures 4.2 and 4.4, the stresses between sections 1 and 3, are approximately 1.6 times higher in section 3 versus section 1 due to increased dynamic force of the BW 225D-3 (85,000 lbf) vs. BW211D (53,000 lbf). Also note however, the stresses variations observed in section 2 for the smaller smooth wheel roller (i.e. passes 7, 8), Fig. 4.3, do not occur in section 3 for the heavier smooth wheel roller. The latter may be due to particle crushing and larger contact area under the compactor for the heavier roller (BW 225D-3). Of interest are the particle motions, which are occurring with the stress changes.

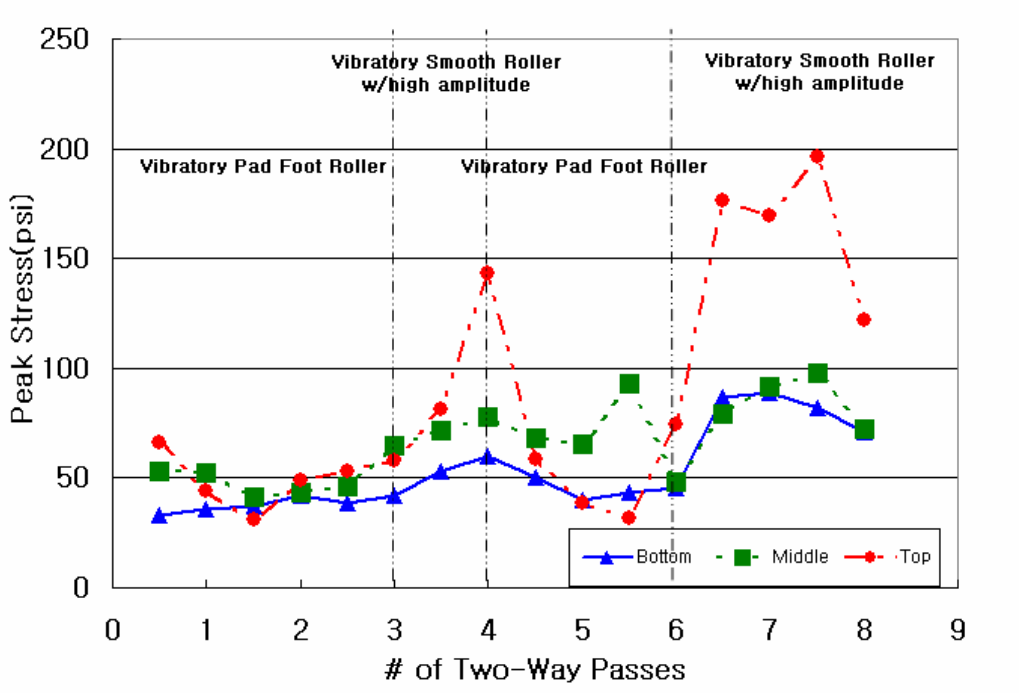

Figure 4.3 Stresses vs. Number of Passes in the Single 12-inch Lift of Section 2

4.2. Compactive Energy

To identify soil particle movement, and subsequent energy transmissions, accelerations were monitored with DC (0-100 Hz) piezo-capacitance instruments attached to the tops of the stress cells at the three depth locations (Figs. 3.4, 3.5, and 3.6). After integrating the accelerations twice, the particle displacements during a pass of a compactor were obtained. Appendix D presents the data reduction process, as well as an example of deformations as a function of time. Of interest is the relationship between stress and deformation as a function of compactor motion. Shown in Figure 4.5 is the typical stress vs. particle motion at the bottom of section 1 during the 4th pass of the Bomag 211D.

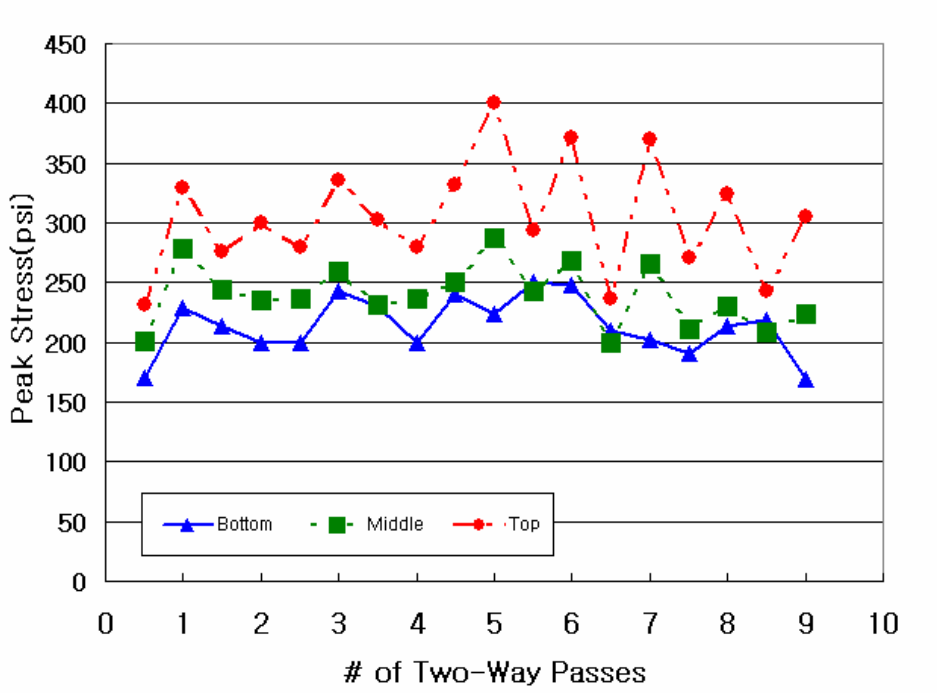

Figure 4.4 Stresses vs. Number of Passes in the Single 12-inch Lift of Section 3

Each loop (ellipse) represents one complete rotation of the eccentric mass within the roller (i.e. 30 Hz or 30cycles/sec). The multiple loops with varying peak stresses are a result of the roller either approaching or moving away from the instrumentation. Note the similarities of Figure 4.5 and Bomag's force vs. displacement measurement of the drum at the ground surface, Figure 4.6. As identified by Bomag, Figure 4.6, the compression is a result of the compactor pressing down on the base, and the expansion (i.e. unloading) is due to the drum unloading the base. In the unloading phase, the particle displacements are negative, i.e. in an upward direction. The energy transmitted to the base for each rotation of eccentric mass within the roller is the area within each loop, Fig. 4.6.

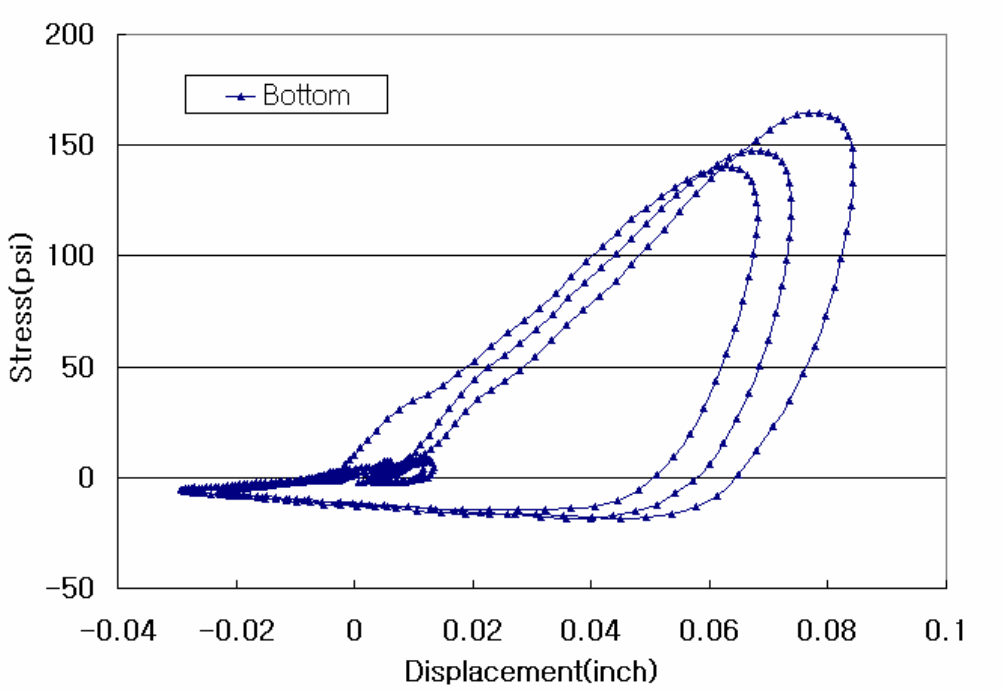

Figure 4.5 Stress vs. Particle Displacements at Bottom of Section 1 During 4th Pass

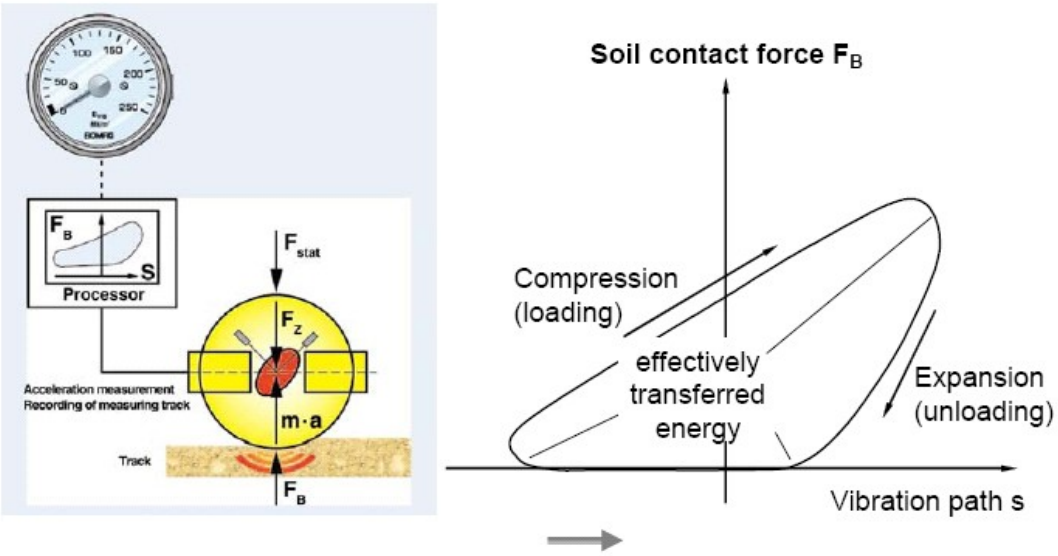

Figure 4.6 Forces on the drum and associated loading loop (Source from Kloubert's presentation at TRB 2004, BOMAG)

Presented in Figure 4.7 are the stresses vs. displacements at the top, middle and bottom of section 2 in the 5th pass of the Bomag 213PD pad-foot roller. Apparent is the

similarities of energies (i.e. areas) at the various depths within the 12" lift, with a slight drop at the bottom. Interestingly, the slopes (i.e. stiffness) of the middle and bottom depths of the lift are higher than the top. The latter may be attributed to the shape of the compactor's contact area, i.e. pad, vs. the smooth wheel.

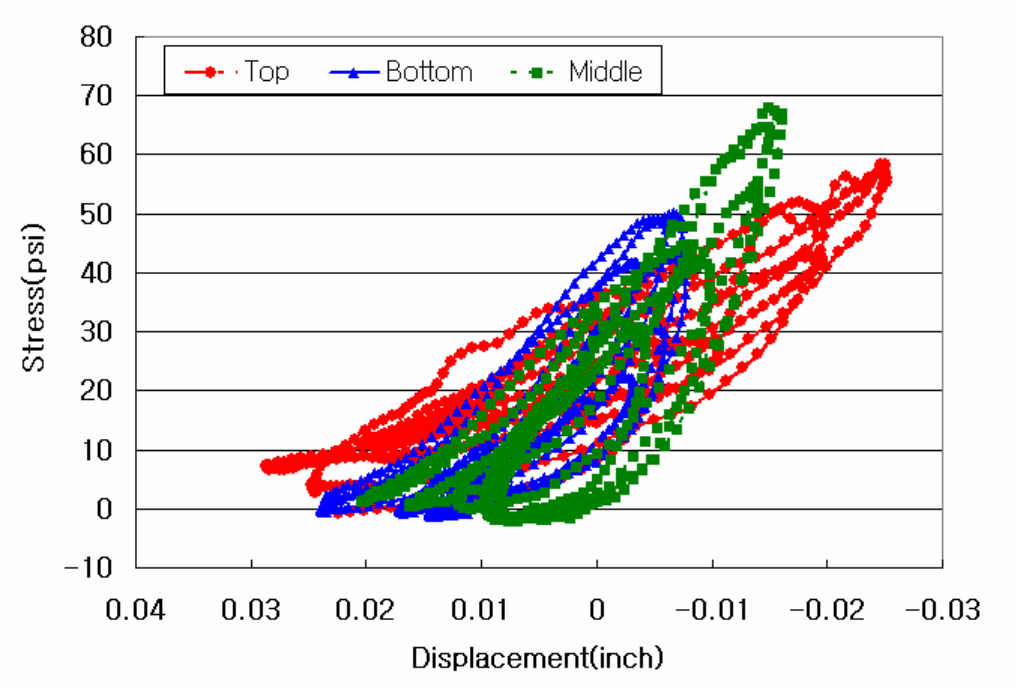

Figure 4.7 Stress vs. Displacement after 5th Pass on Section 2

Shown in Figure 4.8 are the stresses vs. displacements at the top, middle and bottom of section 3 in the 7th pass of the Bomag 225D-3 smooth wheel roller. Evident is the similarities of energies (i.e. areas) at the top and bottom of 12-inch lift, suggesting similar densities throughout the deposit. A comparison of energies (areas) between section 1 (Fig. 4.5) and 3 (Fig. 4.7), suggest higher densities changes or compaction is being performed with one pass of the Bomag 225 vs. 211. Also note that the stiffness (i.e. slopes) of any loop is higher for the Bomag 225 (Fig. 4.8), than the slopes from the

section 1 (Fig. 4.5) with the passing of a Bomag 211. The latter should be evident from Falling Weight Deflectometer (FWD) data discussed later.

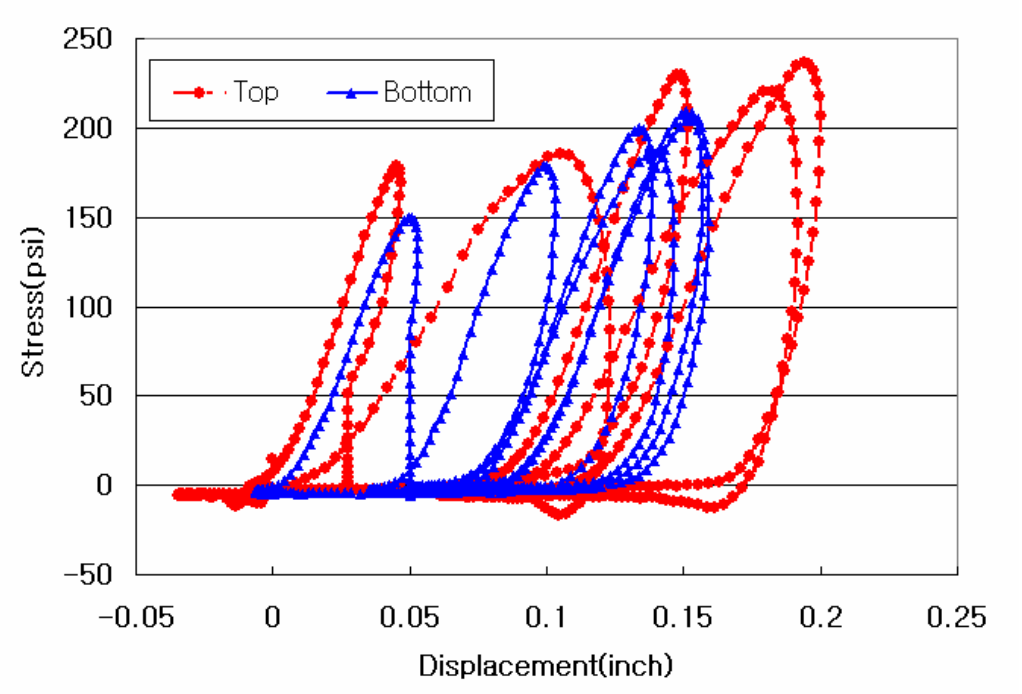

Figure 4.8 Stress vs. Displacement after 7th pass on section 3

4.3. Vertical Strains and Densities

Of interest were the strains, which may be equated to density as function of depth within the base course. Nuclear density probe (NDP) test were performed using probe at depths of 6-inch and 12-inch, Fig. 4.9. Due to the location of the source (various depths) and receiver (surface), the density at 0 to 6-inch (γ_1) is accurate, as well the average 0 to 12-inch (γ_t), however, the density from 6 to 12-inch (γ_2) is generally computed from the following simple averaging assumption:

$$\gamma_1 d_1 + \gamma_2 d_2 = \gamma_t (d_1 + d_2) \qquad (4.1)$$

or solving for γ_2,

$$\gamma_2 = \frac{\gamma_t (d_1 + d_2) - \gamma_1 (d_1)}{d_2}$$

(4.2)

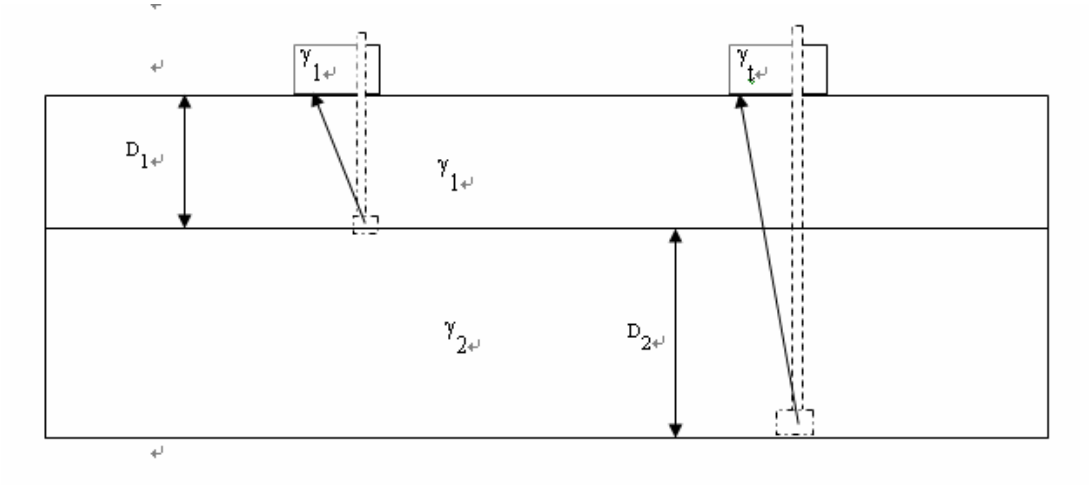

Figure 4.9 Density Calculations with Depth

Knowing the moisture content, ω, the average or individual dry densities (γd1 , γd2) may be found as:

$$\gamma_d = \frac{\gamma}{(1+\omega)} \qquad (4.3)$$

For nuclear density probe (NDP) shown in Fig. 4.9, the moisture content, ω, is computed near the surface (i.e. back scatter). For all calculations to follow, it is assumed that the moisture content with depth is constant (i.e. ω = ω1 = ω2).

Given the uncertainty of the density calculations, it was of interest to check their values with other methods, e.g. strain measurements from LVDT. Knowing the original

spacing between a pair of LVDT plates (i.e. Figs. 3.4 to 3.6), the strain as a function of compactor pass may be found as,

$$\varepsilon_v = \frac{\delta\left(change\,in\,spacing\right)}{L\left(original\,spacing\right)} \tag{4.4}$$

Next, assuming that the initial dry density (γd_initial) of the placed base material is uniform, the final dry density (γd_final) after a pass may be computed as,

$$\gamma_{d\_final} = \frac{\gamma_{d\_initial}}{1-\varepsilon_v} \tag{4.5}$$

Where εv is given by Eq. 4.4, and it is assumed that no horizontal strains develop as the compactor passes over.

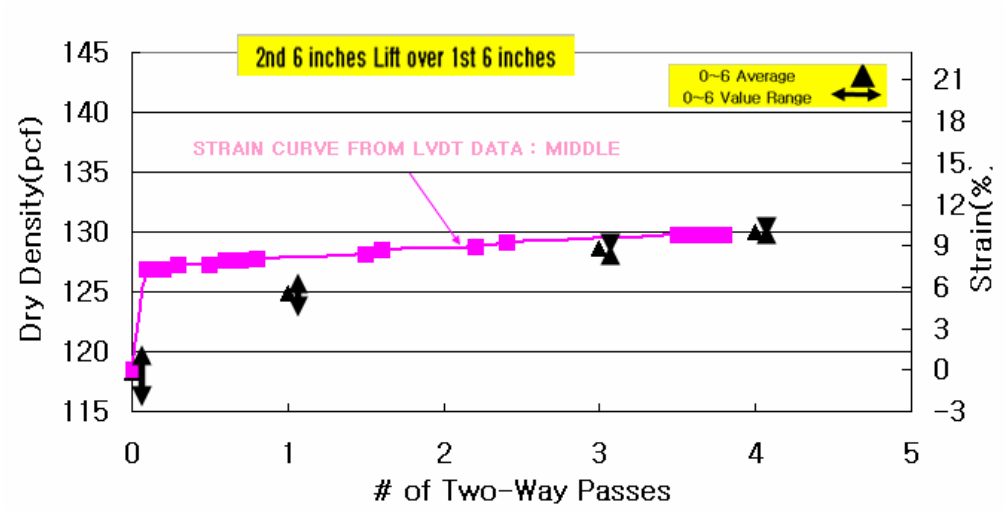

Figure 4.10 Strain from LVDT vs. Dry density from Nuclear Density Probe for Section 1

Shown in Figure 4.10 is a comparison of the strains vs. number of passes in the top 6-inch lift of section 1. Evident the strains increased by 6% in first pass and then to 9% by the 4th pass. Using the strains, initial dry density and Equation 4.5, the computed dry density vs. pass is shown on the left axis. The computed dry density from the nuclear

density probe (NDP) is given in Table 4.1, as well as depicted in Fig. 4.10. Note the moisture and densities were measured at 3 locations within the section, and LVDT occurred at one location. As expected, the measured density variability of the first pass, 3.5 pcf (126.6 to 123.1 pcf), is quite high and if added to the mean (124.8 pcf), covers the density measured by the LVDT (127 pcf), which is at one point.

Table 4.1 Measured Dry Densities from Nuclear Density Probe (NDP) within Section 1

Pass #	Depth	1	2	3	Average	Standard Deviation
0	0~6	120.5	115.2	118.9	118.2	2.7
1	0~6	123.1	126.6	124.8	124.8	1.8
3	0~6	128.8	128.4	N/A	128.6	0.3
4	0~6	129.6	130.2	130.1	129.9	0.3

Presented in Figure 4.11 are the strains in the bottom third and middle third (Fig. 3.6) of section 2 as a function of passes. Evident from the Figure, the strains within the bottom and middle third of the thick (12-inch) lift are quite similar from the pad-foot compactor, suggesting uniform compaction.

Shown in Table 4.2 are nuclear density probe (NDP) test at 3 locations within section 2 for passes 0, 4, and 9. Note, in order to measure density, the surface of the section had to be graded and rolled with the vibratory smooth steel compactor (4th and 6th passes). The table presents the measured values at 6-inch (i.e., 0 to 6-inch), 12-inch (i.e., 0 to 12-inch), as well as the computed value from. 6-inch to 12-inch based on Eq. 4.2. As expected, the highest standard deviation occurred within the 6-inch to 12-inch zone; however, the variability decreased with pass, which is good. A comparison between

densities measured or computed from the nuclear density probe (NDP) or strain LVDT sensors were quite favorable.

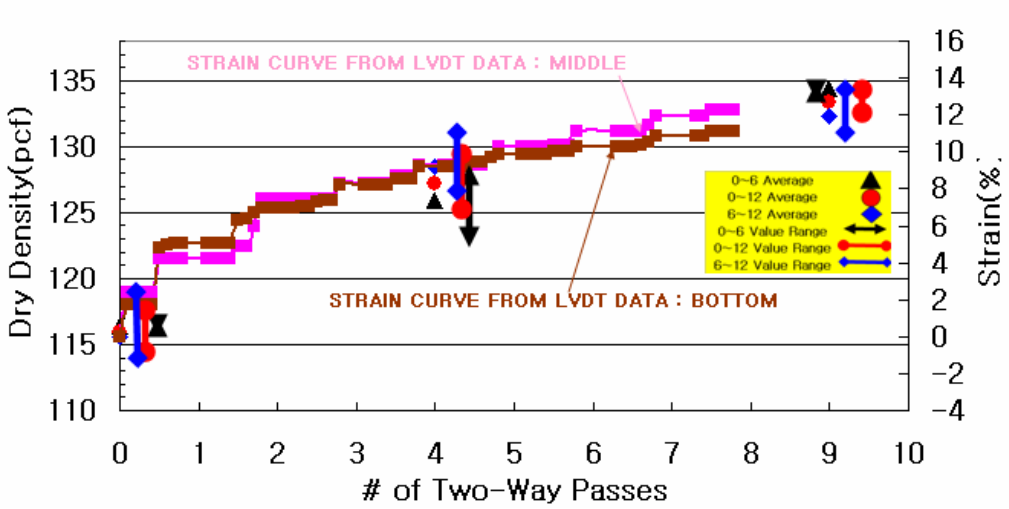

Figure 4.11 Strain from LVDT vs. Dry density from Nuclear Density Probe for Section 2

Table 4.2 Measured & Computed Dry Densities from Nuclear Density Probe (NDP) within Section 2

Pass #	Depth	1	2	3	Average	Standard Deviation
0	0~6	117.0	116.0	116.0	116.3	0.6
	0~12	116.1	117.3	114.4	115.9	1.5
	6~12	115.2	118.6	112.8	115.5	2.9
4	0~6	126.9	128.3	122.6	125.9	3.0
	0~12	126.8	129.8	125.0	127.2	2.4
	6~12	126.7	131.3	127.4	128.5	2.5
9	0~6	134.3	135.0	133.8	134.4	0.6
	0~12	134.5	133.2	132.3	133.3	1.1
	6~12	134.7	131.4	130.8	132.3	2.1

Shown in Figure 4.12 are the measured strains in the bottom and middle third (Fig. 3.7) of section 3 as a function of compactor pass. Apparent from the figure, the strains in section 3 are highest for all sections (max. 20%) due to the dynamic force of compactor,

85,000 lbf. Also evident, the strains within the bottom and middle third of the thick (12-inch) lift are very similar, suggesting uniform compaction.

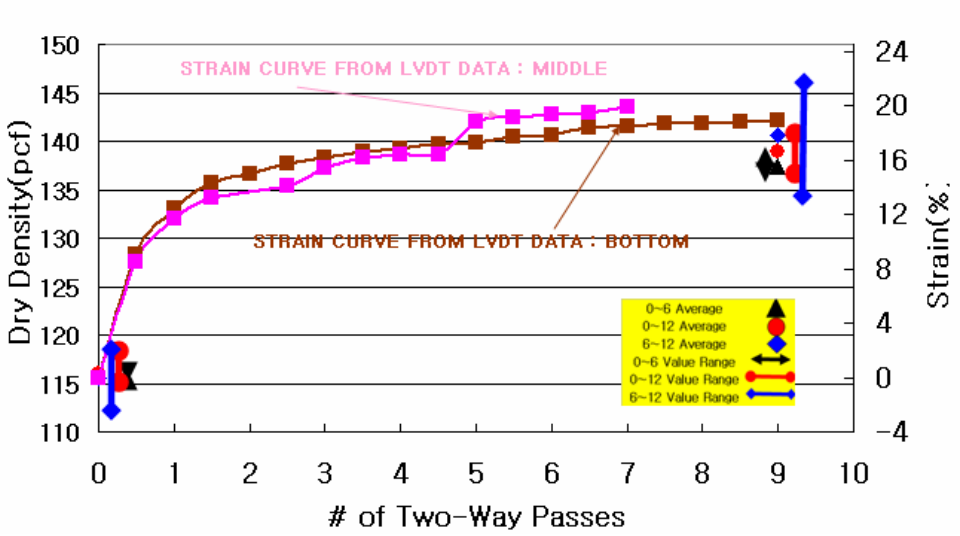

Figure 4.12 train from LVDT vs. Dry density from Nuclear Density Probe for Section

Given in Table 4.3 are nuclear density measurements at 3 locations within the section for passes 0, and 9. No other densities were collected due to time constraints (end of day, darkness). Evident from the table, the densities of section 3 at the end of compaction were the highest and they agreed with the back computed values from the LVDT instrumentation, Fig. 4.12.

Table 4.3 Measured & Computed Dry Densities from Nuclear Density Probe (NDP) within Section 3

Pass #	Depth	1	2	3	Average	Standard Deviation
0	0~6	117.0	116.0	116.0	116.3	0.5
	0~12	116.1	117.3	114.4	115.9	1.2
	6~12	115.2	118.6	112.8	115.5	2.4
9	0~6	135.5	139.3		137.4	1.9
	0~12	141.0	137.0.		139.0	2.0
	6~12	146.5	134.7		140.6	--

4.4. Dry Densities and Moisture Contents

As identified in section 3.1, Modified Proctor (AASHTO T-180) laboratory compaction tests were performed on the SR826 base materials. An optimum dry density of 131 pcf and moisture content of 9% were found. FDOT specification 200 requires a measured field compaction of 98% of T-180 or a dry density of 128.38 pcf.

Presented in Figure 4.13 are measured field dry densities from the nuclear density probe (NDP) for the last passes of lifts 1 and 2 of section 1. Also shown in the figure are the moisture contents measured from the nuclear density probe (NDP) as well as lab oven dried samples recovered from the field. Apparent is the back scatter surface moisture measurement acceptable measurements over the depth of the deposit.

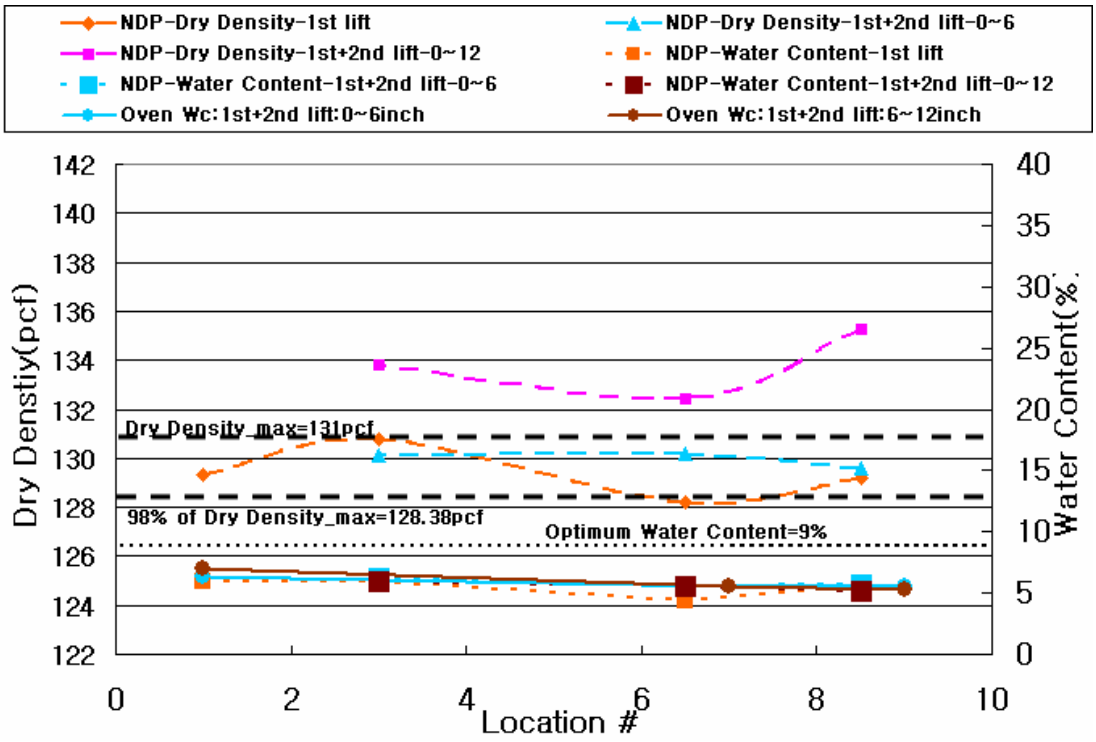

Figure 4.13 Dry densities and Moisture Contents in Section 1

Evident from Fig. 4.13, the dry density measurements in the first lift (129 pcf) increased significantly during the compaction of the overlying second lift (133.5 pcf). The latter may be attributed to the large compactor energy (Fig. 4.5) measured in the bottom of first lift during compaction of 2nd lift. Both lifts are well above FDOT Specification 200 or 98% of the modified Proctor or a dry density of 128.38 pcf. Presented in Figure 4.14 are the measured dry densities and moisture content for the 9th compactor pass on section 2. Evident are similarities of densities for both 0 to 6-inch and 0 to 12-inch zones for all 10 locations within section 2. Also note the similarities of moisture obtained from both the lab oven dried samples and nuclear density probe (NDP). Evident is that the measured densities are well above the required FDOT specification value of 128.38 pcf.

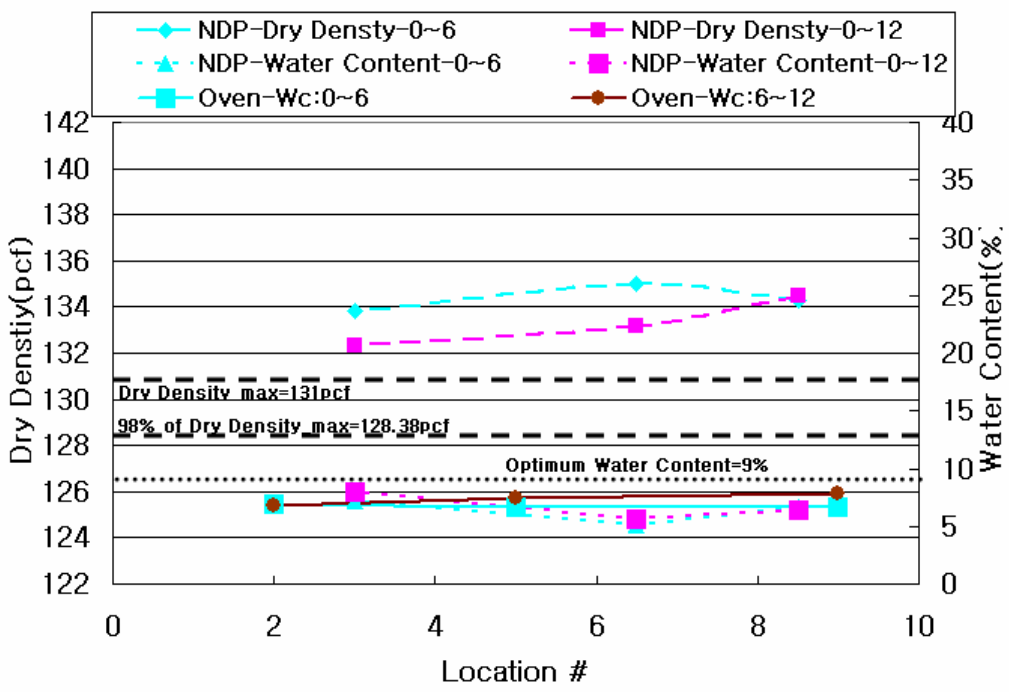

Figure 4.14 Dry Densities and Moisture Contents in Section 2

Presented in Figure 4.15 are measured dry densities and moistures in section 3 for the 9th pass of the Bomag 225D. This section had the highest measured densities, as well as variability along the section. However, the densities were well above FDOT's Specification 200 of 128.3 pcf.

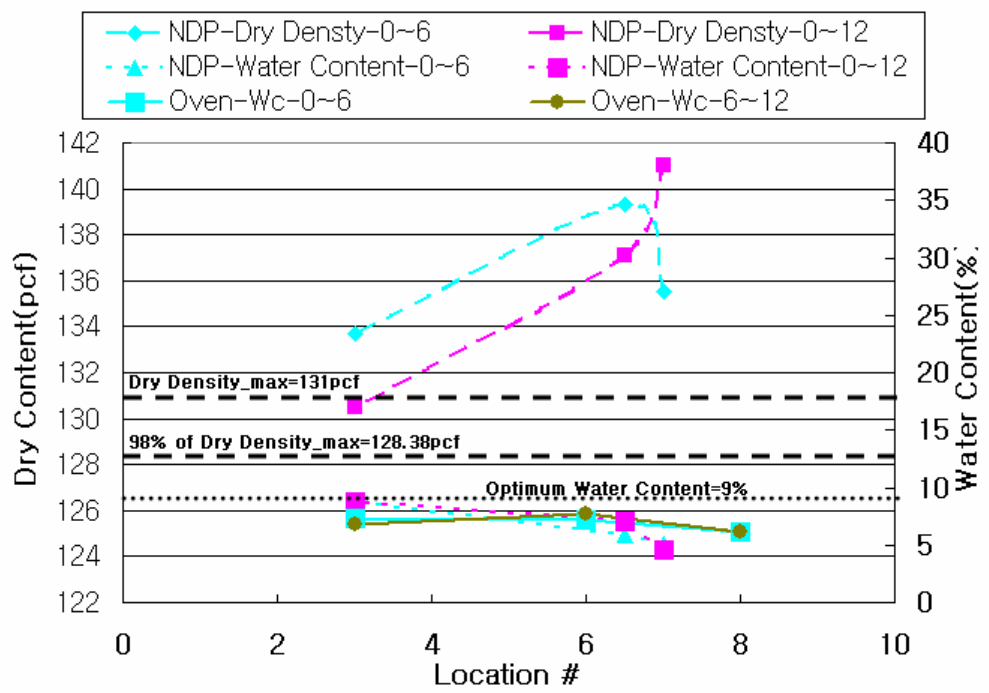

Figure 4.15 Dry Densities and Moisture Contents in Section 3

4.5. Base Stiffness

As identified in section 2.2, the stiffness, and strength of compacted materials are a function of moisture content and compactive effort (energy). Since, future roadway base construction will be based on compacted stiffness, AASHTO (2002), the stiffness of two conventional 6-inch lifts versus the 12-inch thick lift are of great interest. For the stiffness measurements, Falling Weight Deflectometer (FWD), Soil Stiffness Gage (SSG), as well as the E_{vib} from the Bomag Varicontrol measurements on the drum (225D-3) were measured and compared.

Presented in Figure 4.16 are stiffness (Kips/in) measured from the FWD for both lifts of section 1, as well as the thick lift sections 2 and 3 at 10 separate locations. Table 4.4 presents the mean and standard deviation for all ten locations in each section.

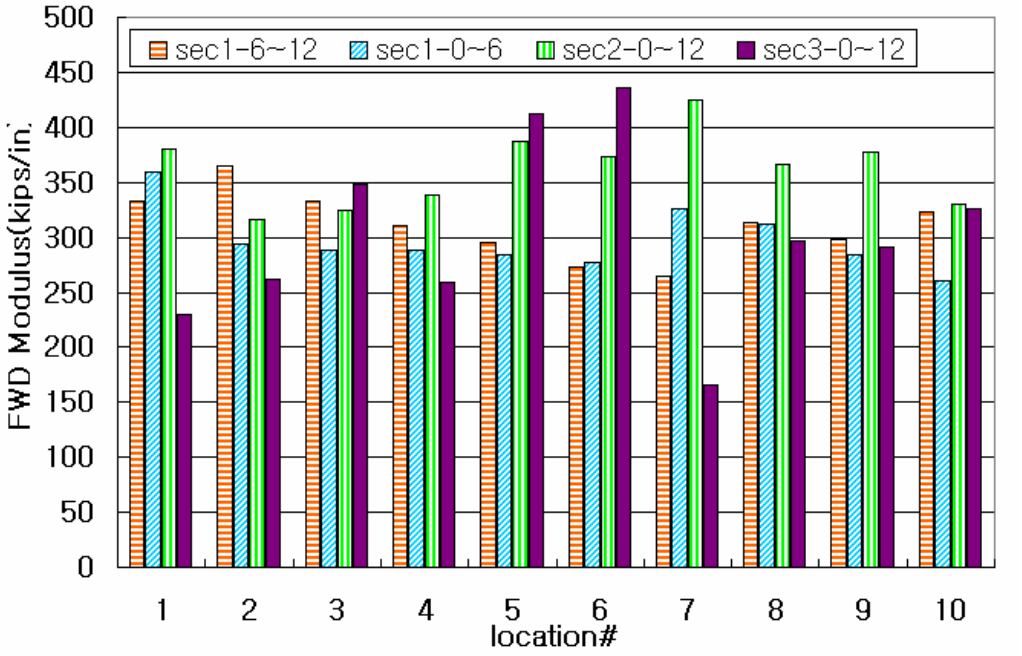

Figure 4.16 Stiffness Measured with FWD in All Sections

As expected, the stiffness of the first lift of section 1 increased with the placement of the second lift due to the compactive effort (energies) improving the underlying layer (Fig. 4.5) densities as shown in Fig 4.13. Interestingly, the FWD stiffness of section 2 had the highest mean for all the tested sites as well as the lowest coefficient of variation, i.e. standard deviation divided by mean. However, section 3, which had the highest compactive effort, and used the vario-control Compactor, had the lowest FWD mean stiffness, as well as the worse variability. Note however, the FWD employs a larger loading surface, i.e. 18” in diameter plate, which has a deeper zone of influence than the vario-control Compactor drum.

Table 4.4 FWD Mean and Standard Deviation on Each Section

Section1	Average	Standard Deviation
0~6inch	297	28.3
6~12inch	311	29.8
0~12inch	304	29.2
Section2	----	-----
0~12inch	362	34.1
Section3	----	----
0~12inch	303	81.8

Presented in Figure 4.17 is the surface stiffness as measured by the soil stiffness Gage (SSG) from Humbolt for each of the ten locations within the 3 sections. Again, section 1 had SSG performed at the end of both the first and second 6-inch lift placement. Shown in Table 4.5 are mean and standard deviation of the SSG data. Interestingly, the mean stiffness for the first 6-inch was higher than the measured mean after compaction of the second 6-inch lift for section 1. This quite different than the FWD results, Table 4.4, suggesting the SSG is measuring a surface phenomenon, whereas, FWD is measuring a depth phenomenon. Again section 2, 12-inch lift with the pad-foot compactor,

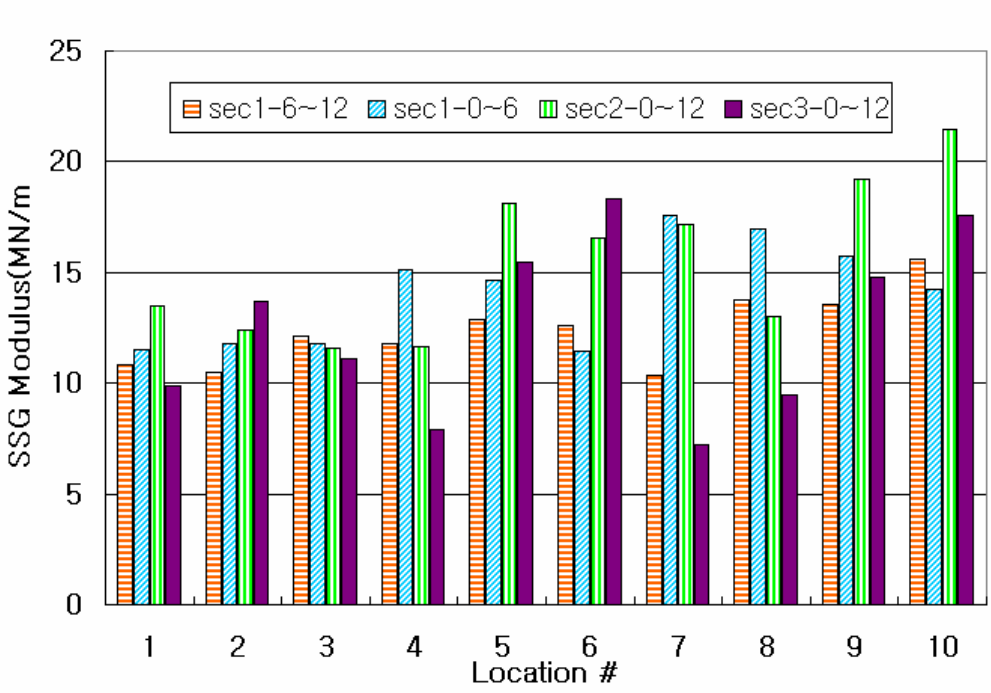

Figure 4.17 Stiffness measured by SSG in All Sections

Table 4.5 SSG Mean and Standard Deviation on Each Section

Section1	Average	Standard Deviation
0~6inch	14	2.3
6~12inch	12	1.6
0~12inch	13	2.1
Section2	---	---
0~12inch	15	3.5
Section3	---	---
0~12inch	13	4.0

had the highest stiffness, whereas section 3 was in between section 1 (2^{nd} lift) and section 2 on average, but had the worst variability (standard deviation 3.98).

Also of interest is a comparison of stiffness and moduli, E_{vib}, as measured with the FWD, SSG, and the vario-control unit for section 3. It is envisioned that intelligent compaction devices (i.e., vario-control, etc.), which continuously monitor stiffness or

moduli, will replace nuclear density probe (NDP) test for quality assessment and control in compaction.

Presented in Figure 4.18 are FWD and SSG stiffness (dashed lines – read on left axis), versus the E_{vib} measurements (read on the right side) as reported by the vario-control unit as a function of location. Note the vario-control Unit was operated in

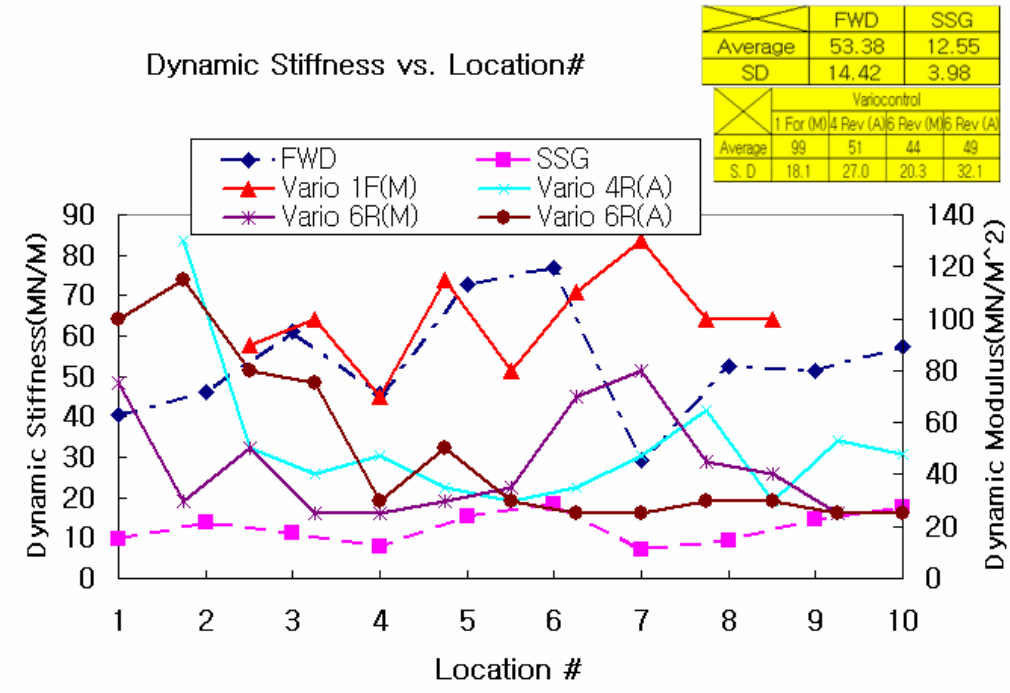

Figure 4.18 Stiffness from FWD & SSG vs. Dynamic Modulus from Vario-System

automatic (A, i.e., preset E_{vib}), and manual (R, i.e., preset amplitude and frequency) modes. Interestingly, after the first pass, all subsequent passes of the vario-control unit, had smaller E_{vib}. Moreover, the variability of the E_{vib} values over the site (i.e. 1-10) is much greater than the initial values (i.e. pass 1) or FWD data. All of the latter suggest that the unit was possibly crushing the surface material in site 3. For instance, particle crushing would result in larger surface deformations or a lower stiffness, k (Eq. 2.2), and a lower E_{vib} (Eq. 2.3) with subsequent pass.

To further verify the particle crushing theory, the stiffness as a function of depth was found from the stress gages and accelerometers located 6-inch, 9-inch and 13-inch below the surface, Fig 3.6. The stiffness was assessed for the loading phase (e.g. Fig 4.8) and was compared to the E_{vib}, in Figure 4.19. Evident from the figure, the stiffness 6-inch or below increased or remained constant for all passes as compared the surface E_{vib} measurements (x axis- decreased). The sensor 6-inch below the surface reached its maximum on the 4th pass, whereas, the bottom (13-inch) reached maximum at the 6th pass. The increasing stiffness values below 6-inch, supported by the higher densities in Fig. 4.15, are in conflict with the decreasing E_{vib} values with pass number. Further confirmation of the influence of compactive effort (energies), Fig. 4.8, are presented in section 4.6, concerning strength vs. depth.

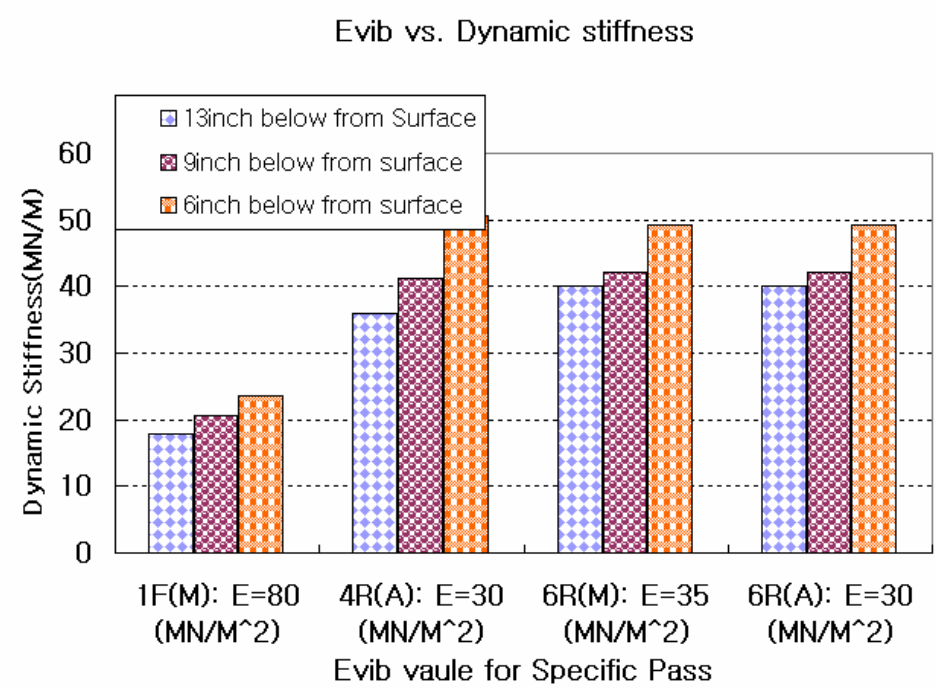

Figure 4.19 Stiffness and E_{vib} Moduli as Function of Depth and Number of Passes

4.6. Base Strength

Besides stiffness, the strength of base materials beneath the roadway is extremely important. The latter controls maximum contact pressures (e.g. semi-truck tire pressures) that the roadway may be exposed without undergoing a bearing failure. One means of assessing strength in the field is with a static or dynamic cone penetration test. For this study, an Automatic Dynamic Cone Penetrometer (ADCP) device owned and operated by the State Materials Office (SMO) in Gainesville was used. SMO recommended the automatic dynamic cone over the static due to its prior success on other base project studies.

Presented in Figure 4.20 is the mean and maximum range of ADCP values as a function of depth for section 1 after the placement of the second 6-inch lift. Appendix G presents the data for all ten locations (Fig 3.5), and Table 4.6 reports the mean and standard deviation of the ten values at depths of 6-inch, 10-inch and 12-inch below the base surface. Of interest is the number of blows required to achieve a specific depth, discontinuities (i.e., jumps due to impenetrable rocks – schist), as well as the slope (blows/distance) over a given layer. Apparent from Fig. 4.20, section 1 after compaction was very uniform with blow count/layer (strength) being similar for each 6-inch lift as well as the subgrade (zone below the base).

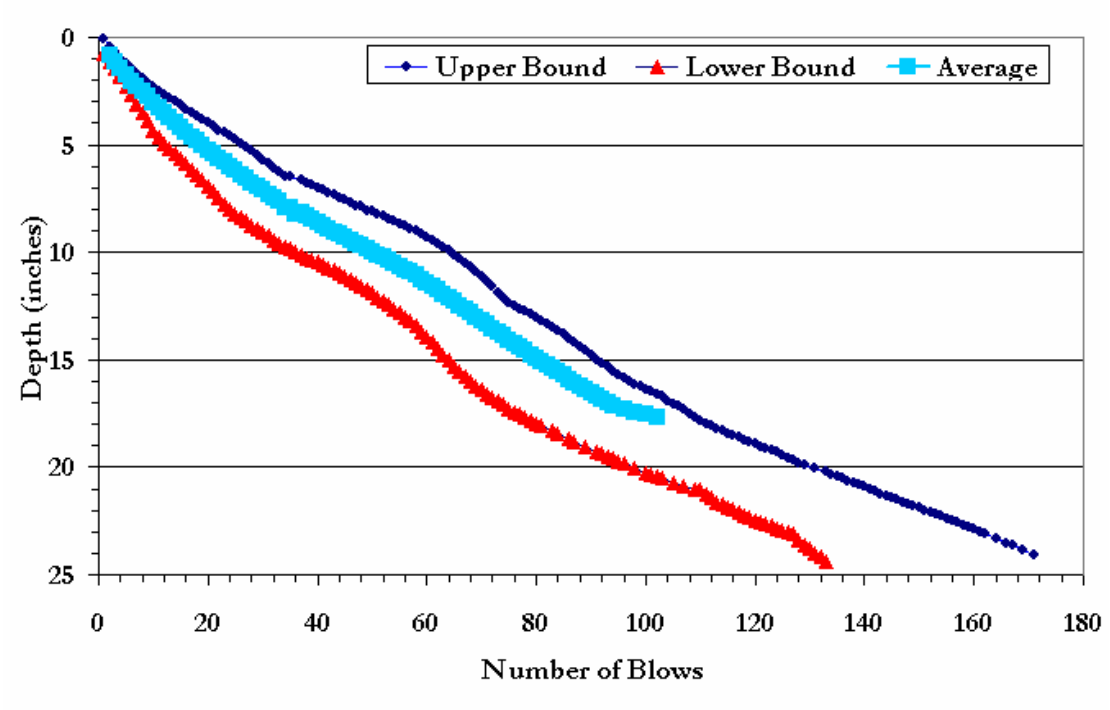

Figure 4.20 ADCP Data for Section 1 After 2nd Layer

Table 4.6 Summary ADCP Results for Section 1

Depth	Average Blow/each depth	Standard Deviation
6	24	5.1
10	51	8.1
12	64	7.7

Shown in Figure 4.21 and Table 4.7 is the mean, range, and variability of ADCP data for section 2. Presented in Table 4.8 and Figure 4.22 is the mean, range and variability of ADCP data for section 3.

A comparison of mean ADCP data between section 1 and 2 is given in Figure 4.23. Evident the mean for both sections are quite similar. However, the mean ADCP data for section 3 is significantly higher than section 1, by a factor of 2. The latter suggests that the significant energies (Fig. 4.8) from Bomag 225D resulted in particle crushing of the

surface (Fig 4.18), but higher strength (Fig 4.22) and stiffness (Fig 4.19) in the underlying materials due to larger contact area and dynamic drum forces in section 3.

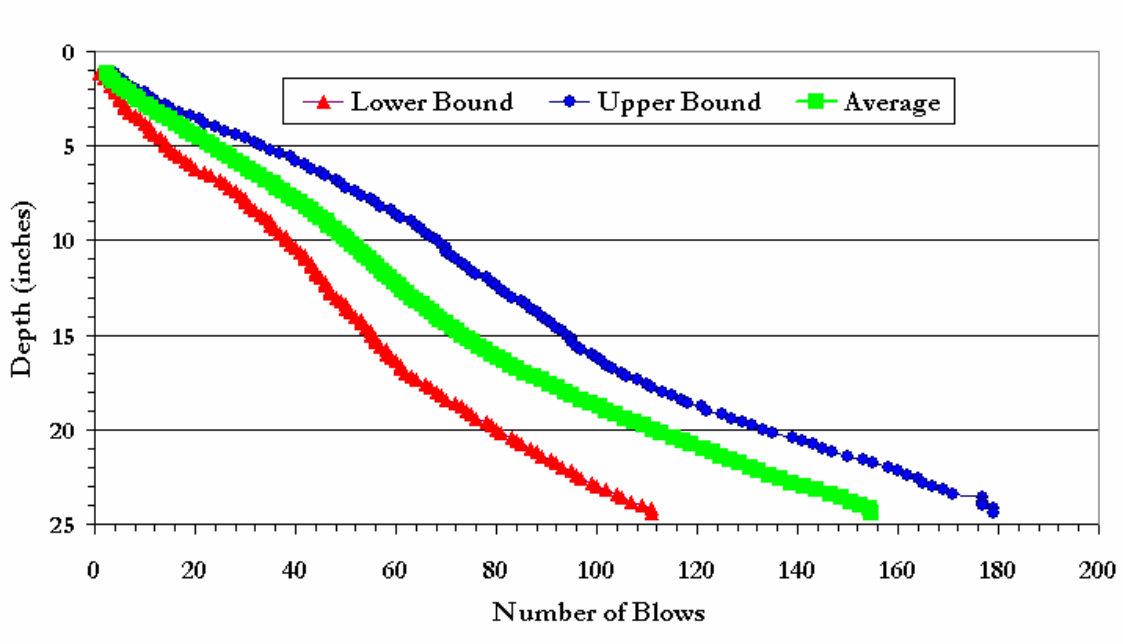

Figure 4.21 ACDP Data for Section 2

Table 4.7 Summary of ADCP Results for Section 2

Depth	Average Blow/each depth	Standard Deviation
6	29	6.7
10	50	9.3
12	59	10.5

Table 4.8 Summary of ADCP Results for Section 3

Depth	Average Blow/each depth	Standard Deviation
6	49	12.3
10	80	12.0
12	94	9.5

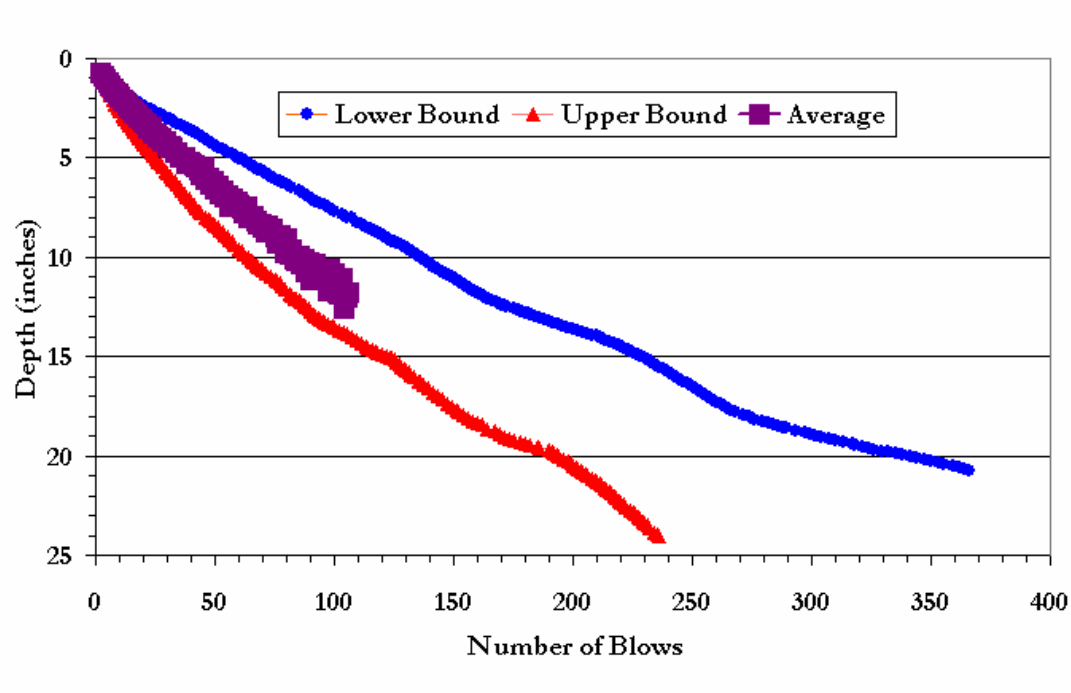

Figure 4.22 ACDP Data for Section 3

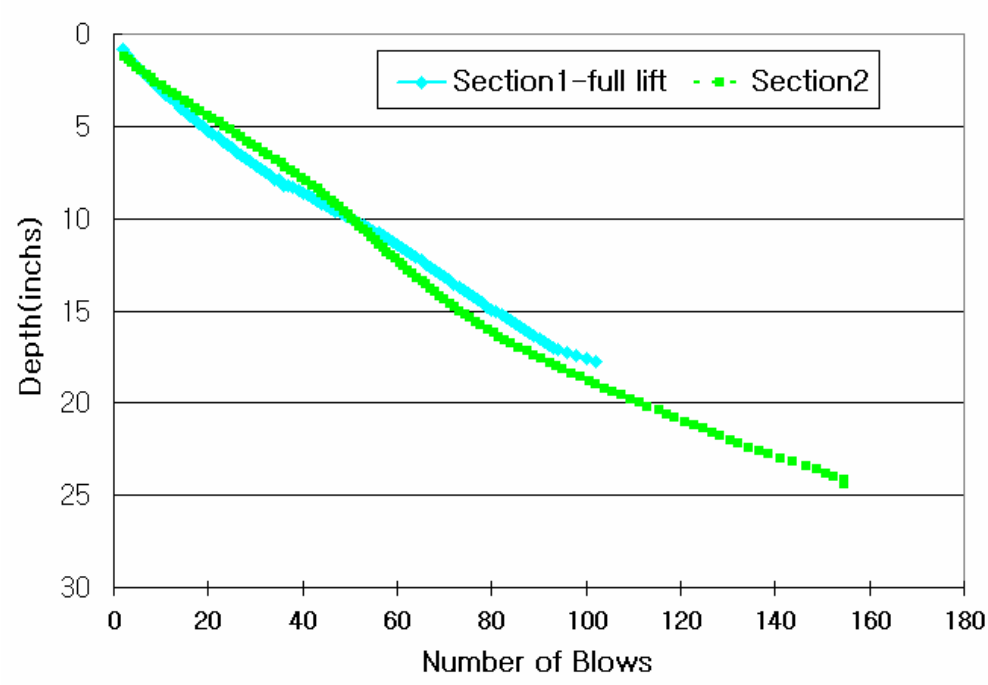

Figure 4.23 Comparison ADCP Data from Section 1 and 2

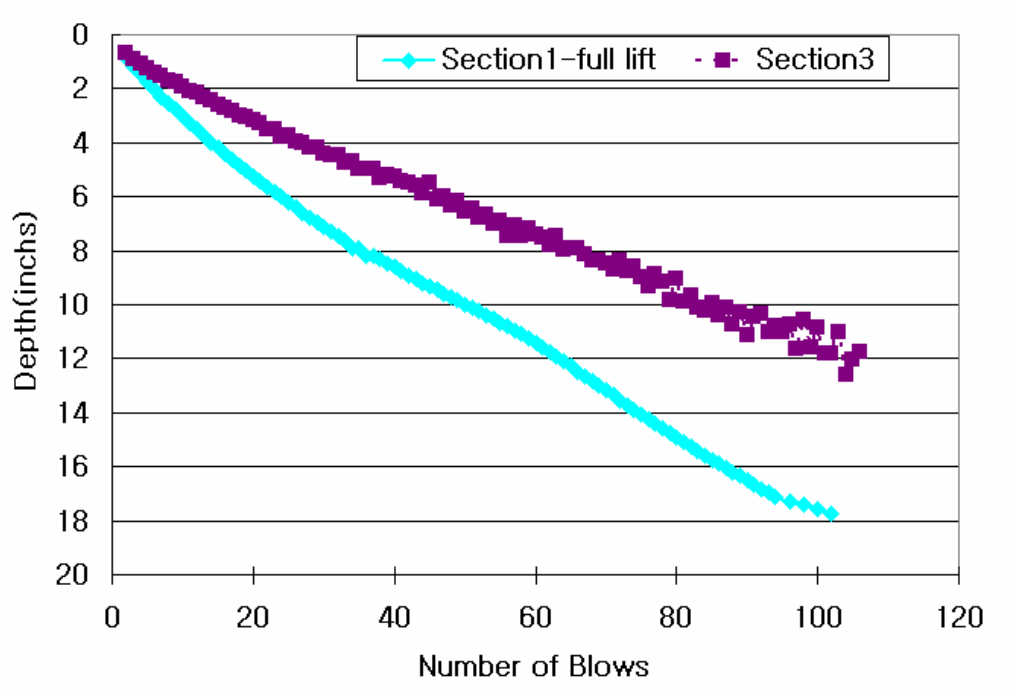

Figure 4.24 Comparison ADCP Data from Section 1 and 3

CHAPTER 5
CONCLUSION AND RECOMMANDATIONS

5.1. Conclusions

Current FDOT specifications for the construction of 12-inch limerock-bases for roadways require placing and compacting two successive 6-inch layers using single or dual smooth-drum vibratory rollers with dynamic forces in the range of 30,000 to 50,000 lbf.

FDOT Construction Specification 200 stipulates that limerock must be compacted to 98% of the maximum dry density as obtained in a laboratory Modified Proctor (AASHTO T-180) test.

Considering the availability of continually evolving heavier compaction equipment that can deliver higher compactive effort with the resulting potential to accelerate roadway construction, and hence to reduce costs, contractors and compactor manufacturers have suggested placement of a single 12-inch base lift instead of two 6-inch layers. For instance, the time required for quality control testing, grading, trucking, scheduling, and delivering a single 12-inch layer instead of two 6-inch lifts might be substantially reduced. In addition, compactor manufacturers have developed intelligent and heavier compactors that are capable of varying the energy delivered to the base, as well as monitoring the stiffness of the compacted material, i.e. QA/QC.

To investigate the possibility of compacting 12-inch thick lifts, the FDOT teamed with Ardaman and Associates with the University of Florida to instrument and monitor 3

test sections, Table 5.1, on SR 826 in Miami Florida. One test section had two conventional 6-inch lifts, and other two test sections were 12-inch thick lifts employing different compaction equipment (i.e. pad-foot vs. smooth wheel, Table 5.1).

The Miami site was selected due to its subgrade stiffness (i.e. LBR>100), as well as properties of its placed limerock: well graded, and low fines content with moisture contents from the mine less than optimum (4% -7%). As identified in the literature and confirmed in laboratory testing (Chapter 2), compacting dry of optimum results in greater stiffness and strength.

Table 5.1 Test Sections and Compactors

Location	Compactor	Weight (lbf)	Compactor Detail	Lift Thickness
Section 1	BOMAG BW 211D-3	53,000	Vibratory Steel Smooth Roller used conventionally	Conventional lifts (e.g. two 6-inch)
Section 2	BOMAG BW 213PD-3	62,000	Vibratory Pad-foot Roller	12-inch thick lift
Section 3	BOMAG BW 225BV-3	85,000	Vibratory Smooth Wheel- ICC Unit	12-inch thick lift

To identify stresses, deformations, and energies within the 6-inch and 12-inch lifts, stress cells, accelerometers, and LVDT deformation sensors were placed in the top, middle and bottom third of each placed layer. After compaction of each lift, Falling Weight Deflectometer (FWD), Soil Stiffness Gage (SSG), and Automatic Dynamic Cone Penetrometer (ADCP) testing were performed at 10 locations within each site. Of interest were the densities, stiffness, and strengths of material as a function of depth for the two

6-inch vs. 12-inch thick lifts. Also of importance was the Moduli, Evib, from Bomag's Intelligent Compaction Control (ICC) unit vs. field measured stiffness.

As expected, the two 6-inch lifts, Section 1, reached 98% of maximum dry densities within 3 to 5 passes of the conventional smooth steel vibratory compactor. Strains within the lifts were 6 to 9% with appreciable increase in density occurring within the lower lift as the upper lift was compacted.

Compaction of Section 2, a 12-inch thick lift, occurred with alternating passes of Bomag 213PD (5 passes), i.e., a vibratory a pad-foot roller, and a Bomag 211D-3, vibratory smooth wheel roller to smooth the base surface in order obtain accurate moisture and density measurements. From the field instrumentation, the strains and back computed densities (nuclear density probe (NDP)) in the bottom and the middle of the section 2 were quite similar. In addition, the energies and stiffness throughout the depth compared quite favorably. Surface stiffness measured with either FWD or SSG were similar or slightly higher with the thick lift, 12-inch section vs. the conventional section 1. Strength measured by ADCP and its associated coefficient of variability were quite similar for both section 1 and section 2.

Section 3 was a 12-inch thick lift base compacted with the smooth wheel Bomag 225 vario-conrol Compactor, which continuously monitor surface stiffness and varies energies based on moduli, E_{vib}. The compactor had the greatest dynamic force, 85,000 lbf, of any of the tested units. The measured strains with depth were quite uniform with depth and the highest of all the test sections, 20%. Similarly, the strength measured with depth by the ADCP was also the highest of all the test sections, i.e. factor of 2. Unfortunately, even though the vario-control unit was run in both the automatic and the manual mode,

the surface stiffness or moduli, $E_{vib,}$ decreased with pass number and was quite variable over the section. The variability attributed to particle crushing of the surface particles, since the measured stiffness, and strength, increased in depth with pass based on buried instrumentation and ADCP results.

From the study, it was concluded that thick lift, 12-inch, compaction of limestone base courses was achievable under the following conditions:

- Subgrade material of sufficient strength and stiffness, i.e., LBR value over 100.
- The compaction process should be conducted with moisture contents on dry part of optimum, i.e., 5~8% vs. 9% optimum moisture content.
- Vibratory padfoot roller with at least 60,000 lbf of dynamic force or vibratory heavy steel smooth roller above 85,000 lbf dynamic force.

5.2. Recommendations for Future Testing

With the successful compaction of thick lift limestone base course in south Florida, the question of its use in central and north Florida remains. Miami was selected due to its expected high potential for success considering characteristic well graded, low-fines limerock materials, moisture content dry of optimum, and stiff subgrade conditions, i.e., typically having LBR values greater than 100.

The next potential test scenario of base thick lift are:

- Base thick lift will be placed on limerock subgrade with stiffness LBR>40.
- Limerock material with higher fine content and moisture content wet of optimum will be used as base material to be compacted with vibratory pad-foot roller with at least 60,000 lbf of dynamic force.

Also, the stiffness (FWD and SSG) and strengths (ADCP) devices should be the minimum instrumentation used in the future study.

CHAPTER 6
ACKNOWLEDGEMENT

FDOT would like to thanks the following:

1. The Research Team for planning and execution of the project

2. State Construction Office, State Materials Office and D-6 Construction Office

3. Ardaman and Associates

4. University of Florida

5. Bomag America for providing both the 213 and 225 compactors.

APPENDIX A
SIEVE ANALYSES

Section 1	Sample #	Location#
	S-1	1
	S-2	1
	S-3	7
	S-4	7
	S-5	9
	S-6	9
Section 2	Sample #	Station
	S-7	2
	S-8	2
	S-9	5
	S-10	5
	S-11	9
	S-12	9
Section 3	Sample #	Station
	S-13	3
	S-14	3
	S-15	6
	S-16	6
	S-17	8
	S-18	8

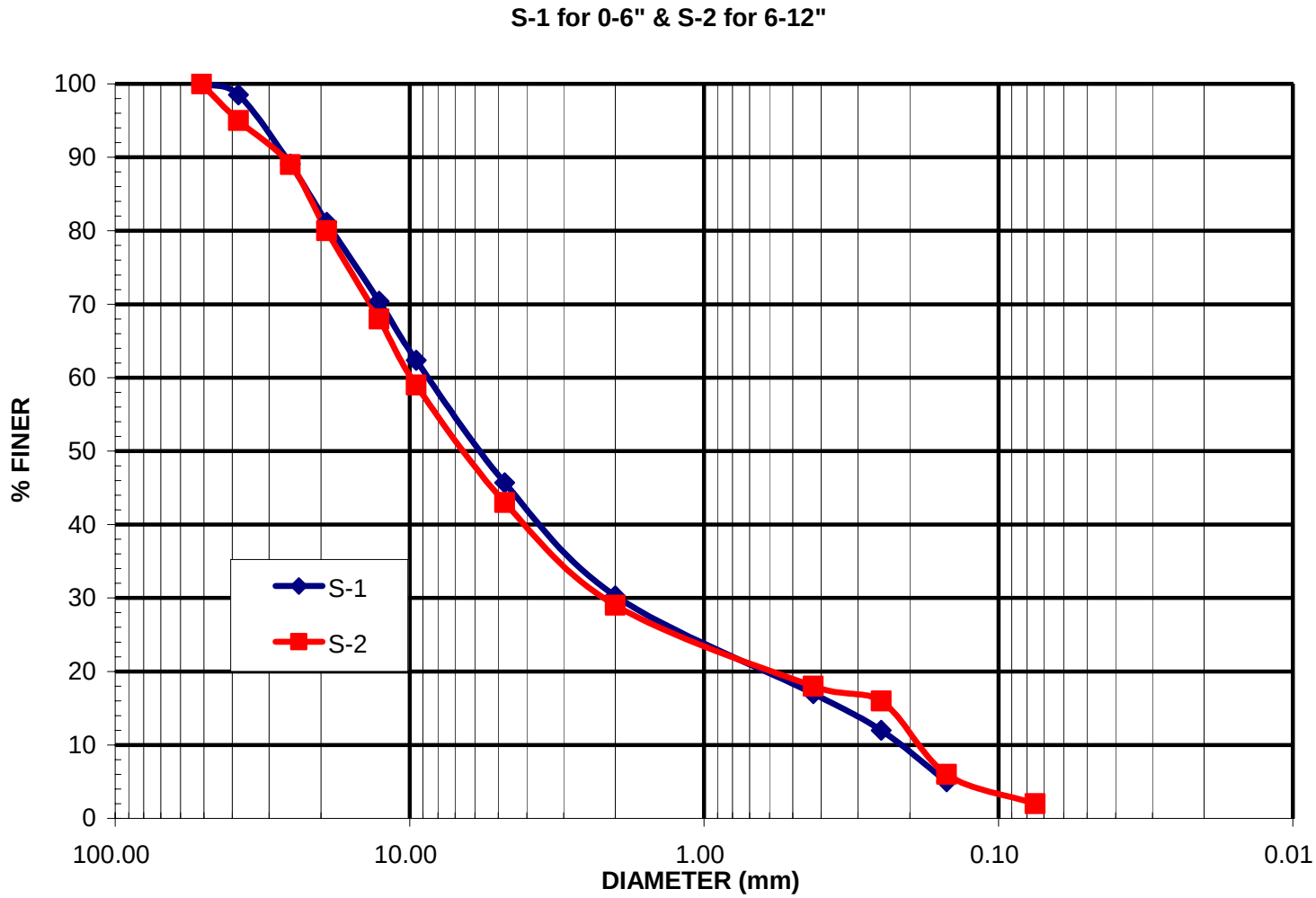
S-1 for 0-6" & S-2 for 6-12"
% FINER
100
90
80
70
60
50
40
30
20
10
0
S-1
S-2
100.00
10.00
1.00
0.10
0.01
DIAMETER (mm)

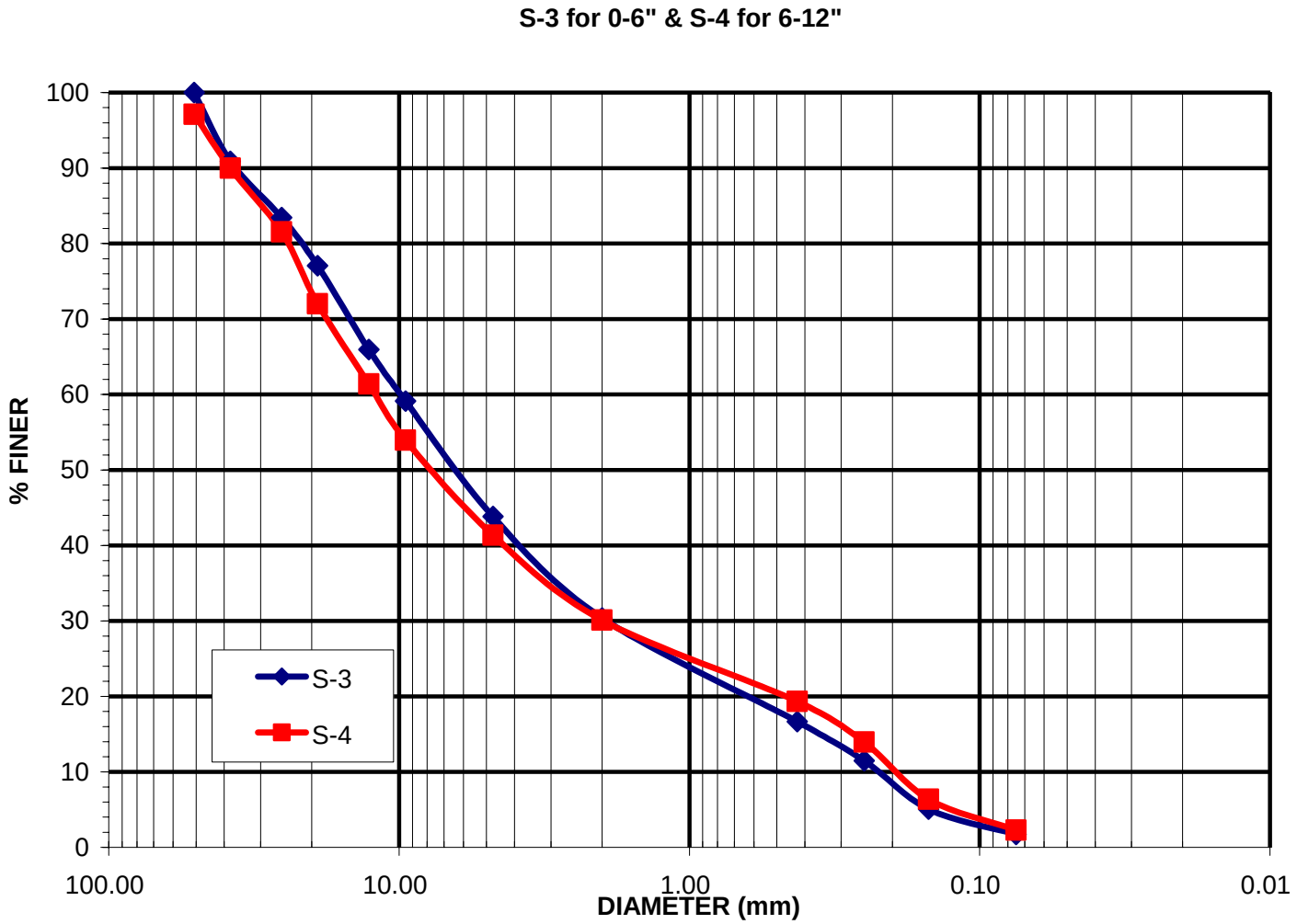
S-3 for 0-6" & S-4 for 6-12"
% FINER
100
90
80
70
60
50
40
30
20
10
0
100.00
10.00
1.00
0.10
0.01
DIAMETER (mm)
S-3
S-4

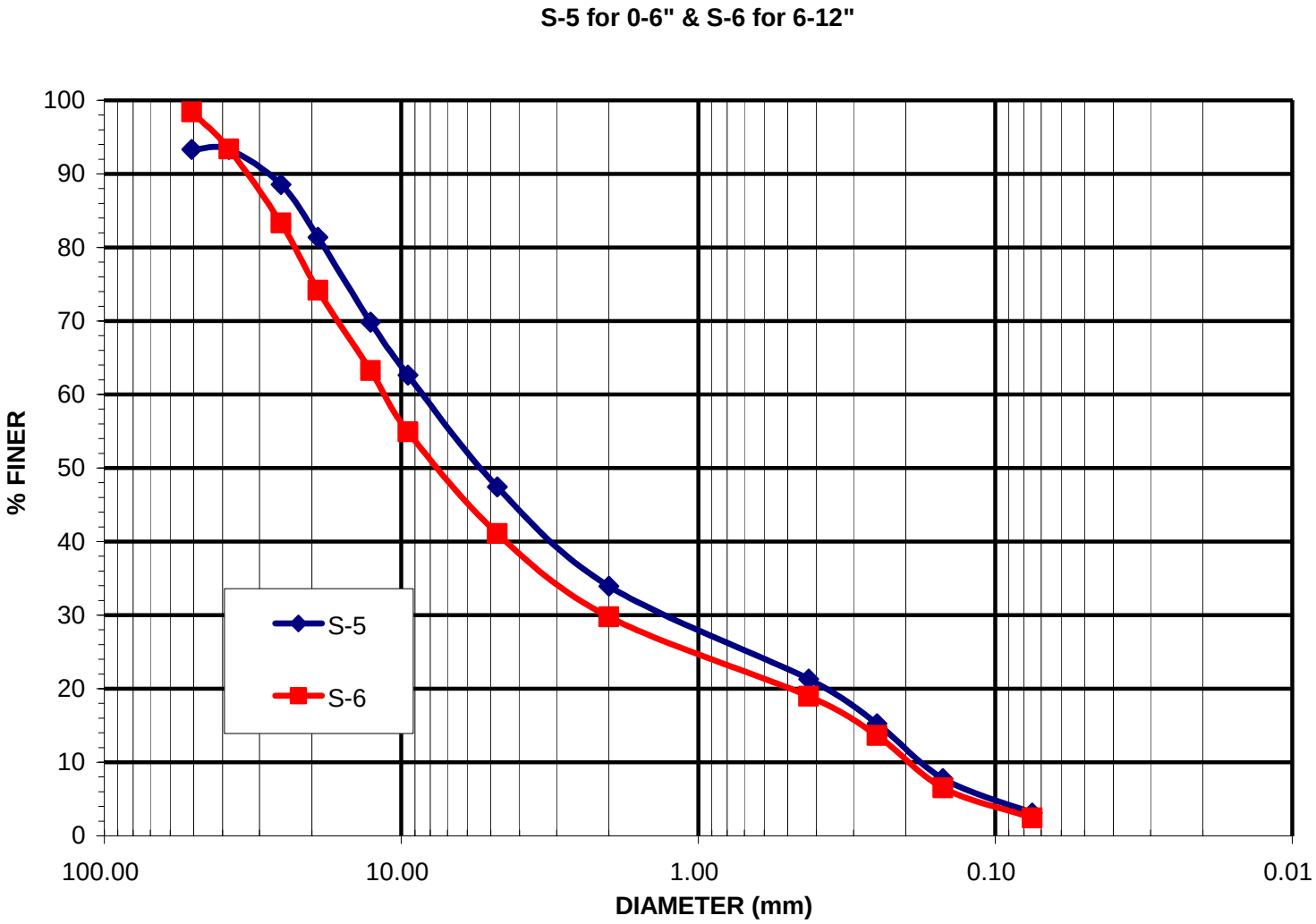
S-5 for 0-6" & S-6 for 6-12"
% FINER
100
90
80
70
60
50
40
30
20
10
0
100.00
10.00
1.00
0.10
0.01
DIAMETER (mm)
S-5
S-6

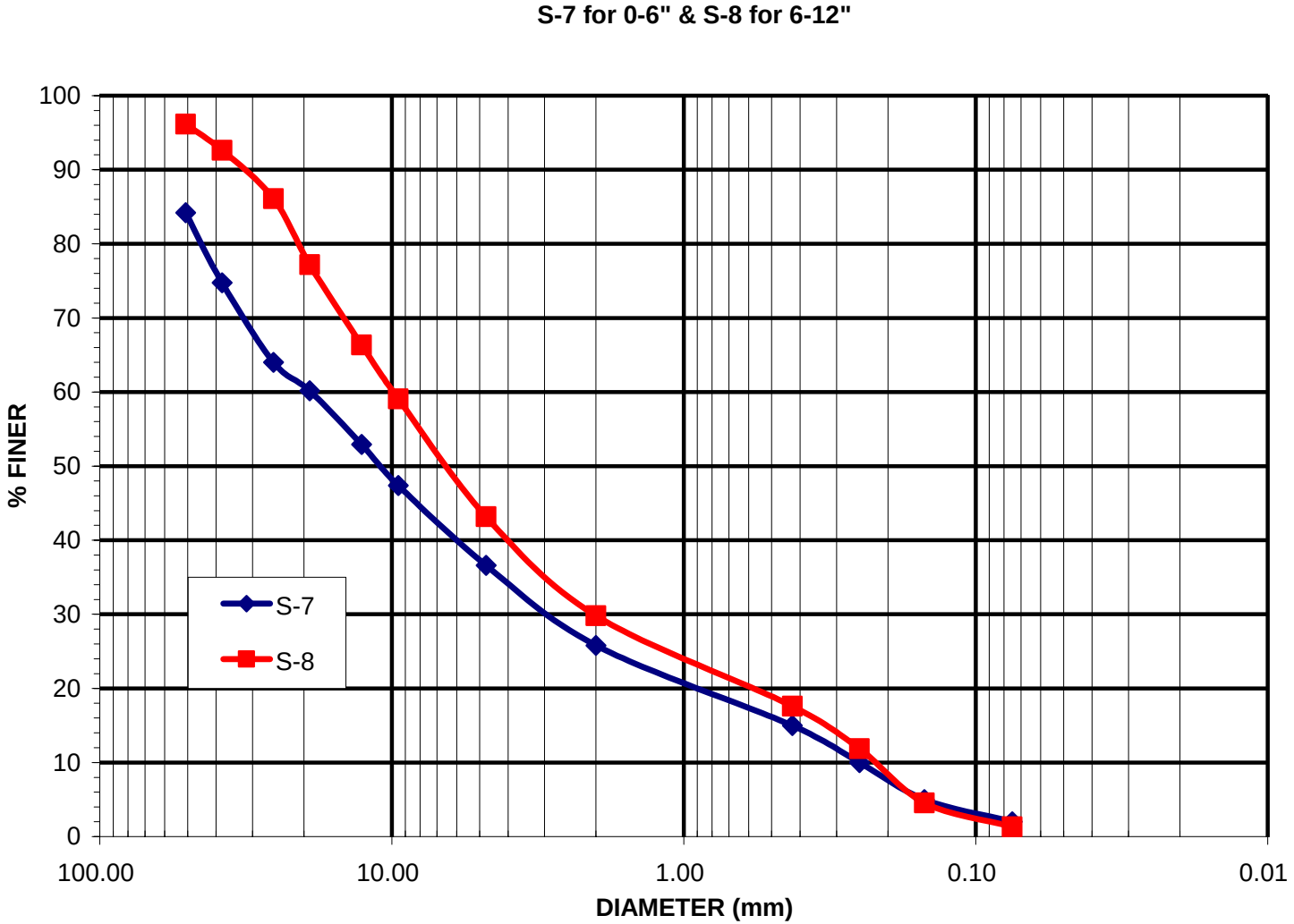
S-7 for 0-6" & S-8 for 6-12"
100
90
80
70
60
50
40
30
20
10
0
% FINER
S-7
S-8
100.00
10.00
1.00
0.10
0.01
DIAMETER (mm)

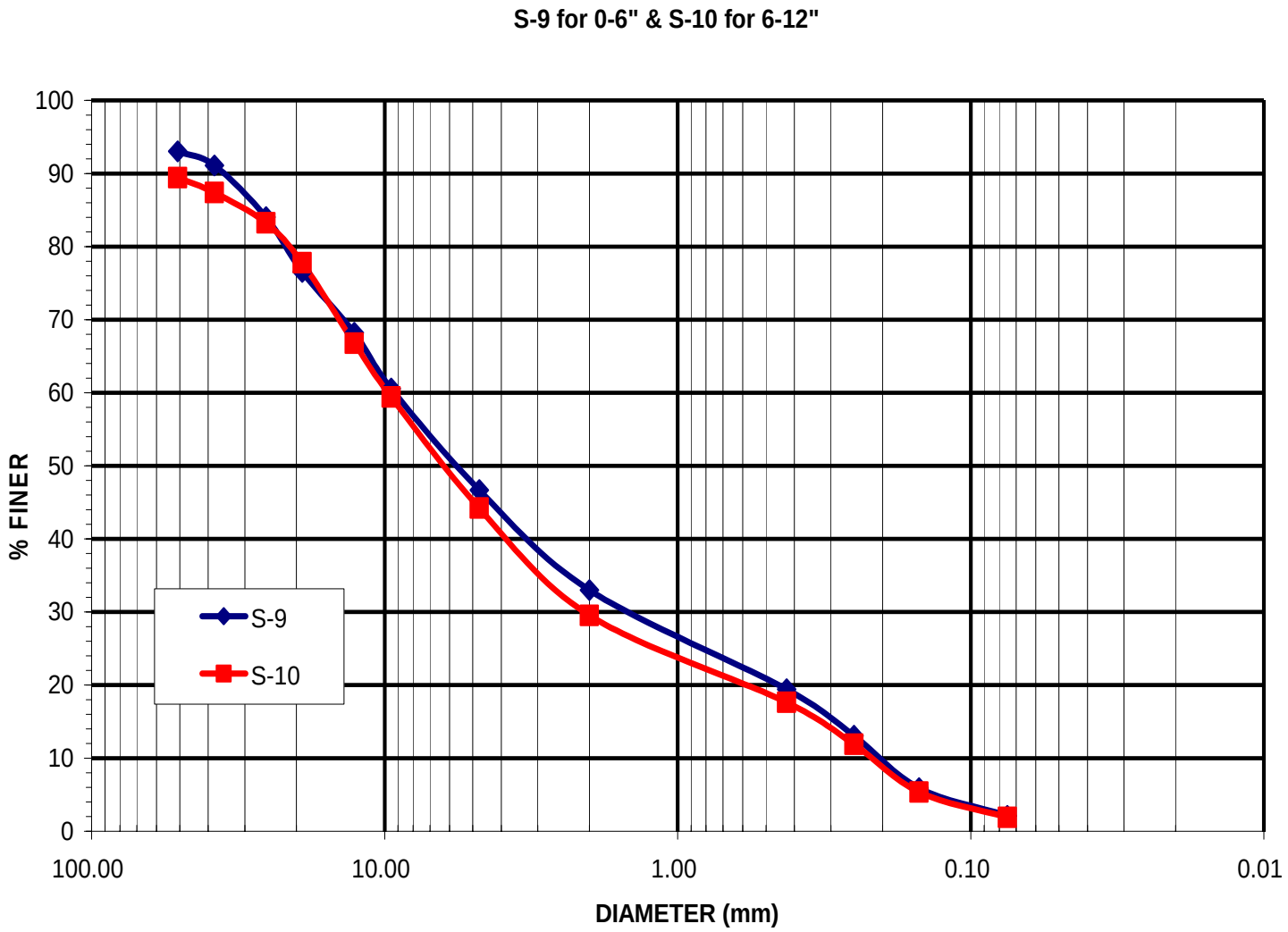
S-9 for 0-6" & S-10 for 6-12"
100
90
80
70
60
50
40
30
20
10
0
% FINER
S-9
S-10
100.00
10.00
1.00
0.10
0.01
DIAMETER (mm)

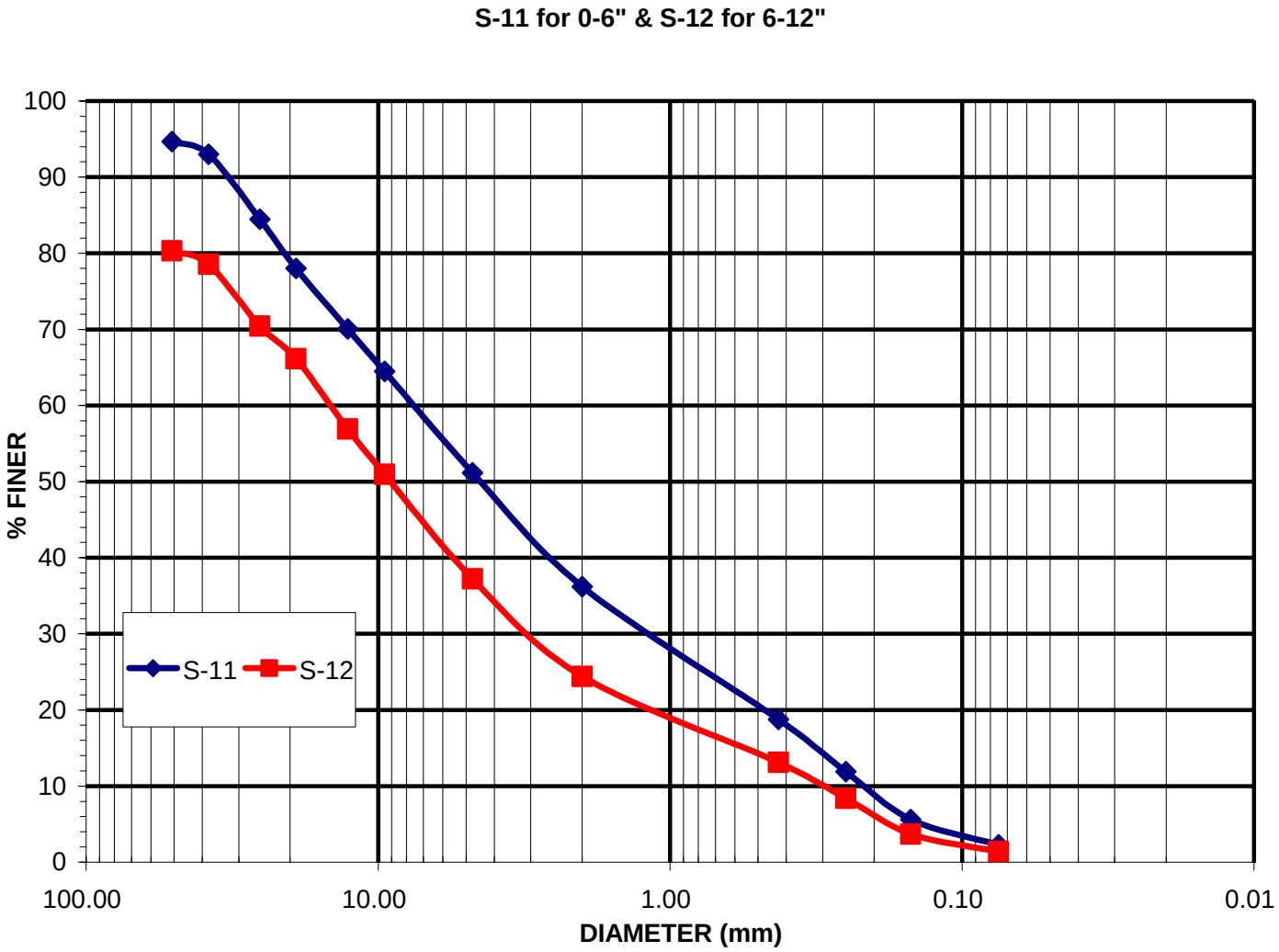
S-11 for 0-6" & S-12 for 6-12"
100
90
80
70
60
50
40
30
20
10
0
% FINER
S-11
S-12
100.00
10.00
1.00
0.10
0.01
DIAMETER (mm)

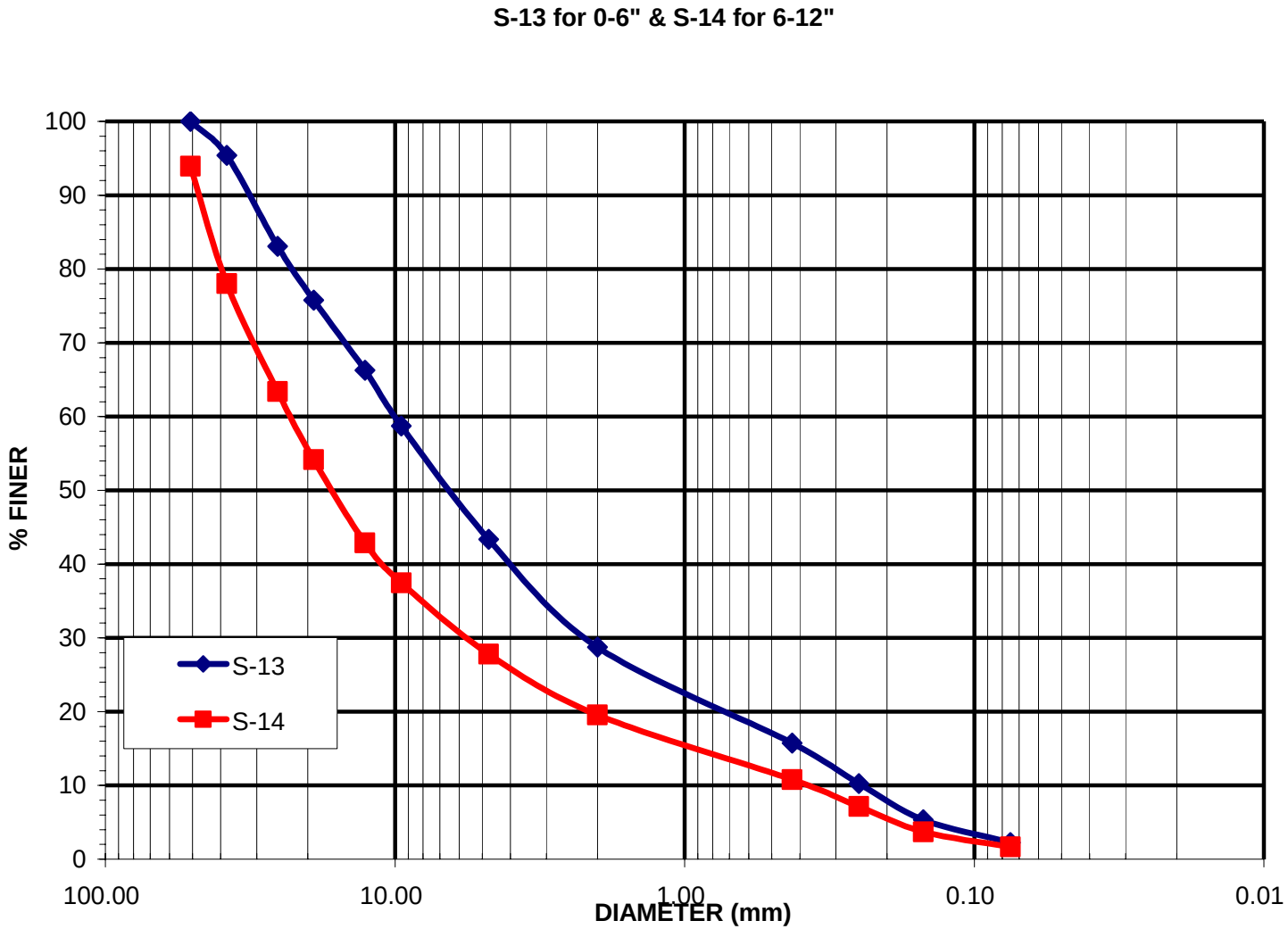
S-13 for 0-6" & S-14 for 6-12"
100
90
80
70
60
50
40
30
20
10
0
% FINER
S-13
S-14
100.00
10.00
1.00
0.10
0.01
DIAMETER (mm)

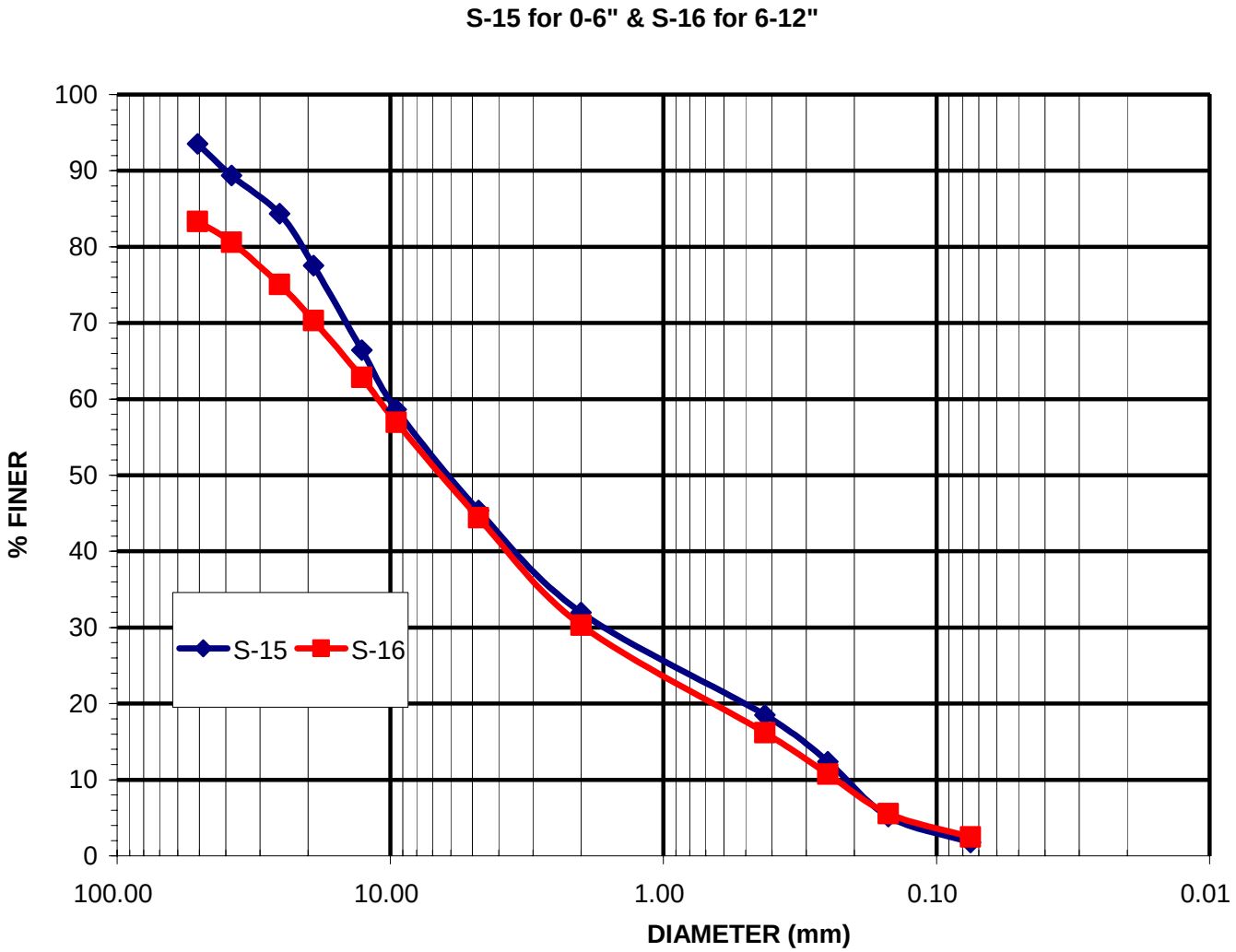
S-15 for 0-6" & S-16 for 6-12"
100
90
80
70
60
50
40
30
20
10
0
% FINER
S-15
S-16
100.00
10.00
1.00
0.10
0.01
DIAMETER (mm)

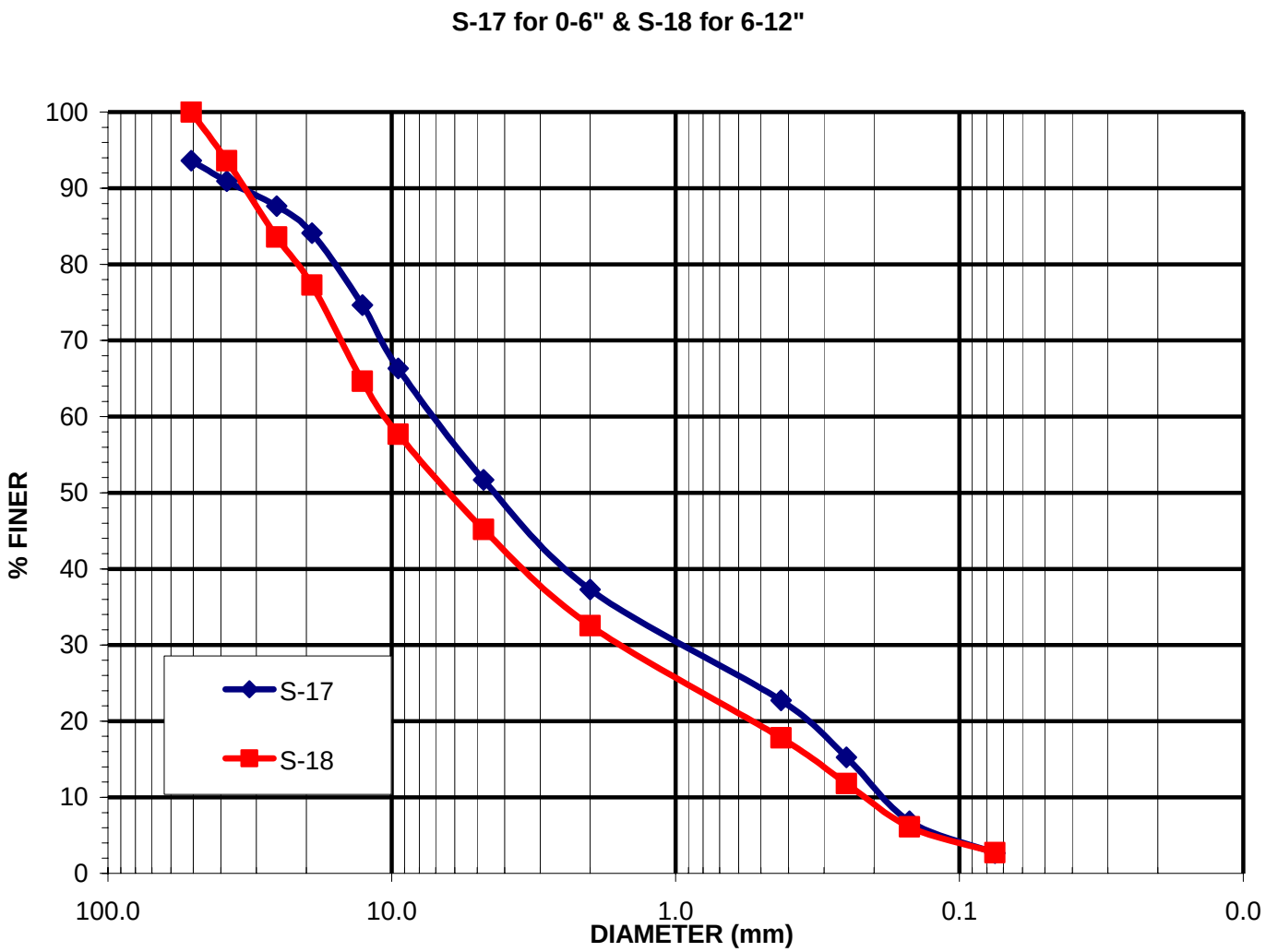
S-17 for 0-6" & S-18 for 6-12"
100
90
80
70
60
50
40
30
20
10
0
% FINER
S-17
S-18
100.0
10.0
1.0
0.1
0.0
DIAMETER (mm)

APPENDIX B
MOISTURE CONTENTS FROM NUCLEAR DENSITY PROBE

Density & Water Content from Nuclear Density Measurment for Section 1													
Station #	Two 6" Layer Test Section1 (control)		Subgrade		After First lift installed (6 inch)		After Second lift installed (12 inch)						
							Before Compaction (6inch)	After 1 Pass		After 3 Pass		After 4 Pass	
			6 inch	12 inch	Pass #2	Pass #3		6 inch	12 inch	6 inch	12 inch	6 inch	12 inch
10		228+00	126.7	129.8									
8.5		227+75			133.8	136.6	126.8	129.2	132.4	136.3	137.5	137	142.4
6.5	Wet Density	227+50	127.1	131.8	134.5	133.9	122	134.4	136.6	135.9	138	137.4	139.7
3		227+25			134.7	138.5	126.3	133.1	139.9			138.2	141.7
1		227+00	129.1	136	134.1	136.9							
10		228+00	3.5	3.7									
8.5		227+75			4.7	5.7	5.3	5	5.4	5.8	5.5	5.7	5.2
6.5	Water Content	227+50	3.4	3.6	4.9	4.4	5.9	6.1	5.3	5.8	5.5	5.6	5.5
3		227+25			5.7	5.9	6.2	6.6	5.4			6.2	5.9
1		227+00	5.9	5.4	5.5	5.9							
10		228+00	122.4	125.1									
8.5		227+75			127.8	129.2	120.5	123.1	125.7	128.8	130.3	129.6	135.3
6.5	Dry Density	227+50	122.8	127.3	128.2	128.2	115.2	126.6	129.7	128.4	131.1	130.2	132.4
3		227+25			127.4	130.8	118.9	124.8	132.7			130.1	133.8
1		227+00	121.9	129	127.1	129.3							

Density & Water Content from Nuclear Density Measurment for Section 2												
Station #	Thick Lift Test w/Pad Foot Rooler Section 2		Subgrade (Initial)		Subgrade After Compacting with Spreading Water		After installed (loose)		During Compaction			
									After 4 Pass		After 9 Pass	
			6 inch	12 inch	6 inch	12 inch	6inch	12inch	6 inch	12 inch	6 inch	12 inch
10	Wet Density	228+00	123.1	131.6	133.6	136.3						
8.5		227+75					123.1	122.5	133.2	133.8	143.3	143.1
6.5		227+50			130.3	134	123.9	125.5	136	137.9	142	140.7
3		227+25					115.4	113.3	131.8	134.5	143.5	142.8
1		227+00			132.4	136.8	123.1	124.7				
10	Water Content	228+00	3.4	3.5	4.7	4.4						
8.5		227+75					5.2	5.5	4.9	5.5	6.7	6.4
6.5		227+50			3.1	3.9	6.8	7.1	6	6.2	5.1	5.6
3		227+25					6.8	7.5	7.5	7.6	7.2	8
1		227+00			4.8	4.9	6.2	5.5				
10	Dry Density	228+00	119	127.1	127.6	130.6						
8.5		227+75					117	116.1	126.9	126.8	134.3	134.5
6.5		227+50			126.3	128.9	116	117.3	128.3	129.8	135	133.2
3		227+25					108	105.3	122.6	125	133.8	132.3
1		227+00			126.3	130.4	116	114.4				

Density & Water Content from Nuclear Density Measurment for Section 3						
Station #	Thick Lift Test w/225D		Subgrade (Initial)		After Compaction	
			6 inch	12 inch	6 inch	12 inch
10	Wet Density	227+00				
7		226+65			142.3	147.6
6.5		226+50	134.4	139.7	147.6	146.6
3		226+25			145.5	141.9
1		226+00	134.8	131.5		
10	Water Content	227+00				
7		226+65			5.1	4.6
6.5		226+50	3.3	2.8	5.9	7
3		226+25			8.8	8.8
1		226+00	3.4	3.4		
10	Dry Density	227+00				
7		226+65			135.5	141
6.5		226+50	130	135.8	139.3	137.1
3		226+25			133.7	130.5
1		226+00	130.3	127.1		

APPENDIX C
LAB OVEN-DRIED MOISTURE CONTENTS

SR 826 Lab Oven-Dried Moisture Contents			
Test Date	11/30/2004		
Sample #	Section1	Location	% M
1	0" to 6"	1	6.98
2	6" to 12"	1	6.39
3	0" to 6"	7	5.53
4	6" to 12"	7	5.50
5	0" to 6"	9	5.28
6	6" to 12"	9	5.55
Test Date	12/1/2004		
Sample #	Section 2	Location	% M
7	0" to 6"	2	6.88
8	6" to 12"	2	6.79
9	0" to 6"	5	6.70
10	6" to 12"	5	7.50
11	0" to 6"	9	6.62
12	6" to 12"	9	7.78
Test Date	12/1/2004		
Sample #	Section 3	Location	% M
13	0" to 6"	3	7.34
14	6" to 12"	3	6.84
15	0" to 6"	6	7.22
16	6" to 12"	6	7.77
17	0" to 6"	8	6.08
18	6" to 12"	8	6.10

APPENDIX D
INSTRUMENTATION DATA REDUCTION

D.1. Calculation for reducing data

D.1.1. Stress Cell

Stress (psi) = (Raw Data-Initial Value) (Volts)*100(psi/Volts)
(Initial Value is the average value of values measured during last 0.4 sec in whole measuring time, 10 sec)

D.1.2. Strain Sensors

Strain= (Raw Data-Initial Value) (Volts)*Factor(in/Volts)/ Initial Gage Height
(Initial Value is measured before test)

Calibration Factors for reducing of Strain Sensors

	Section 1	Section 2	Section 3
CH 6 (Bottom 1/3)	0.4072	0.3966	0.4054
CH 7 (Middle 1/3)	0.4058	0.4054	0.3990

Calibration factors provided by LVDT manufacturer.

D.1.3. Acceleration

Acceleration (in/sec^2) = (Raw Data-Initial Value) (Volts) *Factor (g/Volts) *32.17417*12 (Initial Value is the average value of values measured during last 0.4 sec in whole measuring time, 10 sec)

Calibration Factor for Accelerometers

	Section 1	Section 2	Section 3
CH 1 (Bottom)	2.5497	2.5484	2.5259
CH 3 (Middle)	2.5484	2.5368	2.5510
CH 5 (Top)	2.5478	2.5336	2.5272

Calibration factors provided by accelerometer manufacturer.

D.1.4. Velocity & Displacement from Acceleration Data

$$V_i = (A_{i-1} + A_i)/2 \times (T_i - T_{i-1}) + V_{i-1}$$
$$D_i = (V_{i-1} + V_i)/2 \times (T_i - T_{i-1}) + D_{i-1}$$

Where,

A_i, A_{i-1} is acceleration of desired time and previous time of one step before desired time.

V_i, V_{i-1} is velocity of desired time and previous time of one step before desired time.

D_i, D_{i-1} is displacement of desired time and previous time of one step before desired time.

T_i, T_{i-1} is desired time and previous time of one step before desired time.

D.1.5. Dynamic Stiffness

Stress-displacement curves were generated using displacements derived from accelerometers mounted on the stress cells which represent dynamic soil particle movement. Dynamic stiffness was evaluated using the stress-displacement for the vibratory impact that resulted in the peak measured stress, i.e., for the dynamic loading that occurred when the compactor was located directly above the instrumentation.

Data reduction for dynamic stiffness evaluation involved matching the displacement derived from accelerometer to the displacement measured by the corresponding LVDT. An iterative approach was used in which accelerometer reference values were adjusted to compensate for slight tilt-induced drift until derived velocity and displacement values were consistent with corresponding velocities and displacements measured with the LVDTs.

Example worksheet and plots related with example worksheet

D.2. Using worksheet after 3 passes with vibratory padfoot roller in Section 2

D.2.1. Raw Data

F-DOT Thick Lift Test with 213D-3, Pad-Foot Roller								
Test Date		Dec. 1. 2004						
Data		2500/sec during 10 sec						
File Name		p3-r-c						
	Raw Data							
Locat	Bottom	Bottom	Middle	Middle	Top	Top	M-B	T-M
ID#	1077	6187	1076	30	1087	26	2735	2871
Initial	2.70E-02	4.73E-01	-5.94E-03	4.11E-01	3.89E-02	4.17E-01	0.977	0.907
	Stress Cell	Accelero	Stress Cell	Accelero	Stress Cell	Accelero	LVDT	LVDT
Time	CH00	CH01	CH02	CH03	CH04	CH05	CH06	CH07
msec	V	V	V	V	V	V	V	V
0	3.18E-02	4.94E-01	6.87E-04	4.28E-01	4.28E-02	4.30E-01	-4.84E-01	-8.52E-01
0.4	2.94E-02	4.98E-01	-1.75E-03	4.31E-01	4.34E-02	4.33E-01	-4.83E-01	-8.53E-01
0.8	2.94E-02	5.00E-01	-1.75E-03	4.33E-01	4.22E-02	4.35E-01	-4.84E-01	-8.54E-01
1.2	2.95E-02	5.01E-01	-1.14E-03	4.32E-01	4.46E-02	4.36E-01	-4.83E-01	-8.53E-01
1.6	2.82E-02	5.01E-01	-8.39E-04	4.32E-01	4.22E-02	4.40E-01	-4.84E-01	-8.53E-01
2	2.95E-02	4.99E-01	-1.14E-03	4.35E-01	4.34E-02	4.39E-01	-4.83E-01	-8.52E-01
2.4	2.77E-02	4.99E-01	-1.14E-03	4.32E-01	4.34E-02	4.40E-01	-4.83E-01	-8.53E-01
2.8	3.00E-02	4.98E-01	-2.37E-03	4.32E-01	4.28E-02	4.40E-01	-4.84E-01	-8.52E-01
3.2	2.75E-02	4.95E-01	-1.75E-03	4.32E-01	4.10E-02	4.40E-01	-4.83E-01	-8.53E-01
3.6	3.12E-02	4.93E-01	-8.39E-04	4.29E-01	4.36E-02	4.40E-01	-4.83E-01	-8.52E-01
4	2.82E-02	4.89E-01	-1.14E-03	4.27E-01	4.16E-02	4.38E-01	-4.83E-01	-8.52E-01
9994.4	3.12E-02	4.98E-01	-6.03E-03	4.49E-01	3.73E-02	4.50E-01	-4.93E-01	-8.34E-01
9994.8	3.12E-02	5.02E-01	-6.64E-03	4.46E-01	3.67E-02	4.47E-01	-4.94E-01	-8.35E-01
9995.2	2.63E-02	5.06E-01	-6.03E-03	4.46E-01	3.91E-02	4.45E-01	-4.92E-01	-8.34E-01
9995.6	2.82E-02	5.09E-01	-6.64E-03	4.42E-01	3.98E-02	4.41E-01	-4.93E-01	-8.34E-01
9996	2.88E-02	5.13E-01	-6.64E-03	4.38E-01	3.79E-02	4.37E-01	-4.92E-01	-8.34E-01
9996.4	3.18E-02	5.15E-01	-8.47E-03	4.33E-01	3.98E-02	4.32E-01	-4.92E-01	-8.34E-01
9996.8	3.06E-02	5.14E-01	-7.25E-03	4.27E-01	3.85E-02	4.26E-01	-4.92E-01	-8.34E-01
9997.2	2.94E-02	5.12E-01	-6.64E-03	4.19E-01	3.91E-02	4.22E-01	-4.93E-01	-8.33E-01
9997.6	3.00E-02	5.08E-01	-6.64E-03	4.15E-01	4.10E-02	4.17E-01	-4.92E-01	-8.34E-01
9998	3.00E-02	5.02E-01	-7.25E-03	4.09E-01	4.05E-02	4.12E-01	-4.92E-01	-8.34E-01
9998.4	2.57E-02	4.98E-01	-1.08E-02	4.05E-01	3.85E-02	4.07E-01	-4.93E-01	-8.30E-01
9998.8	2.82E-02	4.90E-01	-7.25E-03	3.99E-01	3.84E-02	4.03E-01	-4.93E-01	-8.34E-01
9999.2	2.75E-02	4.84E-01	-9.08E-03	3.97E-01	3.93E-02	3.99E-01	-4.94E-01	-8.34E-01
9999.6	3.00E-02	4.77E-01	-6.64E-03	3.90E-01	3.79E-02	3.94E-01	-4.94E-01	-8.35E-01

D.2.2. Reduced Data

	F-DOT Thick Lift Test with 213D-3, Pad-Foot Roller													
	Test Date	Dec. 1, 2004							Displacement equivalent to Displacement of CH 5					
	Data	2500/sec during 10 sec												
	File Name	p3-r-c							Maximum and Minimum Value for Each Column					
									Displacement during Compaction					
	Reduced Data 1										Reduced Data 2			
	41.98640959	1578.710127	64.68975334	745.1969956	58.06741369	2428.602177								
	-2.26471041	-649.2598841	-5.013946661	-605.9019451	-4.677426314	-1709.076381	0.003937913	-0.007104637						
	14335		15071		15629			-0.003166724						
	Stress Cell	Accelero	Stress Cell	Accelero	Stress Cell	Accelero	LVDT	LVDT	Velocity from Accelerometer			Displacement from Accelerometer		
Time	CH00	CH01	CH02	CH03	CH04	CH05	CH06	CH07	CH01	CH03	CH05	CH01	CH03	CH05
msec	psi	in/sec2	psi	in/sec2	psi	in/sec2	inch	inch	in/sec	in/sec	in/sec	in	in	in
0	0.48190959	21.54170331	0.662419339	17.0175787	0.388613686	12.17990047	-0.579408804	-0.713094546	0	0	0	0	0	0
0.4	0.23780959	24.54263448	0.418273339	20.00485	0.449613686	15.16340353	-0.579166878	-0.713589134	0.009216868	0.007404486	0.005468661	1.84337E-06	1.4809E-06	1.09373E-06
0.8	0.23780959	26.94337941	0.418273339	21.79721278	0.327513686	16.80677571	-0.579285858	-0.713958048	0.01951407	0.015764898	0.011862697	7.58956E-06	6.11477E-06	4.56E-06
1.2	0.25300959	27.54356564	0.479313339	21.19975852	0.571713686	18.59687755	-0.579107388	-0.71334184	0.030411459	0.024364293	0.018943427	1.75747E-05	1.41406E-05	1.07212E-05
1.6	0.11570959	28.14375188	0.509828339	20.60230426	0.327513686	22.1868632	-0.579408804	-0.71334184	0.041548923	0.032724705	0.027100175	3.19667E-05	2.55584E-05	1.99299E-05
2	0.25300959	26.34319318	0.479313339	23.58957556	0.449613686	20.99346198	-0.579166878	-0.713094546	0.052446312	0.041563081	0.03573624	5.07658E-05	4.0416E-05	3.24972E-05
2.4	0.06990959	25.74300694	0.479313339	21.19975852	0.449613686	22.1868632	-0.579166878	-0.71334184	0.062863552	0.050520948	0.044372306	7.38278E-05	5.88328E-05	4.85189E-05
2.8	0.29880959	25.14282071	0.357243339	20.60230426	0.388613686	22.1868632	-0.579349314	-0.71328103	0.073040717	0.05888136	0.053247051	0.000101009	8.07132E-05	6.80428E-05
3.2	0.05470959	22.28947632	0.418273339	20.60230426	0.205413686	21.59016259	-0.579166878	-0.71334184	0.082527177	0.067122282	0.062002456	0.000132122	0.000105914	9.10927E-05
3.6	0.42090959	20.34133084	0.509828339	18.21248722	0.464913686	21.59016259	-0.578924952	-0.713094546	0.091053338	0.07488524	0.070638521	0.000166838	0.000134315	0.000117621
4	0.11570959	16.14002721	0.479313339	16.42012444	0.266513686	19.80006075	-0.578924952	-0.713094546	0.09834961	0.081811763	0.078916566	0.000204719	0.000165655	0.000147532
9994.4	0.42090959	24.54263448	-0.008976661	37.34081788	-0.160786314	31.734073	-0.58304166	-0.705918966	3.602013542	2.039331699	8.845916672	19.50389722	13.29622328	62.16390309
9994.8	0.42090959	29.34412434	-0.070016661	34.95100084	-0.221786314	28.75056394	-0.583283586	-0.70616626	3.612790894	2.053790063	8.858013601	19.50534018	13.2970419	62.16744388
9995.2	-0.06739041	32.95508086	-0.008976661	34.50046156	0.022313686	27.10719776	-0.582795768	-0.705918966	3.625250735	2.067680355	8.869185154	19.50678779	13.2978662	62.17098932
9995.6	0.11570959	35.95601203	-0.070016661	30.76882102	0.083413686	23.38026443	-0.58304166	-0.705854102	3.639032954	2.080734211	8.879282647	19.50824065	13.29869588	62.17453901
9996	0.17670959	40.15731566	-0.070016661	27.18409546	-0.099686314	19.19357816	-0.582795768	-0.705854102	3.654255619	2.092324795	8.887797415	19.50969931	13.29953049	62.17809243
9996.4	0.48190959	41.35768813	-0.253126661	21.79721278	0.083413686	13.82327265	-0.582795768	-0.705671672	3.67055862	2.102121056	8.894400785	19.51116427	13.30036938	62.18164887
9996.8	0.35980959	40.7575019	-0.131046661	16.42012444	-0.038686314	8.452967139	-0.582795768	-0.705854102	3.686981658	2.109764524	8.898856033	19.51263578	13.30121176	62.18520752
9997.2	0.23780959	38.35675696	-0.070016661	8.643424725	0.022313686	4.276062852	-0.58304166	-0.705424378	3.70280451	2.114777234	8.901401839	19.51411374	13.30205667	62.18876757
9997.6	0.29880959	34.75563956	-0.070016661	3.863790643	0.205413686	-0.507324025	-0.582795768	-0.705671672	3.717426989	2.117278677	8.902155587	19.51559778	13.30290308	62.19232828
9998	0.29880959	28.74393811	-0.131046661	-1.513297699	0.159713686	-5.280928925	-0.582795768	-0.705671672	3.730126305	2.117748775	8.900997936	19.51708729	13.30375008	62.19588891
9998.4	-0.12849041	24.54263448	-0.482046661	-5.69547752	-0.038686314	-10.05453382	-0.58304166	-0.704183854	3.740784219	2.11630702	8.897930844	19.51858147	13.3045963	62.1994487
9998.8	0.11570959	16.74021344	-0.131046661	-11.08236019	-0.053986314	-14.24122009	-0.58304166	-0.705671672	3.749040789	2.112951453	8.893071693	19.52007944	13.30544275	62.2030069
9999.2	0.05470959	11.48612412	-0.314156661	-13.47217724	0.037613686	-18.41812438	-0.583283586	-0.705918966	3.754686056	2.108040545	8.886539824	19.52158018	13.30628695	62.20656282
9999.6	0.29880959	4.726649658	-0.070016661	-20.0441741	-0.099686314	-23.19172928	-0.58322013	-0.70616626	3.757928611	2.101337275	8.878217853	19.52308271	13.30712882	62.21011577

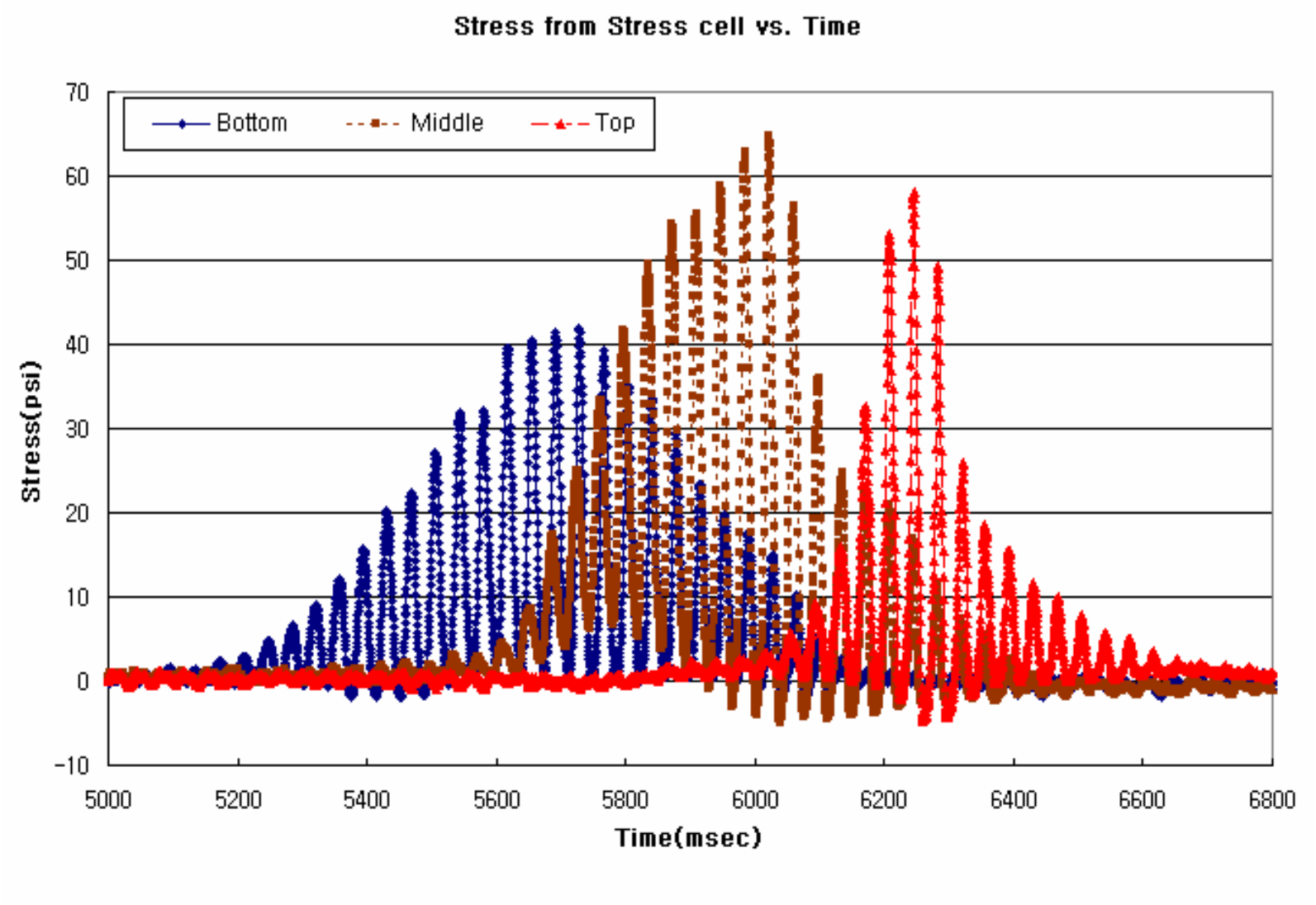
Stress from Stress cell vs. Time
Bottom
Middle
Top
Stress(psi)
70
60
50
40
30
20
10
0
-10
5000
5200
5400
5600
5800
6000
6200
6400
6600
6800
Time(msec)

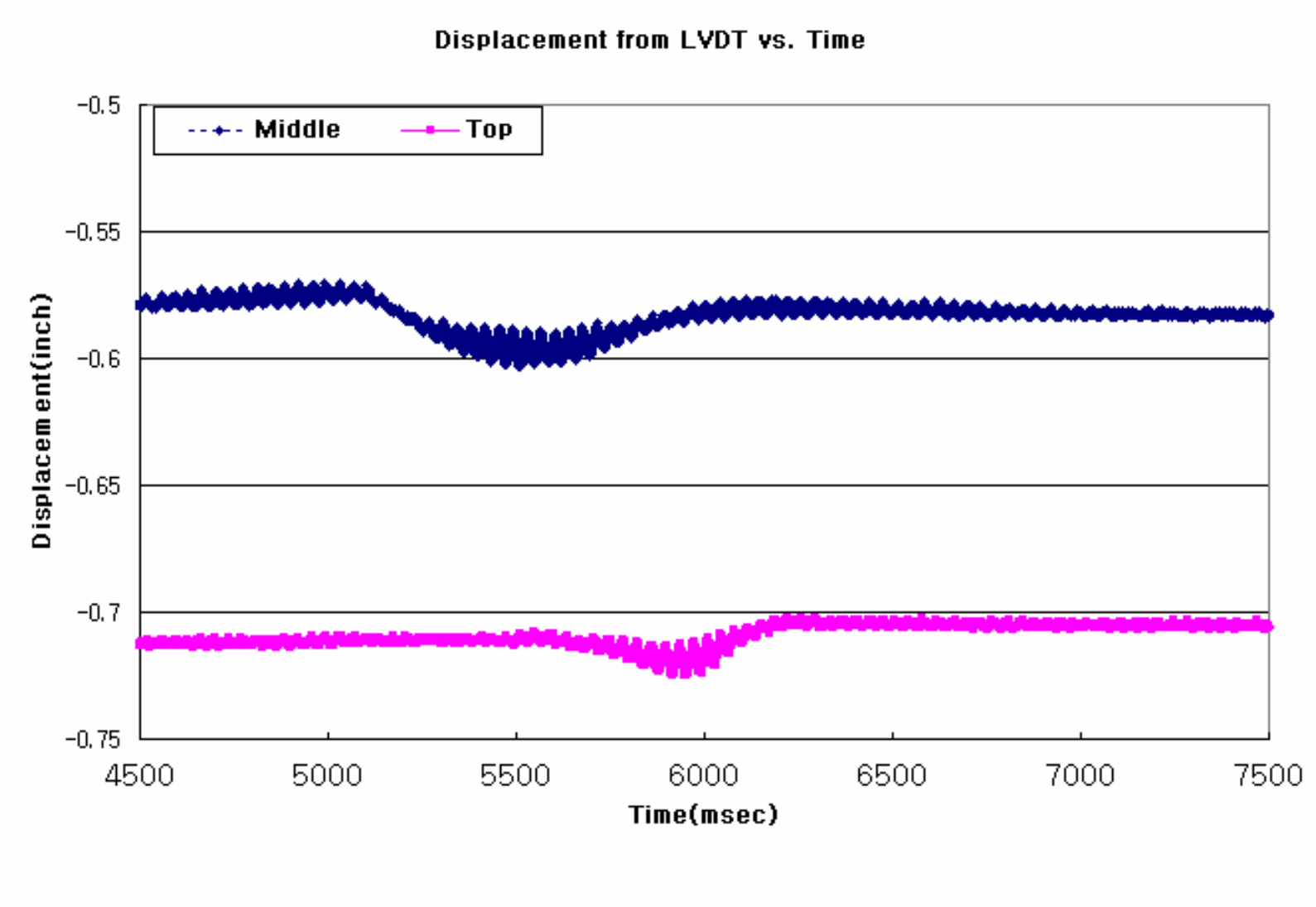
Displacement from LVDT vs. Time
Middle
Top
-0.5
-0.55
-0.6
-0.65
-0.7
-0.75
Displacement(inch)
4500
5000
5500
6000
6500
7000
7500
Time(msec)

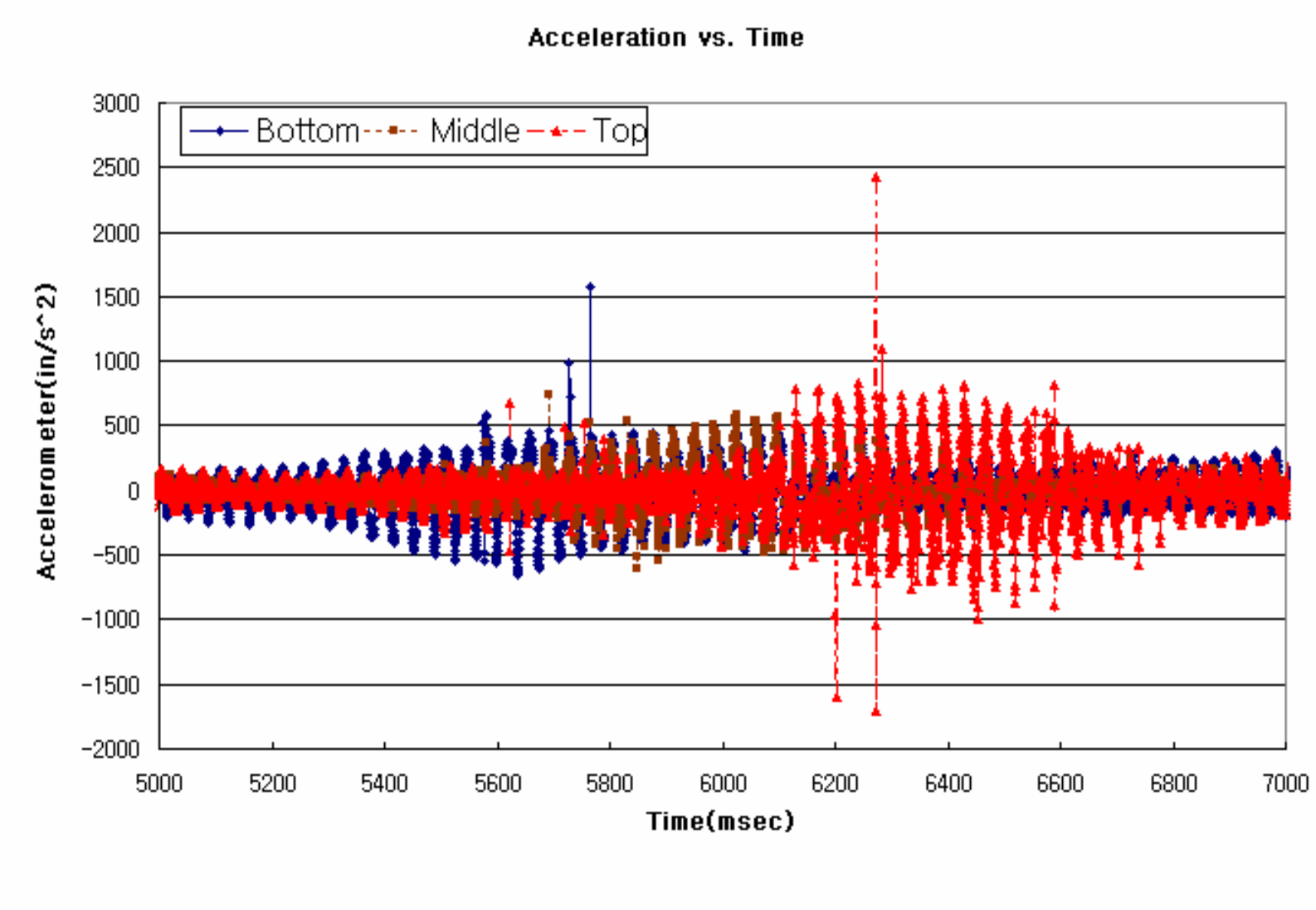
Acceleration vs. Time
Bottom
Middle
Top
3000
2500
2000
1500
1000
500
0
-500
-1000
-1500
-2000
Accelerometer(in/s^2)
5000
5200
5400
5600
5800
6000
6200
6400
6600
6800
7000
Time(msec)

APPENDIX E
SSG RESULTS

SSG READINGS

Strip: Section 1 (Control)

Roller: BW 211 D

1st 6" lift

	Subgrade			Cover#	2		Cover#	3
	STD DEV	SSG VALUE		STD DEV	SSG VALUE		STD DEV	SSG VALUE
1	7.12	11.46	1	2.37	7.69	1	1.41	10.82
2	2.28	11.04	2	1.44	8.93	2	1.48	10.48
3	1.45	7.90	3	1.40	11.26	3	1.51	12.12
4	2.57	12.28	4	1.22	9.83	4	1.49	11.80
5	1.47	10.85	5	1.22	9.59	5	1.73	12.86
6	1.70	11.94	6	2.06	7.95	6	3.12	12.57
7	2.08	12.81	7	1.52	11.79	7	1.38	10.35
8	1.70	12.68	8	1.59	12.15	8	1.78	13.74
9	2.47	13.46	9	1.83	13.03	9	1.81	13.55
10	1.85	11.53	10	1.48	14.69	10	2.23	15.57

2nd 6" lift

	Cover#	1		Cover#	3		Cover#	4
	STD DEV	SSG VALUE		STD DEV	SSG VALUE		STD DEV	SSG VALUE
1	1.39	7.32	1	1.59	13.21	1	1.58	11.49
2	1.11	7.22	2	1.84	12.61	2	1.34	11.80
3	1.20	9.02	3	1.87	14.46	3	1.86	11.80
4	1.61	12.24	4	1.98	13.00	4	2.40	15.10
5	1.36	11.20	5	1.62	12.54	5	1.83	14.66
6	1.41	9.26	6	2.27	16.69	6	1.43	11.43
7	1.39	12.52	7	2.03	15.05	7	2.31	17.56
8	1.25	10.21	8	1.96	14.36	8	1.98	16.97
9	1.19	8.87	9	1.69	13.12	9	1.49	15.76
10	1.52	9.02	10	2.42	12.11	10	1.72	14.24

SSG READINGS								
Strip: Section 2								
Roller: Padfoot - BW 213P D								
	Subgrade			Cover# 4			Cover# 9	
	STD DEV	SSG VALUE		STD DEV	SSG VALUE		STD DEV	SSG VALUE
1	1.74	13.83	1	1.13	10.61	1	1.35	13.51
2	2.36	15.11	2	1.20	8.18	2	1.35	12.37
3	2.09	16.03	3	1.42	8.72	3	1.37	11.59
4	2.19	15.95	4	1.22	10.28	4	1.66	11.64
5	2.14	12.02	5	1.37	11.62	5	2.21	18.11
6	2.13	15.91	6	1.59	11.59	6	1.90	16.53
7	2.02	12.91	7	1.27	11.06	7	2.22	17.14
8	2.32	16.97	8	1.26	10.64	8	1.43	13.03
9	1.54	11.17	9	2.53	9.31	9	2.57	19.23
10	1.91	14.15	10	1.40	12.64	10	2.93	21.47
Note: subgrade not done with Padfoot			Note: 3 covers with Padfoot 1 cover with BW 211 D			Note: 2 covers with Padfoot 3 covers with BW 211 D		

SSG READINGS					
Strip: Section 3					
Roller: BW 225 D Variocontrol					
	Subgrade			Cover# 9	
	STD DEV	SSG VALUE		STD DEV	SSG VALUE
1	6.66	17.99	1	1.33	9.90
2	2.58	16.41	2	1.63	13.69
3	3.32	24.13	3	1.43	11.08
4	2.45	16.32	4	1.29	7.87
5	3.24	17.26	5	8.97	15.46
6	2.32	14.13	6	2.26	18.34
7	2.17	15.98	7	1.57	7.23
8	1.75	13.18	8	2.08	9.50
9	2.09	15.52	9	1.84	14.81
10	2.63	14.95	10	2.18	17.59

APPENDIX F
FWD RESULTS

D0 Impulse Stiffness Modulus
Dade County SR 826 SBTL
Section 1

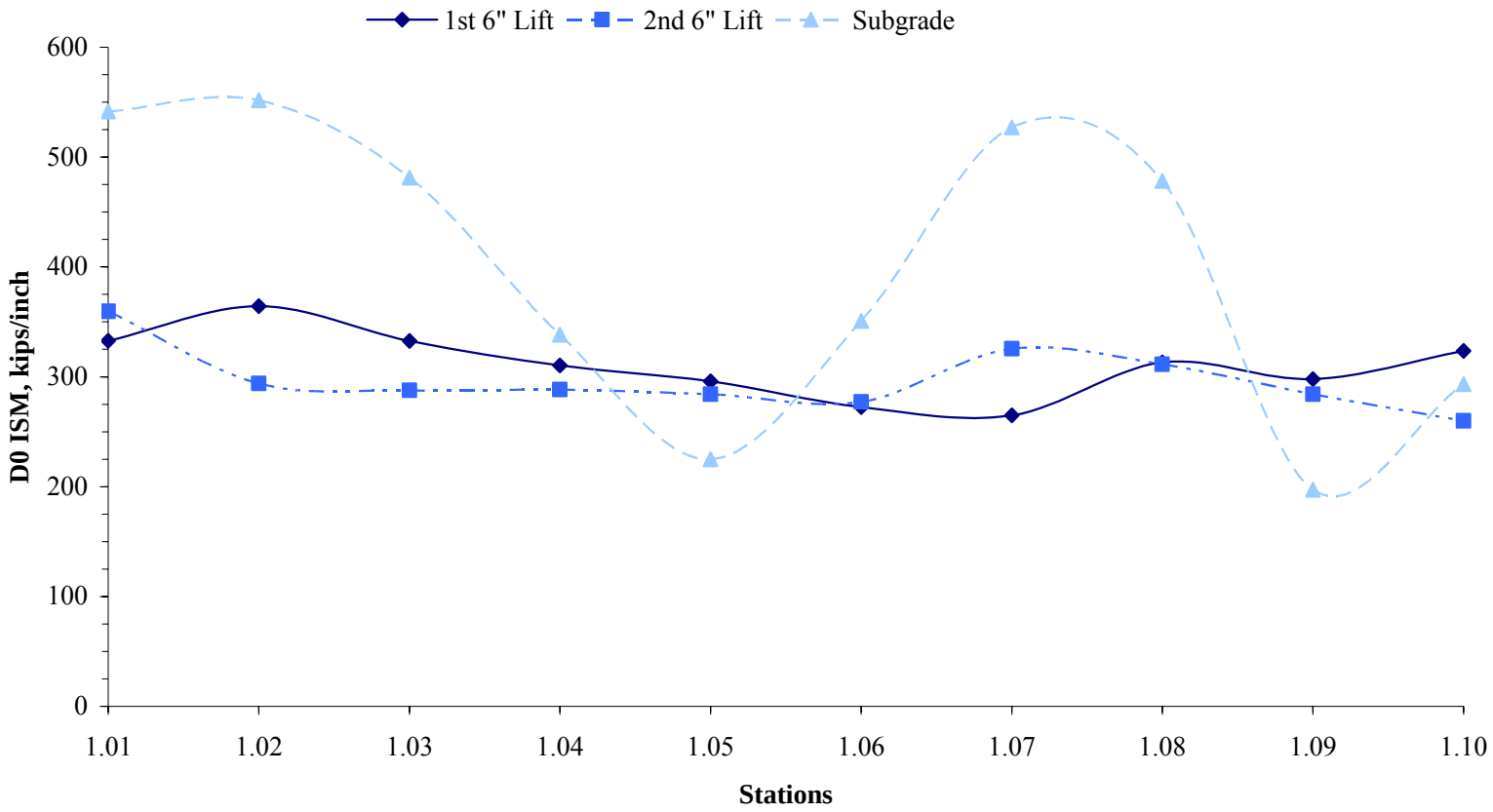

D0 Impulse Stiffness Modulus
Dade County SR 826 SBTL
Section 2

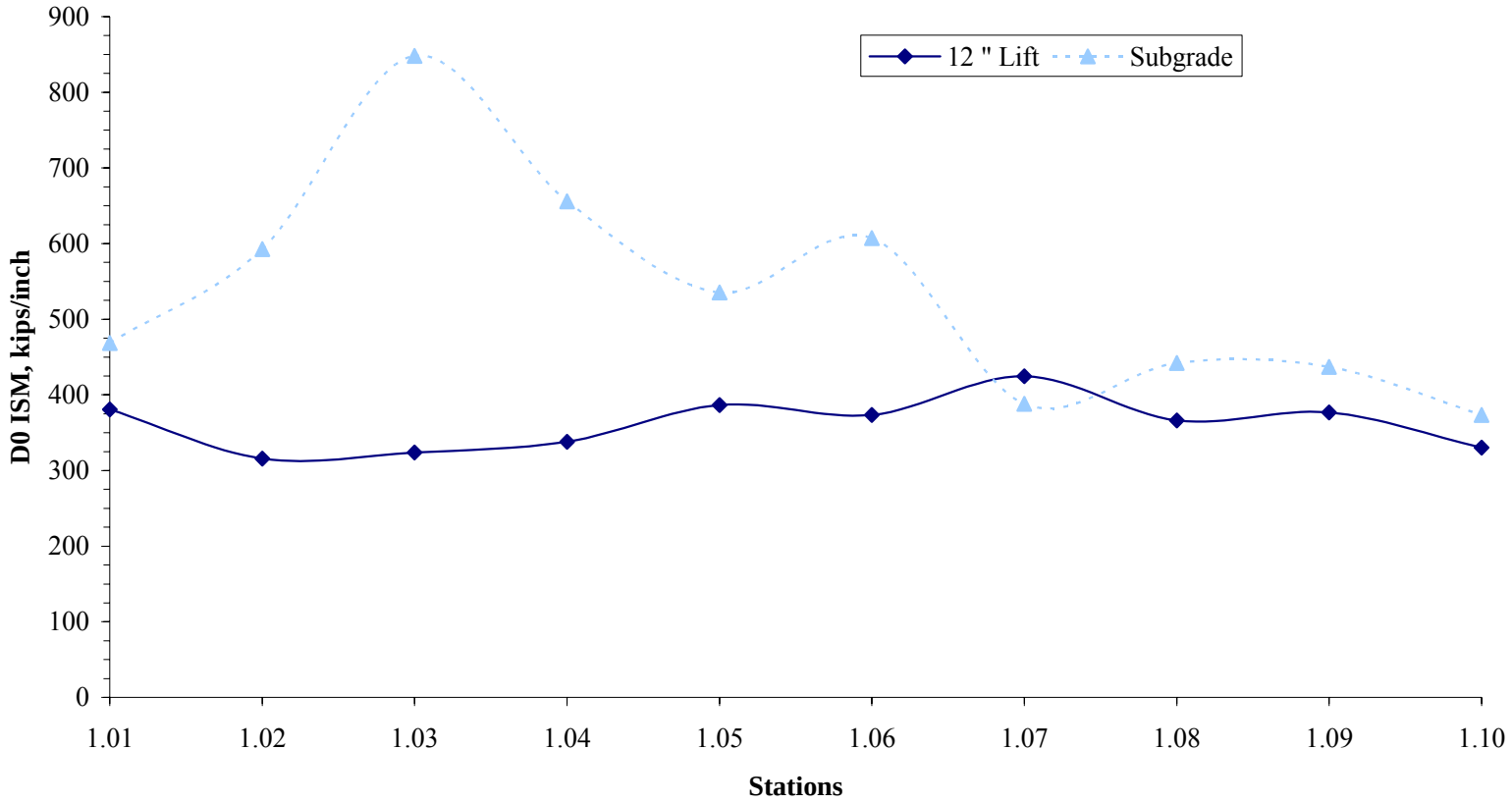

D0 Impulse Stiffness Modulus
Dade County SR 826 SBTL
Section 3

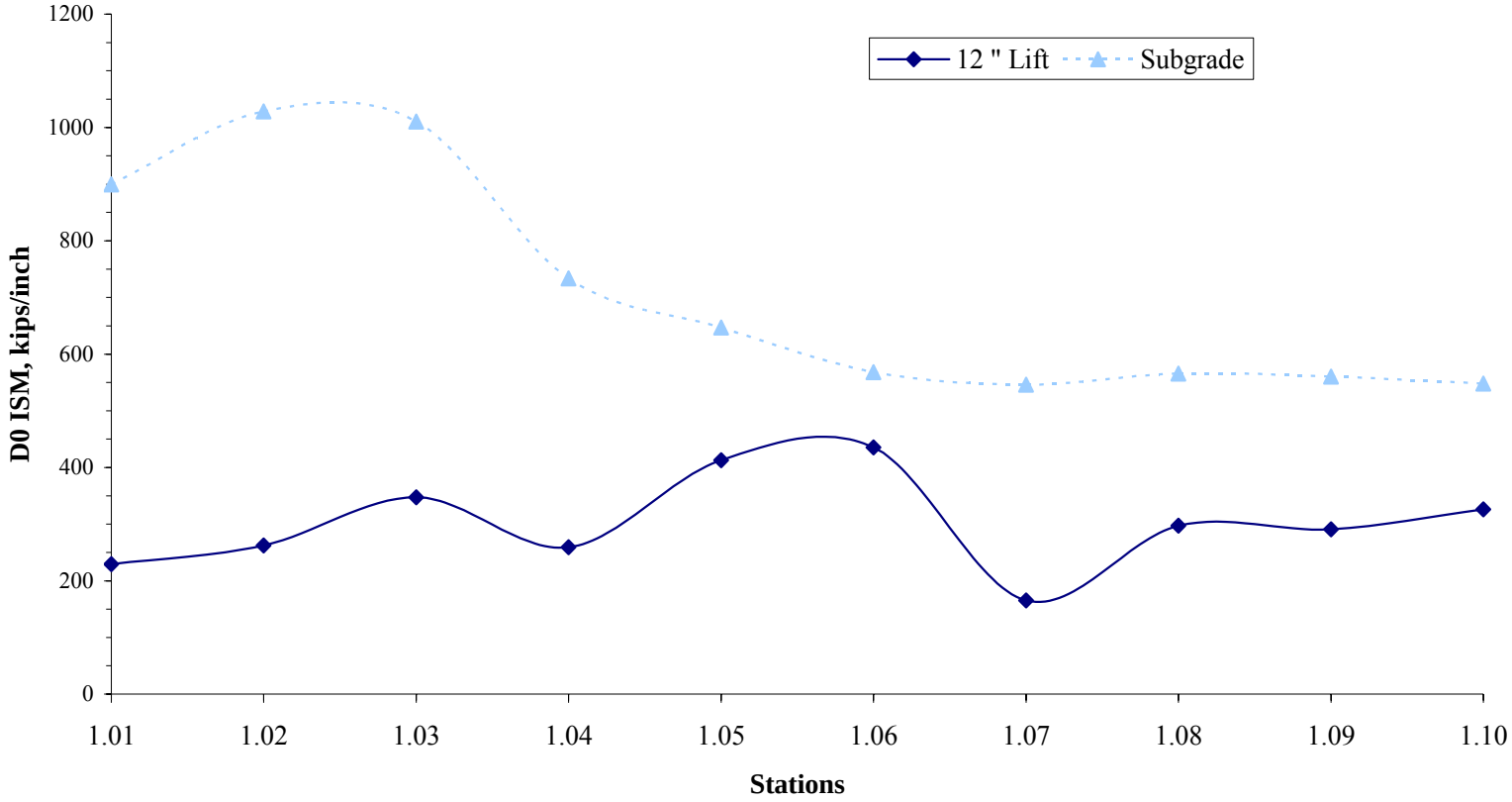

APPENDIX G
ADCP RESULTS

SR 826 - Miami Dade - Control Section
DCP Slope Summary (Depth vs. Blows)

Section 1 (BW 211D)	Slope (Depth vs. Blows)						
	Base - 1st Lift			Base - 2nd Lift			Subgrade
Location	0" - 6"	6" - 12"	12" - 24"	0" - 6"	6" - 12"	12" - 24"	0" - 12"
1	0.397	0.251	0.231	0.358	0.156	0.125	0.094
2				0.357	0.165	0.148	
3	0.283	0.209	0.158	0.308	0.143	0.144	0.164
4				0.272	0.140	0.180	
5	0.324	0.354	0.273	0.206	0.128	0.208	0.327
6				0.180	0.130	0.156	
7	0.209	0.228	0.126	0.171	0.139	0.123	0.219
8				0.237	0.113	0.131	
9	0.251	0.196	0.189	0.191	0.147	0.143	0.216
10				0.173	0.168	0.148	
Average =	**0.293**	**0.247**	**0.196**	**0.245**	**0.143**	**0.151**	**0.204**
St. Dev. =	**0.072**	**0.063**	**0.058**	**0.074**	**0.017**	**0.026**	**0.086**
COV =	**0.246**	**0.255**	**0.298**	**0.302**	**0.120**	**0.173**	**0.420**

SR 826 - Miami Dade - Section 2
DCP Slope Summary (Depth vs. Blows)

Section 2 (BW 211D)	Slope (Depth vs. Blows)			
	Base - 1st Lift			Subgrade
Location	0" - 6"	6" - 12"	12" - 24"	0" - 12"
1	0.173	0.235	0.138	
2	0.198	0.192	0.152	0.099
3	0.223	0.243	0.115	
4	0.278	0.232	0.210	0.170
5	0.192	0.230	0.146	
6	0.179	0.203	0.107	0.128
7	0.160	0.140	0.183	
8	0.174	0.213	0.123	0.163
9	0.130	0.224	0.125	
10	0.121	0.169	0.135	0.279
Average =	**0.190**	**0.213**	**0.144**	**0.140**
St. Dev. =	**0.042**	**0.032**	**0.034**	**0.033**
COV =	**0.222**	**0.149**	**0.233**	**0.237**

SR 826 - Miami Dade - Section 3
DCP Slope Summary (Depth vs. Blows)

Section 3 (BW 225D)	Slope (Depth vs. Blows)			
	Base - 1st Lift			Subgrade
Location	0" - 6"	6" - 12"	12" - 24"	0" - 12"
1	0.1397	0.1409	0.0546	
2	0.1314	0.1145	0.0906	0.1285
3	0.1311	0.1105	0.0736	
4	0.1709	0.1151	0.0608	0.0859
5	0.0708	0.0677	0.0883	
6	0.1019	0.1132	0.0716	0.1941
7	0.1255	0.1027	0.0812	
8	0.0856	0.0598	0.0408	0.2811
9	0.1041	0.0913	0.0706	
10	0.1009	0.0967	0.0973	0.1684
Average =	**0.1179**	**0.1015**	**0.0702**	**0.1724**
St. Dev. =	**0.0304**	**0.0253**	**0.0161**	**0.0850**
COV =	**0.2582**	**0.2483**	**0.2291**	**0.4932**

SR 826 - Miami Dade - Control Section
DCPI Summary (DCPI vs. Depth)

Section 1 (BW 211D)	Base - 1st Lift				Base - 2nd Lift						Subgrade	
	0" - 6" Limerock		6" - 12" Subgrade		0" - 6" Limerock		6" - 12" Limerock		12" - 24" Subgrade		0" - 6" Subgrade	
Location	Average	St. Dev.	Average	St. Dev.	Average	St. Dev.	Average	St. Dev.	Average	St. Dev.	Average	St. Dev.
1	0.414	0.153	0.326	0.060	0.365	0.082	0.169	0.042	0.151	0.034	0.218	0.218
2					0.356	0.107	0.179	0.058	0.172	0.047		
3	0.281	0.062	0.246	0.047	0.297	0.077	0.149	0.024	0.159	0.061	0.199	0.120
4					0.263	0.100	0.149	0.036	0.177	0.038		
5	0.327	0.047	0.333	0.047	0.209	0.048	0.141	0.051	0.210	0.025	0.430	0.140
6					0.196	0.051	0.139	0.038	0.155	0.036		
7	0.231	0.105	0.228	0.065	0.189	0.053	0.147	0.050	0.126	0.036	0.227	0.075
8					0.246	0.033	0.131	0.058	0.140	0.045		
9	0.263	0.043	0.230	0.044	0.203	0.040	0.158	0.038	0.140	0.021	0.268	0.134
10					0.185	0.039	0.172	0.055	0.153	0.040		
Average =	**0.303**		**0.273**		**0.251**		**0.153**		**0.158**		**0.268**	
St. Dev. =	**0.071**		**0.052**		**0.068**		**0.016**		**0.024**		**0.094**	
COV =	**0.234**		**0.192**		**0.271**		**0.102**		**0.150**		**0.350**	

SR 826 - Miami Dade - Section 2
DCPI Summary (DCPI vs. Depth)

Section 2 (BW 211D)	Base						Subgrade	
	0" - 6" Limerock		6" - 12" Limerock		12" - 24" Subgrade		12" Subgrade	
Location	Average	St. Dev.	Average	St. Dev.	Average	St. Dev.	Average	St. Dev.
1	0.180	0.025	0.237	0.024	0.160	0.057		
2	0.210	0.045	0.198	0.042	0.177	0.052	0.159	0.078
3	0.234	0.062	0.241	0.036	0.183	0.067		
4	0.296	0.105	0.229	0.068	0.206	0.041	0.218	0.040
5	0.199	0.039	0.230	0.028	0.151	0.036		
6	0.188	0.048	0.198	0.029	0.129	0.033	0.181	0.064
7	0.168	0.052	0.141	0.032	0.206	0.042		
8	0.188	0.048	0.213	0.047	0.130	0.038	0.199	0.120
9	0.149	0.051	0.228	0.082	0.131	0.037		
10	0.132	0.053	0.166	0.040	0.138	0.034	0.329	0.209
Average =	**0.194**		**0.208**		**0.161**		**0.217**	
St. Dev. =	**0.046**		**0.033**		**0.030**		**0.066**	
COV =	**0.237**		**0.158**		**0.189**		**0.305**	

SR 826 - Miami Dade - Section 3
DCPI Summary (DCPI vs. Depth)

Section 3 (BW 225D)	Base						Subgrade	
	0" - 6" Limerock		6" - 12" Limerock		12" - 24" Subgrade		12" Subgrade	
Location	Average	St. Dev.	Average	St. Dev.	Average	St. Dev.	Average	St. Dev.
1	0.153	0.049	0.138	0.026	0.075	0.026		
2	0.151	0.047	0.134	0.049	0.139	0.051	0.169	0.110
3	0.136	0.037	0.111	0.042				
4	0.178	0.045	0.134	0.041	0.088	0.033	0.128	0.077
5	0.099	0.035	0.090	0.035				
6	0.117	0.041	0.129	0.044	0.103	0.030	0.290	0.174
7	0.139	0.046	0.106	0.026	0.138	0.041		
8	0.099	0.047	0.085	0.031	0.097	0.037	0.541	0.351
9	0.109	0.039	0.098	0.036	0.103	0.038		
10	0.106	0.042	0.116	0.044	0.106	0.033	0.189	0.116
Average =	**0.129**		**0.114**		**0.106**		**0.264**	
St. Dev. =	**0.027**		**0.019**		**0.022**		**0.166**	
COV =	**0.209**		**0.169**		**0.210**		**0.631**	

SR 826 Miami-Dade
Control Section (2nd Lift)
Smooth Roller (BW 211 D)

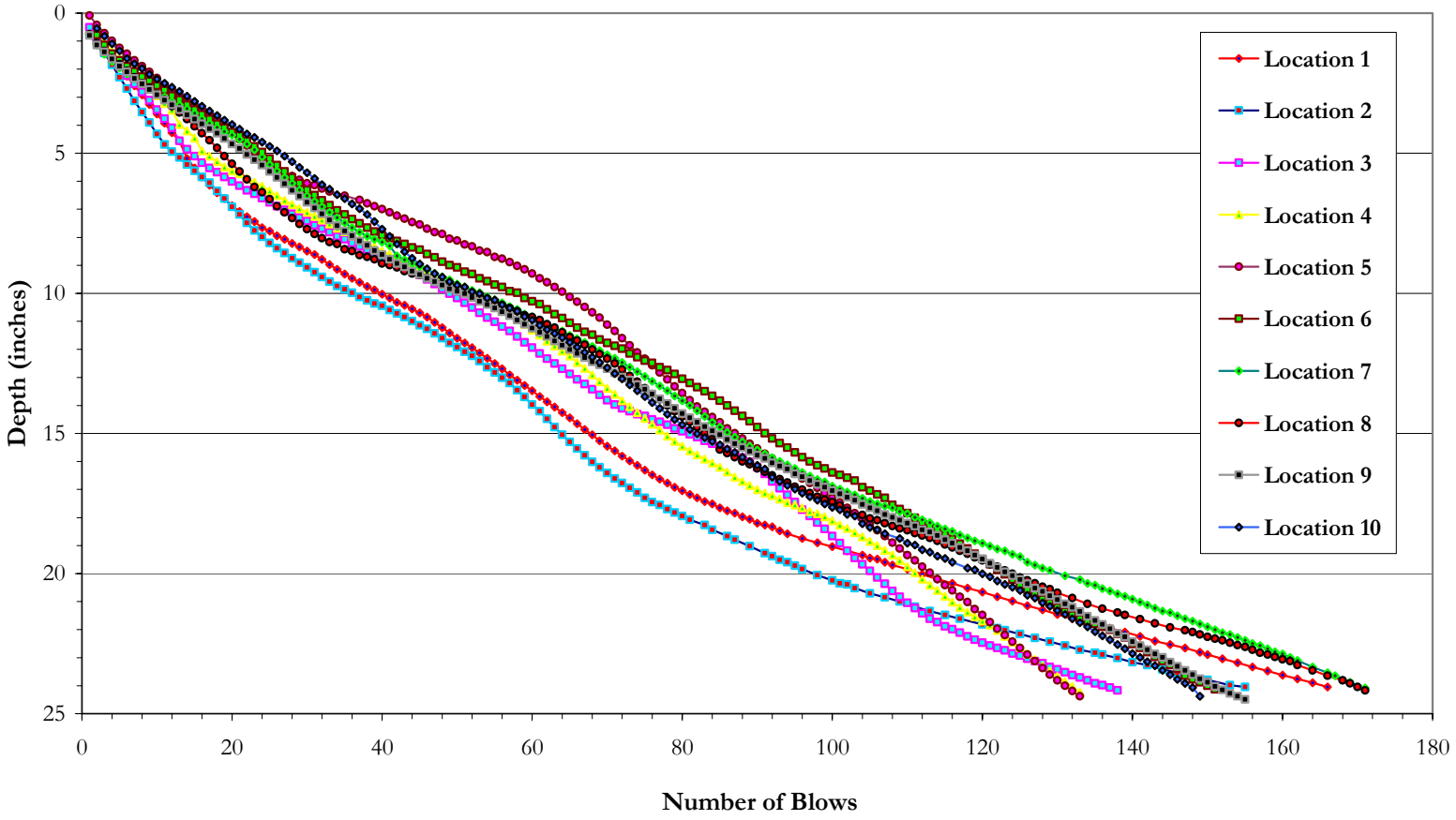

SR 826 Miami-Dade
Section 2, Base
Pad Foot Roller (BW 213 PD)

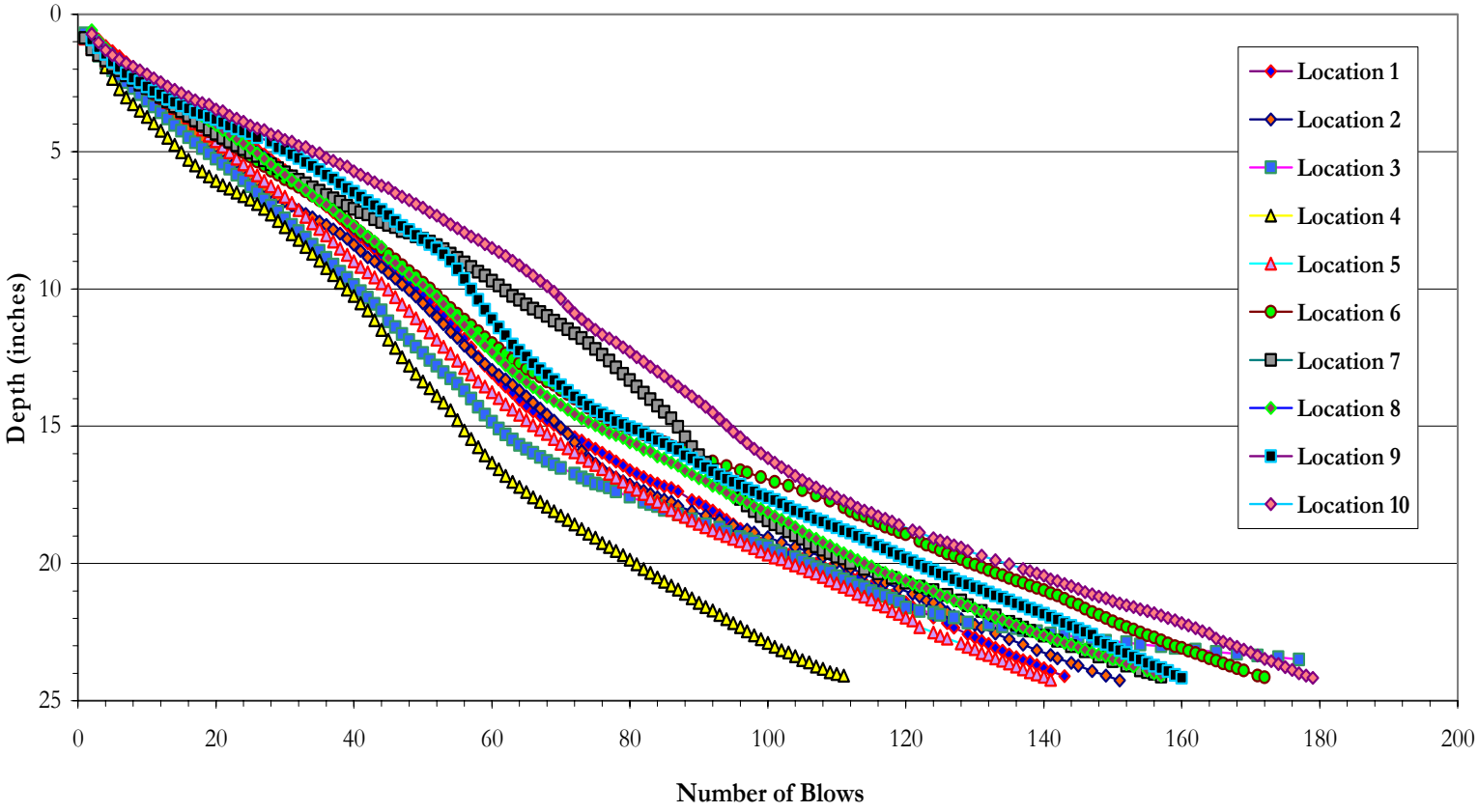

SR 826 Miami-Dade
Section 3, Base
Heavy Roller (BW 225 D)

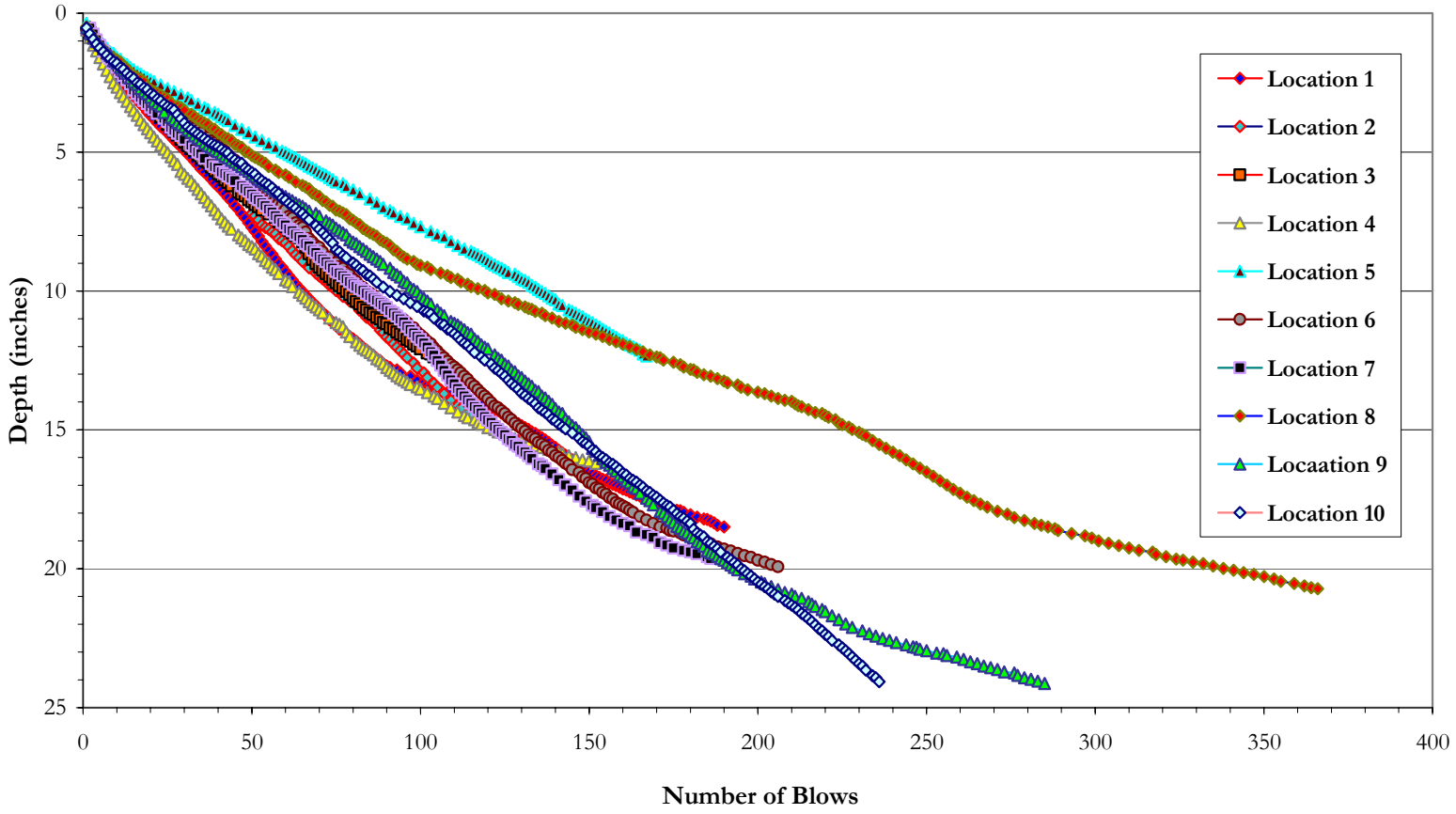

LIST OF REFERENCES

Forssblad, L.,1977, "Vibratory Compaction in the Construction of Roads, Airfields, Dams, and Other Projects," Research Report No. 8222, Dynapac, S-171, No. 22, Solna, Sweden as referenced in Hausmannn(1990).

US Army Engineering Waterways Experiment Station COE, 1976, "Notes for Earthwork Construction Inspectors Course," Vicksburg, MS.

Townsend, F.C. & Anderson, B., 2004, "A Compendium of Ground Modification Techniques," Research Report BC-354, pp. 16~60. Florida Department of Transportation (FDOT).

Forssblad, L., 1965, "Investigations of Soil Compaction by Vibration" Acta Polytechnica Scandinavia, No. Ci-34, Stockholm.

Bernhard,R.K., 1952, "Static and Dynamic Soil Compaction," Proc. HRB, Vol. 31, 1952, pp. 563~591.

Parsons, A.W., Krawczyk, J. and Cross, J.E., Mar.1962, "An Investigation of the performance of an 8.5 ton Vibrating Roller for the Compaction of Soil" Road Research Laboratory Note. LN/64/ AWP.JK.JEC.

Turnbull, W.J., and Foster, C.R., 1956, "Stabilization of Materials by Compaction", Journal of the Soil Mechanics and Foundations Division, American Society of Civil Engineers, Vol. 82, No.SM2, pp.934-1~934-23.

Seed, H.B., and Chan, C.K., 1959, "Structure and Strength Characteristics of Compacted Clays", Journal of the Soil Mechanics and Foundations Division, American Society of Civil Engineers, Vol.85, No. SM5, pp.87~128.

Kloubert, H.J, 2001, "New intelligent compaction system for vibratory rollers" Report for IRF in Paris.

Yoo, T.S., 1975, "A Theory for Vibratory Compaction of Soil", The Dissertation for Degree of Doctor of Philosophy to University of New York at Buffalo